



SCHOOL of
GRADUATE STUDIES
EAST TENNESSEE STATE UNIVERSITY

East Tennessee State University
Digital Commons @ East Tennessee
State University

Electronic Theses and Dissertations


Student Works

12-2018

SIP-428, a SIR2 Deacetylase Enzyme and Its Role in Biotic Stress Signaling Pathway

Bal Krishna Chand Thakuri
East Tennessee State University

Follow this and additional works at: <https://dc.etsu.edu/etd>

 Part of the [Biochemistry Commons](#), [Biology Commons](#), [Molecular Biology Commons](#), [Molecular Genetics Commons](#), and the [Plant Sciences Commons](#)

Recommended Citation

Thakuri, Bal Krishna Chand, "SIP-428, a SIR2 Deacetylase Enzyme and Its Role in Biotic Stress Signaling Pathway" (2018). *Electronic Theses and Dissertations*. Paper 3505. <https://dc.etsu.edu/etd/3505>

This Dissertation - Open Access is brought to you for free and open access by the Student Works at Digital Commons @ East Tennessee State University. It has been accepted for inclusion in Electronic Theses and Dissertations by an authorized administrator of Digital Commons @ East Tennessee State University. For more information, please contact digilib@etsu.edu.

SIP-428, a SIR2 Deacetylase Enzyme and Its Role in Biotic Stress Signaling Pathway

A dissertation
presented to
the faculty of the Department of Biomedical Sciences
East Tennessee State University
In partial fulfillment
of the requirements for the degree
Doctor of Philosophy in Biomedical Sciences

by
Bal Krishna Chand Thakuri
December 2018

Dhirendra Kumar, Chair
Alok Agrawal
Antonio Rusinol
Cecilia McIntosh
William L. Stone

Key Words: Plant Defense, Salicylic Acid, Salicylic Acid Binding Protein 2, PR1, SIP-428, SIR2
Deacetylase, Deacetylation

ABSTRACT

SIP-428, a SIR2 Deacetylase Enzyme and Its Role in Biotic Stress Signaling Pathway

by

Bal Krishna Chand Thakuri

SABP2 (Salicylic Acid Binding Protein 2) plays a vital role in the salicylic acid signaling pathway of plants both regarding basal resistance and systemic acquired resistance against pathogen infection. SIP-428 (SABP2 Interacting Protein-428) is a Silent information regulator 2 (SIR2) like deacetylase enzyme that physically interacts with SABP2 in a yeast two-hybrid interaction and confirmed independently by a GST pull-down assay. We demonstrated that SIP-428 is an NAD⁺ dependent SIR2 deacetylase enzyme. Transgenic tobacco plants silenced in SIP-428 expression via RNAi showed enhanced basal resistance to microbial pathogens. Moreover, these SIP-428-silenced lines also exhibited a robust induction of systemic acquired resistance. In contrast, the transgenic tobacco lines overexpressing SIP-428 showed compromised basal resistance and failed to induce systemic acquired resistance. These results indicate that SIP-428 is likely a negative regulator of SA-mediated plant immunity. Experiments using a SABP2 inhibitor showed that SIP-428 likely functions upstream of SABP2 in the salicylic acid signaling pathway. It also indicates that SABP2 is dependent on SIP-428 for its role in the SA signaling pathway. Subcellular localization studies using confocal microscopy and subcellular fractionation showed that SIP-428 localized in the mitochondria. These results clearly show a role for SIP-428 in plant immunity.

DEDICATION

To my loving wife Bishakha Rana Chand: words cannot express how much I appreciate the undying support you have given me through the process of obtaining my degree. To my brother Rabi Chand Thakuri and sisters Sarita Thakuri and Chandrawati Thakuri for their love, support, and guidance. Bandana Rana, Avinaya S.J.B Rana, Ambarish S.J.B Rana and Ayushma Malla Rana for all the support and blessings. Similarly, Brian Evanshen and Dr. Pamela Evanshen for their help and encouragement throughout my stay in ETSU.

In memoriam to my late father Mohan Bahadur Thakuri and late mother, Subdhara Chand Thakuri. I humbly dedicate everything in my life to my late parents.

ACKNOWLEDGMENTS

First, I owe my deepest gratitude to my advisor Prof. Dhirendra Kumar for his continuous support, patience, motivation, dedication, and immense knowledge. I would also like to thank my dissertation committee members: Dr. Cecilia A. McIntosh, Dr. Alok Agrawal, Dr. Antonio Rusinol, and Dr. William L. Stone for their guidance, constructive criticism, insightful comments, and the hard questions that helped me widen my research knowledge throughout the project. My sincere thanks go to Dr. McIntosh and Dr. Kilaru who gave me access to their laboratories and research facilities. I would like to thank my fellow lab mates for their constant experimental help and stimulating discussions. Also, I thank my friend Dr. Xiaohui Wang for helping me with research related writing and troubleshooting. I would like to thank all the staff members of Biological Sciences and Biomedical Sciences for their support as well as the ETSU Graduate School for a graduate assistantship. Last but not least, I am also thankful to my wife Bishakha Rana Chand for her help and encouragement throughout my dissertation project as well as my family members and friends for their support and love.

ETSU supported this work with RDC grant (14-021M to DK), and NSF grant (MCB 1022077 to DK) to support this project

TABLE OF CONTENTS

	Page
ABSTRACT.....	2
DEDICATION.....	3
ACKNOWLEDGMENTS	4
LIST OF TABLES.....	11
LIST OF FIGURES	12
Chapter	
INTRODUCTION	16
Synthesis of SA.....	19
Regulation of NPR1 by SA.....	21
Systemic Acquired Resistance (SAR).....	22
SABP2 and SIP (SABP2 Interacting Protein).....	23
Deacetylation/Acetylation in Plant Immunity.....	24
Silent Information Regulator2 (SIR2).....	26
Sirtuins in Plants.....	29
Non-Histone Protein De/acetylation.....	30
Hypothesis.....	34
MATERIALS AND METHODS.....	35
Plant Material	35
Chemicals/Reagents	35
Other Materials.....	37
Oligonucleotides (Primers)	37
Bioinformatics Analysis.....	38

Expression of The Full-length SIP-428 Protein in <i>E. coli</i>	39
Cloning of SIP-428.....	39
Transformation of Chemically Competent <i>E. coli</i> Cells	41
Screening of Transformed Cells using Colony PCR.....	42
Agarose Gel Electrophoresis	42
Isolation of TOPO-SIP-428 Plasmid DNA	43
DNA Sequencing of Recombinant Plasmids.....	43
Restriction Digestion of TOPO-SIP-428 Plasmid and Destination Plasmid (pET28a (+))...	43
Cloning of SIP-428 into Destination Plasmid (pET28a (+)).....	44
Solubility Test of Full-length SIP-428	44
Sodium Dodecyl Sulfate-Polyacrylamide Gel Electrophoresis (SDS PAGE) and Western Blot	45
Expression and Purification of SIP-428-72 Protein	46
Cloning and Expression of SIP-428-72.....	46
Purification of SIP-428-72 Using Ni-NTA Chromatography	47
Purification of SIP-428-72 Using Mono-Q.....	48
Dialysis of SIP-428-72	49
Deacetylase Enzyme Assay.....	49
HDAC Deacetylase Enzyme Assay.....	49
GST-Pull Down Assay	50
Verification of SIP-428 Homolog Mutant	51
Confirmation of T-DNA Insertion.....	52
Confirmation of SIP-428 Homolog Mutant	52
Role of SIP-428 in Biotic Stress	53
Role of SIP-428 in Basal Resistance	53

Role of SIP-428 in Systemic Acquired Resistance (SAR)	54
Role of SIP-428 in Abiotic Stress	54
Generation of RNAi Lines Silenced in SIP-428 and Homologs of SIP-428	55
PCR Amplification of SIP-428 Silencing and Homolog Silencing Fragment	56
Agarose Gel Electrophoresis and Gel Extraction	57
Cloning of SIP-428 (Silencing and Homolog Silencing) into pDONR221	57
Isolation of pDONR221-SIP-428 Plasmid DNA	58
Cloning of SIP-428 (Silencing and Homolog Silencing) into pHELLSGATE8	58
Isolation of pHELLSGATE8-SIP-428 Plasmid DNA	59
Transformation of pHELLSGATE8-SIP-428 Silencing and Homolog Silencing Plasmid into Competent <i>Agrobacterium tumefaciens</i>	59
Screening of Transformed <i>Agrobacterium</i>	59
Generation of Inducible SIP-428 Overexpressing Transgenic Lines	60
Cloning of SIP-428 into pER8 Plasmid	60
Preparation of Competent <i>Agrobacterium tumefaciens</i> LBA4404	61
Transformation of the pER8-SIP-428 Plasmid into Competent <i>Agrobacterium</i>	62
Transient Expression of SIP-428 in <i>Nicotiana benthamiana</i>	62
Generation of Stable Transgenic Tobacco Lines with Verified pER8-SIP-428 and pHELLSGATE8-SIP-428 Plasmid in <i>Agrobacterium</i>	63
Screening of SIP-428 Silenced and Homolog Silenced Transgenic Lines	65
Screening of SIP-428 Overexpressing Transgenic Lines	66
Role of SIP-428 in Biotic Stress	67
Role of SIP-428 in Basal Resistance	67
Role of SIP-428 in SAR	68
Subcellular Localization of SIP-428	68

Time Course Expression of SIP-428	69
Confocal Microscopy	69
Subcellular Fractionation.....	70
SDS PAGE Electrophoresis and Western Blot Analysis.....	72
Statistical Analysis	72
RESULTS	73
Bioinformatics Analysis of SIP-428	73
Putative Conserved Domains of SIP-428	73
Protein Structure of SIP-428.....	74
Expression of Full-length SIP-428 in <i>E. coli</i>	76
Expression of SIP-428-72 Protein in <i>E. coli</i>	78
Expression and Purification of SIP-428-72 using Ni-NTA	80
Purification of SIP-428-72 Using Mono-Q Ion Exchange Chromatography	81
Dialysis of SIP-428-72	83
Enzyme Assay	84
SIR2 Deacetylase Enzyme Assay	84
Histone Deacetylase Enzyme Assay.....	85
GST Pull-Down Assay	86
Screening of SIP-428 Homolog Mutant.....	87
T-DNA Insertion Confirmation	87
Confirmation of <i>atsrt2</i> Mutant	88
Role of AtSRT2 in Biotic Stress	89
Arabidopsis Mutant of SIP-428 and Basal Resistance	89
Arabidopsis Mutant of SIP-428 and SAR	91

Role of AtSRT2 in Abiotic Stress	93
Generation of SIP-428 Silenced, and Homolog Silenced Tobacco Lines.....	95
PCR Amplification of SIP-428 Silencing and Homolog Silencing Fragment	96
Cloning of SIP-428 into pDONR221 by BP Reaction	99
Isolation of pDONR221-SIP-428 Plasmid DNA.....	99
Sequencing of Entry Plasmid (pDONR221)	100
Cloning of SIP-428 (Silencing and Homolog Silencing) into pHELLSGATE8.....	102
Isolation of pHELLSGATE8-SIP-428 Plasmid DNA.....	102
Screening of SIP-428 Silenced and Homolog Silenced Transgenic Lines.....	103
Role of SIP-428 in SABP2 Expression.....	108
Role of SIP-428 in Biotic Stress Using Silenced Lines	109
SIP-428 Negatively Regulates Basal Resistance.....	109
SIP-428 Negatively Regulates SAR.....	111
Role of SIP-428 in SABP2 Dependent Signaling Pathway	113
Generation of Inducible SIP-428 Overexpressing Transgenic Lines.....	115
PCR Amplification of SIP-428 Coding Sequence.....	115
Cloning of SIP-428 into pGEMT Plasmid	116
Sequencing of Recombinant pGEMT-SIP-428-OE Plasmid.....	117
Cloning of SIP-428-OE into pER8 Plasmid	119
Verification of Destination Plasmid (pER8-SIP-428-OE)	120
Transient Expression of SIP-428 (pER8-SIP-428-OE) in <i>Nicotiana benthamiana</i>	122
Generation of Stable SIP-428 Overexpressing Transgenic Lines.....	123
Generation of T2 Generation of Stable SIP-428 Overexpressing Lines	124
SIP-428 Overexpressing Lines and Biotic Stress.....	125

Overexpression of SIP-428 Compromised Basal Resistance	125
Overexpression of SIP-428 Compromised SAR	127
Subcellular Localization of SIP-428	130
PCR Amplification of SIP-428.....	131
Cloning of SIP-428 into Entry Plasmid (pDONR221) by BP Reaction.....	133
Cloning of SIP-428 into Destination Plasmid (pSITE-2CA) by LR reaction	134
Transient Expression of SIP-428.....	136
Confocal Microscopy of SIP-428 Expression.....	138
Subcellular Fractionation of SIP-428	140
DISCUSSION	142
SIP-428 Negatively Regulates Plant Immune System	143
SIP-428 in SABP2 Signaling Pathway.....	145
Subcellular Localization of SIP-428	146
Future Directions.....	146
REFERENCES	148
APPENDIX A – Abbreviations	171
APPENDIX B – Buffers and Reagents.....	173
APPENDIX C – Figures and Tables.....	181
VITA	184

LIST OF TABLES

Table 1: List of The Non-Histone Target Proteins for De/acetylation in human	32
Table 2: Some of The Putative Non-Histone Target Proteins in Plant for De/acetylation	33
Table 3: List of Primers Used for This Study	37
Table 4: List of Primers Used for Screening of SIP-428 Silenced and Homolog Silenced.....	41
Table 5: Details of T-DNA Insertion Lines	51
Table 6: Primer Details of Arabidopsis AtSRT2 mutants	52
Table 7: List of Arabidopsis AtSRT2 primer	53
Table 8: The Bacterial Growth of <i>Pseudomonas syringae</i> pv <i>maculicola</i>	90
Table 9: The Bacterial Growth of <i>Pseudomonas syringae</i> pv <i>maculicola</i>	90
Table 10: The Bacterial Growth of <i>Pseudomonas syringae</i> pv <i>maculicola</i>	92
Table 11: The Bacterial Growth of <i>Pseudomonas syringae</i> pv <i>maculicola</i>	93
Table 12: The Bacterial Growth of <i>Pseudomonas syringae</i> pv <i>tabaci</i>	110
Table 13: The Bacterial Growth of <i>Pseudomonas syringae</i> pv <i>tabaci</i>	110
Table 14: Average Size of TMV necrotic lesion (mm).	112
Table 15: Average Size of TMV necrotic lesion (mm).	112
Table 16: The Bacterial Growth of <i>Pseudomonas syringae</i> pv <i>tabaci</i>	114
Table 17: The Bacterial Growth of <i>Pseudomonas syringae</i> pv <i>tabaci</i>	125
Table 18: The Bacterial Growth of <i>Pseudomonas syringae</i> pv <i>tabaci</i>	126
Table 19: <i>In silico</i> Analysis of SIP-428 Signal Peptide.....	131

LIST OF FIGURES

Figure 1: Schematic Diagram of The SA Signaling Mechanism.....	19
Figure 2: Proposed Pathways of Salicylic Acid (SA) Biosynthesis.....	20
Figure 3: SIR2 Deacetylase Enzyme-Mediated Reaction.....	27
Figure 4: Prediction of SIP-428 Signal Peptide Cleavage Site.....	47
Figure 5: Generation of Stable SIP-428 Transgenic Tobacco Lines	65
Figure 6: NCBI Protein Blast Analysis of SIP-428	73
Figure 7: Multiple Protein Sequence Alignment	74
Figure 8: Predicted 3D Structure of SIP-428, AtSRT2, and Human Sirtuin-4.....	75
Figure 9: Bioinformatic Analysis of SIP-428	76
Figure 10: Expression of Full-Length SIP-428.....	77
Figure 11: Colony PCR of SIP-428-72	78
Figure 12: Isolation of Plasmid DNA.	78
Figure 13: Solubility Test of SIP-428-72 Protein.....	79
Figure 14: Purification of SIP-428-72 Protein Using Ni-NTA column.....	81
Figure 15: Chromatography Profile of Protein in Mono Q column Purification.....	82
Figure 16: Purification of SIP-428-72 by Mono Q Chromatography.....	83
Figure 17: Purification of SIP-428-72 Protein From <i>E.coli</i>	84
Figure 18: SIR2 Deacetylase Enzyme Activity	85
Figure 19: Histone Deacetylase Enzyme Activity	86
Figure 20: Figure: Glutathione-S-transferase (GST) Pull-Down Assay.....	87
Figure 21: Confirmation of T-DNA Insertion in AtSRT2 Mutant	88

Figure 22: Confirmation of AtSRT2 Mutant Plant (<i>atsrt2</i>)	89
Figure 23: Bacterial Growth Assay in Arabidopsis	90
Figure 24: Bacterial Growth Assay in Arabidopsis	91
Figure 25: SAR in Arabidopsis Wild-Type Col-0, and <i>atsrt2</i> Mutant..	92
Figure 26: SAR in Arabidopsis Wild-Type Col-0, and <i>atsrt2</i> Mutant	93
Figure 27: Effect of Salinity on Chlorophyll Content	94
Figure 28: Effect of Osmotic Stress on Chlorophyll Content.....	94
Figure 29: Vector Map of pHELLSGATE8	95
Figure 30: SIP-428 cDNA Nucleotide Sequence.....	96
Figure 31: SIP-428 cDNA Nucleotide Sequence.....	97
Figure 32: Sol Genomic Blast Analysis of SIP-428.	98
Figure 33: Sol Genomic Blast Analysis of SIP-428	98
Figure 34: PCR Amplification of SIP-428.....	99
Figure 35: Colony PCR of pDONR221	100
Figure 36: Sequence Alignment of Entry Plasmid.	101
Figure 37: Colony PCR of Destination Plasmid.....	102
Figure 38: Colony PCR of Transformed Agrobacterium	103
Figure 39: RT-PCR Screening of SIP-428 Silenced and Homolog Silenced Lines	104
Figure 40: Densitometric Analysis of The Relative Expression Level of SIP-428	105
Figure 41: RT-PCR Screening of T2 Generation of SIP-428 Silenced Lines	106
Figure 42: Densitometric Analysis of The Relative Expression Level of SIP-428	106
Figure 43: RT-PCR Screening of T3 Generation of SIP-428 Silenced Plants.	107
Figure 44: Densitometric Analysis of The Relative Expression Level of SIP-428	108

Figure 45: Expression of SABP2 in The T3 generation of SIP-428 Silenced Line.....	109
Figure 46: Bacterial Growth Assay of SIP-428 Silenced Lines.	110
Figure 47: Bacterial Growth Assay of SIP-428 Silenced Lines	111
Figure 48: Systemic Acquired Resistance in SIP-428 Silenced Lines	112
Figure 49: Systemic Acquired Resistance in SIP-428 Silenced Lines	113
Figure 50: SIP-428 Regulate The SABP2 Signaling Pathway	115
Figure 51: Verified Nucleotides Sequence of Full-Length SIP-428 cDNA	116
Figure 52: Generation of Entry Plasmid For SIP-428 Overexpression	117
Figure 53: Isolation of Plasmid DNA From The Positive Entry Clones.	117
Figure 54: Sequence Alignment of pGEMT-SIP-428-OE and SIP-428 cDNA	118
Figure 55: Restriction Digestion of Entry Plasmid DNA and Destination Vector	120
Figure 56: Colony PCR Detection of pER8-SIP-428-OE.....	120
Figure 57: Isolation of Plasmid DNA.	121
Figure 58: In Frame Cloning of SIP-428-OE.	121
Figure 59: Transient Expression of SIP-428 in <i>Nicotiana benthamiana</i>	122
Figure 60: Western Blot Screening of T1 Generation of SIP-428 Overexpressing Lines.....	123
Figure 61: Western Blot Screening of T2 Generation of SIP-428 Overexpressing Lines.....	124
Figure 62: Bacterial Growth Assay of SIP-428 Overexpressing Lines	126
Figure 63: Bacterial Growth Assay of SIP-428 Overexpressing Lines	127
Figure 64: Western Blot Screening of T2 generation of SIP-428 Overexpressing Lines.....	128
Figure 65: Systemic Acquired Resistance in SIP-428 Overexpressing Lines.	129
Figure 66: Systemic Acquired Resistance in SIP-428 Overexpressing Lines	130
Figure 67: PCR Amplification of SIP-428.....	132

Figure 68: Gel Extraction of The SIP-428 Fragment.....	132
Figure 69: Colony PCR of Entry Plasmid (pDONR221-428).	133
Figure 70: Isolation of Entry Plasmid (pDONR221-428).....	134
Figure 71: Colony PCR of Destination Plasmid (pSITE-2CA-428).....	135
Figure 72: Isolation of Destination Plasmid (pSITE-2CA-428).	135
Figure 73: Colony PCR Screening of Transformed Agrobacterium	136
Figure 74: Time Course Expression of The SIP-428 Protein	137
Figure 75: Time Course Expression of PR1.	138
Figure 76: Confocal Microscopy of SIP-428 Expression.....	139
Figure 77: Confocal Microscopy of SIP-428 Expression.....	140
Figure 78: Western Blot Analysis of Subcellular Fractions	141
Figure 79: Western Blot Analysis of Subcellular Fractions.	141
Figure 80 (A-1): 35S CaMV Promoter Sequence of pHELLSGATE8 Vector.	181
Figure 81 (A-2): Sequence Alignment of SIP-428.	183

CHAPTER 1

INTRODUCTION

Plants are continuously exposed to various biotic and abiotic stresses. Being immobile, plants have evolved multifaceted and highly complex innate immunity mechanisms. Innate immunity is the first line of defense that prevents the growth and development of invading pathogens (Garner *et al.* 2016). Innate immunity has evolved in plants, resulting in a broad range of defense mechanisms against invading pathogens.

Plants have evolved various pathways to combat pathogens by restricting their entry, by sequestering and limiting their nutrient supply, or by killing them. Physical barriers such as leaf hairs, trichomes, wax, thick cell walls, cuticle and much more help to combat invading pathogens. In response to pathogen infection, various physiological changes in the plants take places such as strengthening the cell wall through lignification, suberization, and callose-deposition that prevent entry of the pathogens (Luna *et al.* 2011; Malinovsky *et al.* 2014). Callose is an amorphous, high-molecular weight β -(1, 3)-glucan polymer matrix where antimicrobial compounds are deposited (Brown *et al.* 1998). It provides a site for delivery of chemical defense molecules at the cellular sites of infection. Callose deposition is triggered during the early stage of infection by conserved pathogen-associated molecular pattern (PAMPs) of pathogens (Brown *et al.* 1998; Luna *et al.* 2011).

Pathogenic bacteria, fungi, nematodes, and oomycetes enter the plants through various routes (Melotto *et al.* 2008; Qiao *et al.* 2013). Many of these pathogens deliver virulence factor or effector molecules such as endotoxin, exotoxin, and vascular permeability factors inside the plant cell to neutralize the host defense mechanisms (Fink Jr 1993; Li *et al.* 2014).

Invading pathogens are perceived in one of two ways: the recognition of conserved distinctive signature patterns (PAMP) or molecular-associated recognition pattern or damage-associated molecular patterns by pattern recognition receptors (PRRs) present on the surface of plant cells (Choi and Klessig 2016). PRRs at the plasma membrane of cells perceive extracellular signals while cytoplasmic sensors such as ‘Nibblers’ (NB-LRR receptors) recognize cytoplasmic danger signals (Hein *et al.* 2009; Liu *et al.* 2009; Monaghan and Zipfel 2012; Heil and Land 2014). Recognition of these signals results in PTI (PAMP-triggered immunity) (Boller and Felix 2009). The induced PTI results in the production of reactive oxygen species (ROS), activation of mitogen-activated protein kinase cascade, and deposition of callose around the site of infections. PTI also results in induction, synthesis, and accumulation of plant hormones such as salicylic acid (SA) (Schwessinger and Zipfel 2008).

Some pathogens can evade the PTI, and release effector molecules (such as *Pseudomonas* type III effector AvrPtoB) inside the plant cell causing the development of effector-triggered susceptibility (ETS) (Abramovitch *et al.* 2003). ETS results in enhanced susceptibility of the host to pathogens and provides better opportunities for pathogen growth and survival. Effector molecules interact directly or indirectly with polymorphic nucleotide binding and leucine-rich repeat proteins of plant cells that result in the development of effector-triggered immunity (ETI), an amplified version of PTI immunity (Jones and Dangl 2006). ETI leads to local necrosis and apoptotic cell death collectively known as hypersensitive response (Nimchuk *et al.* 2003). Activation of the innate immune system, synthesis, and release of plant hormones (e.g., SA, ethylene, and jasmonic acid) result in activation of a robust immune response against the invading pathogens (Figure 1) (Kumar 2014; Shah 2003).

Plants activate a defense response by inducing resistance (*R*) and pathogenesis-related (*PR*) genes and by producing phenolic compounds such as phytoalexins in response to pathogen infection (Bowles 1990; Wanderley-Nogueira *et al.* 2012). *R*-genes induced the expression of PR1 proteins to confer resistance against more than one pathogen (Tai *et al.* 1999; Zhao *et al.* 2005; Gururani *et al.* 2012). Neighboring healthy adjacent cells produce phytoalexin to localize damaged and necrotic cells while PR proteins accumulate both locally in infected and surrounding uninfected cells (Jeandet *et al.* 2002).

PR protein in plants was first discovered in tobacco plants infected with tobacco mosaic virus (TMV) (Antoniw *et al.* 1980). Subsequently, these proteins were isolated from other plant species such as tomato and barley (Sels *et al.* 2008). PR proteins are low molecular weight, acid-soluble, and protease-resistant proteins (Gaffney *et al.* 1993). Production and accumulation of PR proteins in uninfected parts of plants can prevent subsequent infections (Weissmann 1991; White 1979). PR1 proteins bind to sterols and inhibit the growth of pathogen by sequestering the sterols needed by pathogens for their growth (Wanderley-Nogueira *et al.* 2012; Gamir *et al.* 2017). PR1a protein is an acidic protein that binds to ergosterols in fungal membranes causing cellular leakage. P14c in tomato is an orthologue of PR-1a and basic protein (Niderman *et al.* 1995). P14c is stored in the vacuole and released when cells damaged and lysed due to pathogen infections. P14c damages the plasma membrane before pathogen sterol biosynthesis begins (Gamir *et al.* 2017). PR2 protein possesses β -1,3-glucanase activity while PR3 possess putative chitinase activity (Legrand *et al.* 1987). SA dependent expression of PR1/2/5 has been observed in arabidopsis challenged with the biotrophic fungus *Peronospora parasitica* (Curto *et al.* 2006).

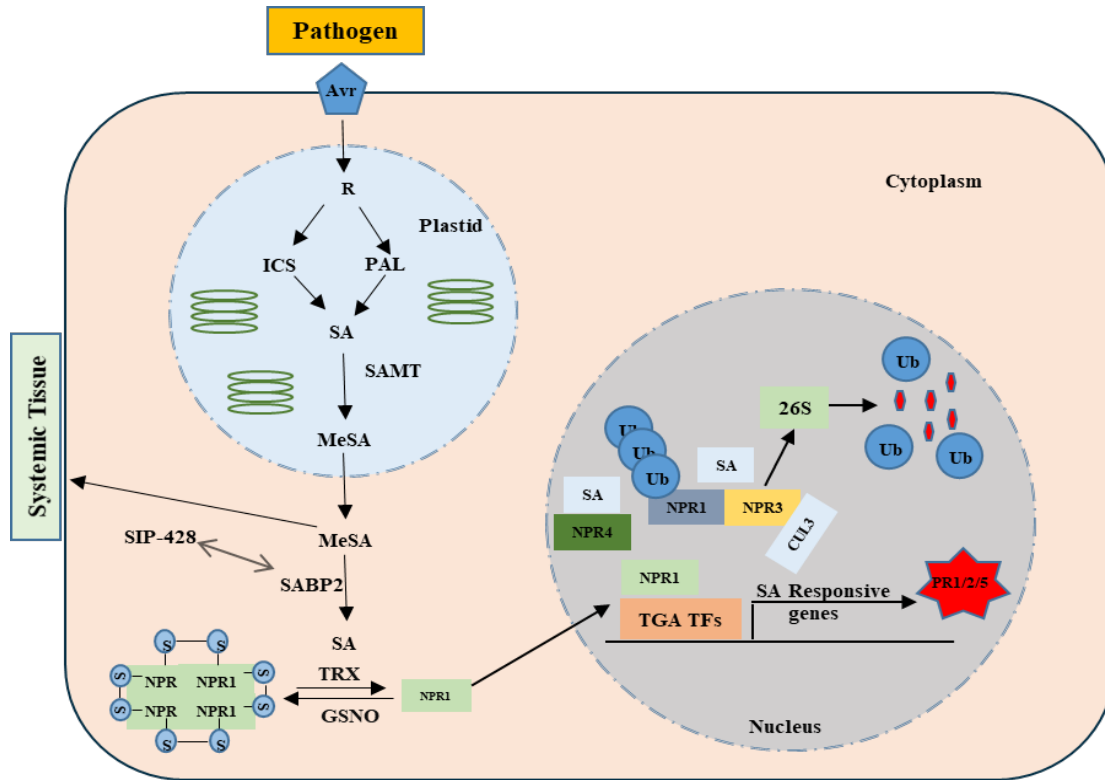


Figure 1: Schematic diagram of the SA signaling mechanism (Kumar 2014). Pathogen infection induces the synthesis of SA in plastids. SAMT converts SA into methyl salicylate (MeSA). MeSA transported to the cytoplasm. SABP2 binds and converts MeSA to active SA, which facilitates the depolymerization of the NPR1 oligomer. Free monomers of NPR1 induce the expression of SA responsive genes such as *PRI/2/5*. CUL3 mediates the degradation of NPR1.

Synthesis of SA

Primarily isochorismate synthase (ICS) and phenylalanine ammonia-lyase (PAL) mediated pathways synthesize SA in the plants (Figure 2) (Klessig *et al.* 1994; Chen *et al.* 2009). In a plant, PAL produces SA from phenylalanine. PAL is a crucial regulator of the phenylpropanoid pathway that is induced in response to biotic and abiotic stress signals (Chen *et al.* 2009). SA is synthesized from cinnamate via benzoate in tobacco and rice (Figure 2) (Leon *et al.* 1995; Silverman *et al.* 1995). ICS mediates the conversion of chorismate to isochorismate (Figure 2). Isochorismate pyruvate lyase enzyme mediates synthesis of SA from isochorismate

(Serino *et al.* 1995; Wildermuth *et al.* 2001). In plants, chorismate is synthesized in plastids by ICS (Schmid and Amrhein 1995). Arabidopsis contains two ICS genes: *ICS1* and *ICS2* (Wildermuth *et al.* 2001). Isochorismate synthase-mediated pathway is the major biosynthetic pathway of SA in Arabidopsis infected with pathogens. Mutation in either of the PAL or ICS mediated pathways resulted in defective immune responses. In Arabidopsis, an overlapping role of PAL gene in defense had been reported (Huang *et al.* 2010). Some reports had also suggested the PAL-mediated pathway as a significant source of SA biosynthesis in other plants such as tomatoes (Chadha and Brown 1974; Shine *et al.* 2016).

Most of the SA synthesized in plants modified by glycosylation or methylation or both (Klessig *et al.* 1994; Chen *et al.* 1995). Glycosylation of SA yields SA 2-O- β -D-glucoside, which is an inactive form stored in the cell's vacuole and released when needed (Dean and Mills 2004; Dean *et al.* 2005). SAMT convert SA into MeSA which is an active and volatile form of SA (Figure 1) (Rivas-San Vicente and Plasencia 2011).

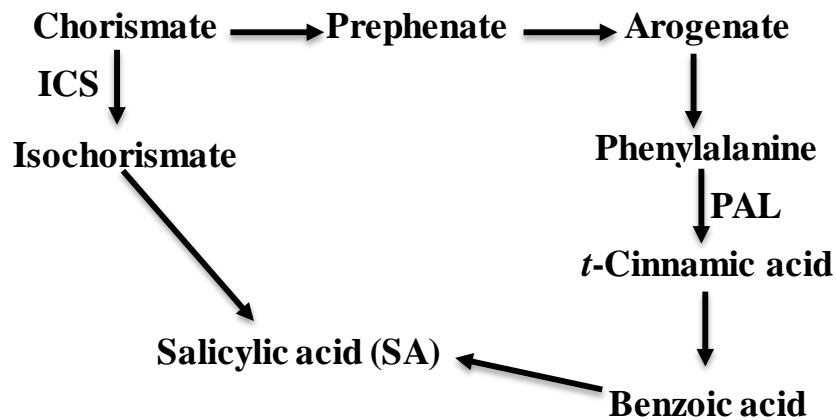


Figure 2: Proposed pathways of salicylic acid (SA) biosynthesis (Ribnicky *et al.* 1998; Chen *et al.* 2009). Isochorismate synthase (ICS) mediates the synthesis of SA from chorismate. Phenylalanine ammonia lyase (PAL) mediate the synthesis of SA from phenylalanine.

Regulation of NPR1 by SA

NPR1 is the master regulator of the SA signaling pathway that regulates 95% of SA-induced defense genes (Pajerowska-Mukhtar *et al.* 2013). SA synthesized in plastids converted into MeSA by SA carboxyl salicylic acid methyltransferase enzyme (SAMT) (Figure 1). MeSA translocate/diffuses into the cytoplasm where it interacts with SABP2. SABP2 catalyzes the conversion of MeSA into SA by its methylesterase activity increasing the concentration of SA in the cytosol (Kumar and Klessig 2003; Forouhar *et al.* 2005). High levels of SA in cytosol alter the redox potential of the cell (Mou *et al.* 2003). Change of redox potential in a cell causes dissociation of NPR1 oligomers into monomers facilitated by thioredoxins (TRXs) (Figure 1) (Tada *et al.* 2008). Monomeric NPR1 thus released then translocates to the nucleus where it interacts with TGA-bZIP (TGA-basic leucine zipper) transcription factor (Tada *et al.* 2008). This interaction induces the expression of various SA-dependent genes including *PRI/2/5* (Zhang *et al.* 1999; Zhou *et al.* 2000; Fan and Dong 2002).

A change in redox potential induced by SA also determines the sub-cellular localization and DNA binding ability of the NPR1 that induces the expression of the *PRI/2/5* gene (Zhou *et al.* 2000; Spoel *et al.* 2006). The polyubiquitination of NPR1 by CUL3, NPR3, and NPR4 depends on the level of SA (Moreau *et al.* 2012). The low level of SA results in the 26S proteasome-mediated degradation of NPR1 thereby preventing the induction of immune responses in uninfected cells (Spoel *et al.* 2006; Fu *et al.* 2012). SA prevents the proteasome-mediated degradation of NPR1 by CUL3 while abscisic acid (ABA) promotes the degradation (Ding *et al.* 2016). SA induces expression of WRKY70 and WRKY33 that are negative regulators of JA signaling (Li *et al.* 2004; Zheng *et al.* 2006). WRKY is an essential transcription factor that responds to pathogen infections and SA (Duan *et al.* 2015). An SA-mediated defense

mechanism gets activated against hemi- and biotrophic pathogens while JA-mediated defense mechanism gets activated against necrotrophic pathogens (Pieterse *et al.* 2012). S-nitrosoglutathione (GSNO) induced nitrosylation of cysteine-156 of NPR1 results in oligomerization of NPR1 (Figure 1). SA induced activation of MPK6 that acts upstream of WRKY6. WRKY6 binds directly to the promoter of NPR1 and induces expression of NPR1 (Chai *et al.* 2014). A high level of SA induces sumoylation of NPR1 that facilitate depolymerization of NPR1 and the transcriptional activation of defense-related genes (Spoel *et al.* 2009; Saleh *et al.* 2015).

TGA transcription factors belong to a group of basic region/leucine zipper (bZIP) transcription factors that are common in eukaryotes (Pontier *et al.* 2002; Kesarwani *et al.* 2007). In response to free monomeric NPR1, TGA transcription factors bind to specific canonical sequence TGACGTCA (Jakoby *et al.* 2002) and mediate SAR and *PR* gene expression (Despres *et al.* 2000; Fan and Dong 2002).

Systemic Acquired Resistance (SAR)

SAR is a long-distance defense signaling mechanism in plants that are dependent on SA accumulation. It provides robust, long-lasting, broad-spectrum, and heightened resistance to secondary infection by pathogens (Gao *et al.* 2015). SA, along with nitric oxide and ROS, is an essential downstream component of SAR (Wendehenne *et al.* 2014). Infected tissue produces SAR mobile signaling molecules such as MeSA, abietane diterpenoid dehydroabietinal, azelaic acid and glycerol-3 phosphate that travels to uninfected systemic tissues where these molecules regulate expression of various resistance genes manifesting SAR (Banday and Nandi 2015). PTI

is elicitor of SAR response, as infected tissues produce and accumulate SA at the higher level (Dong 2001).

Some putative receptors of SA are NPR1, NPR3, and NPR4 (Fu *et al.* 2012). In Arabidopsis, NPR1 transcription cofactor is required for SAR induction. Degradation of NPR1 acts as a molecular switch (Fu *et al.* 2012). Both NPR3 and NPR4 are paralogues of NPR1, which binds to SA with different affinities. On low level of SA, degradation of NPR1 depends upon NPR3 and NPR4 (Fu *et al.* 2012). The *npr3/npr4* Arabidopsis double mutants were defective in pathogen effector-triggered programmed cell death and SAR (Yan and Dong 2014).

Levels of SA in cells is maintained by salicylic acid carboxyl methyltransferase (SAMT) enzyme, which catalyzes the conversion of SA to methyl salicylate (Ross *et al.* 1999; Park *et al.* 2007; Lin *et al.* 2016). SAMT, initially isolated from petals of *Clarkia breweri*, plays an essential function in plant defense responses (Raguso and Pichersky 1995; Raguso *et al.* 1996; Dudareva *et al.* 1998). Phloem mediates transportation of MeSA to various uninfected systemic tissues (Bonnemain *et al.* 2013).

SABP2 and SIP (SABP2 Interacting Protein)

SABP2 is one of the SA binding proteins that belong to α/β hydrolase family. SABP2 is a 29 kDa soluble tobacco protein with high affinity for SA ($K_d = 90$ nM). SABP2 essential for both local immunity and SAR (Kumar and Klessig 2003; Chigurupati *et al.* 2016). SABP2 binds and converts MeSA to free SA by its methylesterase activity (Kumar and Klessig 2003; Forouhar *et al.* 2005)

NPR3 and NPR4 both bind to SA and modulate its defense function in the presence of JA. JA is involved in the defense mechanism against the necrotrophic pathogen like *Botrytis*

cinerea (AbuQamar *et al.* 2017). NPR3 and NPR4 induce SA and JA in parallel, which results in the degradation of JAZ proteins that repress JA responsive genes (Liu *et al.* 2016a). SABP2, by its esterase activity, converts MeSA to free SA altering the cellular redox potential. Change in redox potential results in depolymerization and subsequent migration of NPR1 monomers into the nucleus. NPR1 monomers induce expression of various SA-responsive genes (PR1/3/5) that result in high resistance against invading pathogens (Spoel *et al.* 2006).

The competition of different compounds (e.g., MeSA, methyl jasmonate,) with SA for binding with SABP2 influences physiological responses of a cell (Forouhar *et al.* 2005). Yeast two-hybrid library was constructed from tobacco leaf mRNA constructed and used to screen for the SABP2 interacting proteins (SIPs) (Kumar *et al.*, 2018 unpublished) that could potentially bind SABP2 and effect SA signaling pathway. Full-length SABP2 used as bait and tobacco leaf cDNA as prey (Y2H library). Several SIPs were identified including SIP-428, which shows high homology to Silent Information Regulator 2 (SIR2) family of human proteins.

Deacetylation/Acetylation in Plant Immunity

Plants have complex mechanisms for countering pathogen infections. Many of the genes responsible for defense mechanism are under epigenetic control and mediated by acetylation (van Lohuizen 1999; Zhou *et al.* 2005; Alvarez-Venegas *et al.* 2007). Two antagonistic reactions, one catalyzed by histone acetyltransferase (HAT) and another histone deacetylase (HDAC), regulate acetylation of lysine residues.

Plants have a plant-specific type II-HDAC (histone deacetylase) family of enzymes, reduced potassium dependency 3 (RPD3), HDA1, and SIR2 based on the homology to yeast counterparts (Ding and Wang 2015). Expression of *HDA19* (*HISTONE DEACETYLASE* 19) in *Arabidopsis*, which belongs to RPD3 subfamily is induced by pathogen infections, and its

overexpression increases resistance against the pathogenic fungi, *Alternaria brassicicola* (Zhou *et al.* 2005). *HDA19* represses SA-mediated defense responses in Arabidopsis (Zhou *et al.* 2005).

PR1 and PR2 are marker genes for SA-mediated basal and R gene-mediated defense against pathogen infections (Rairdan and Delaney 2002; van Loon *et al.* 2006). *HDA19* associated with promoters of PR1 and PR2 maintains repressive chromatin state under normal physiological conditions to ensure a low level of defense gene expressions (Choi *et al.* 2012).

Flagellin is the motility unit of the bacterial pathogens that serves as a molecular pattern recognized by pattern recognition receptors (PRRs) in plants (Chinchilla *et al.* 2007). Flagellin activated MAP kinases that in turn phosphorylate histone deacetylase HD2B and regulates the expressions of biotic stress response genes by modulating the H3K9ac histone (Latrasse *et al.* 2017).

Histone deacetylase701 (HDT701), is a member of the plant-specific HD2 subfamily of HDACs in rice (*Oryza sativa*). HDT701 expression changes upon infection with the fungal pathogen *Magnaporthe oryzae* (Ding *et al.* 2012). Overexpression of HDT701 caused decreased levels of histone H4 acetylation and increased susceptibility to rice pathogens. HDT701 modulates the acetylation levels of histone H4 of PRRs and defense-related genes in rice thereby negatively regulating innate immunity (Ding *et al.* 2012).

HDA6 from Arabidopsis is an RPD3-type HDAC that suppresses pathogen defense responses by inhibiting acetylation of the promoter region of defense genes including PR1 and PR2 (Wang *et al.* 2017). HDA6 was induced by treatment with the ethylene precursor ACC and JA while expression of other members of RPD3 in Arabidopsis was not reported (Zhou *et al.* 2005). HDA6 mediates the JA signaling pathway by interacting with coronatine insensitive-1,

which is F-box proteins that mediate 26S proteasome-mediated degradation of targeted protein by ubiquitination (Devoto *et al.* 2002).

Silent Information Regulator2 (SIR2)

Silent mating-type Information Regulation 2 (SIR2) or sirtuin is an NAD⁺ dependent deacetylase enzyme evolutionarily conserved from bacteria to mammals (Frye 2000). Sirtuin contains a highly conserved catalytic domain with NAD⁺ binding, metal ion (Zn⁺) binding, and substrate-binding domains. Sirtuin transfers the acetyl moiety from acetylated lysine residues of proteins to NAD⁺ via cleavage of nicotinamide glycosidic bond resulting in the formation of the unique product, O-acetyl-ADP-ribose (Figure 3) (Imai *et al.* 2000). Enzymes belonging to Nudix hydrolase family hydrolyze O-acetyl-ADP-ribose (Rafty *et al.* 2002). Sirtuin mediates this reaction, where NAD⁺ cleavage and deacetylation are directly coupled (Tanner *et al.* 2000).

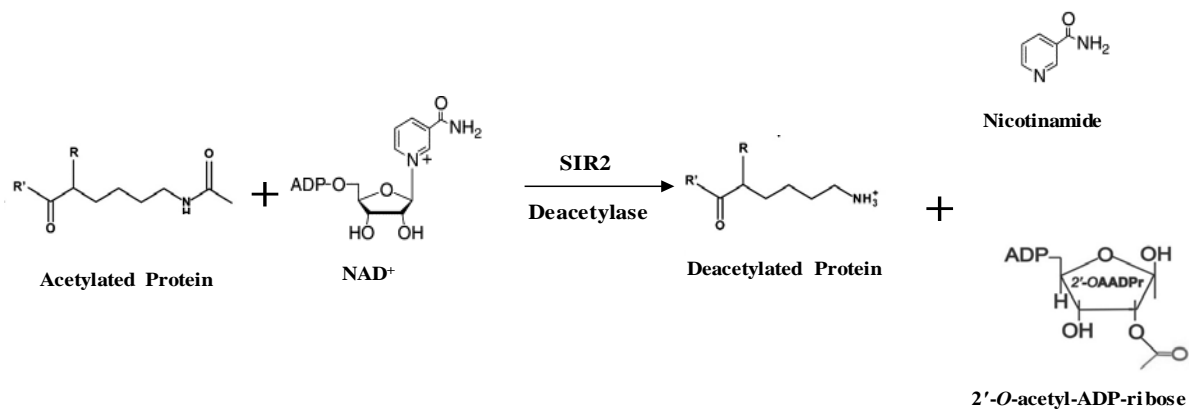


Figure 3: SIR2 deacetylase enzyme-mediated reaction (Losson et al. 2016). In the presence of NAD⁺ SIR2 deacetylase enzyme, catalyze deacetylation of proteins with acetylated lysine residues resulting in the formation of deacetylated proteins and nicotinamide and 2'-O-acetyl-ADP-ribose as a byproduct.

First reported in yeast, SIR2 is known for its anti-aging effect via caloric restriction (Lin *et al.* 2000). Calorie restriction in yeast and *Drosophila* induce expression of the nicotinamidase gene that recycles nicotinamide (Balan *et al.* 2008). Under calorie restriction, NADH levels were reduced due to high mitochondrial respiration that results in a high NAD/NADH ratio (Anderson *et al.* 2003a; Anderson *et al.* 2003b). As the inner membrane of mitochondria is impermeable to NADH and NAD, an electron translocated by the malate-aspartate shuttle system. SIR2 mediates genomic silencing at telomeres, repeated ribosomal DNA (rDNA) and mating type loci (Kaeberlein *et al.* 1999). Yeast SIR2p, not only involved in transcriptional silencing but also controlled the genomic stability of cells (Defossez *et al.* 2001).

The seven isoforms of sirtuins (SIRT1-SIRT7) found in humans and yeast has five form of sirtuins (SIR2 and HST1-4) (Brachmann *et al.* 1995). Initially, sirtuin was known for deacetylating core histone proteins, but evidence suggests possible sirtuin targets in mitochondria, cytoplasm, and transcriptional factors indicating a possible non-histone

deacetylase activity (Patel *et al.* 2004; Glozak *et al.* 2005; Yuan *et al.* 2005). The activity of sirtuin is dependent on the availability of NAD⁺ indicating a possible role of sirtuin in the fine-tuning of energy metabolism (König *et al.* 2014). The activity of sirtuin depends on the availability of NAD⁺ but not NADH, NADP⁺, or NADPH (Blander and Guarente 2004). Sirtuin is responsible for the hypoacetylation of histone H4 in rDNA sites (Hekimi and Guarente 2003). Sirtuin absence results in hyperacetylation of mating type loci, subtelomeric region, H3 and H4 histone of rDNA (Buck *et al.* 2002; Robyr *et al.* 2002).

Several compounds activate or inhibit the activity of sirtuins. Sirtinol (Sir two-inhibitor naphthol) and splitomicin inhibit NAD⁺ dependent deacetylase activity of sirtuin in Arabidopsis and yeast (Grozinger *et al.* 2001; Hirao *et al.* 2003). Nicotinamide, the product of deacetylation reactions, also inhibits the activity of sirtuins in a negative feedback mechanism (Bitterman *et al.* 2002). On the other hand, piceatannol and quercetin are potential activators of SIR1 (Howitz *et al.* 2003).

Sirtuin regulates critical cellular process such as inflammation, fine-tuning of metabolism, apoptosis, demalonylation, and desuccinylation (Poulose and Raju 2015). Embryonic developments and muscle differentiation of humans SIR1 (orthologue of SIR2) dependent (Cheng *et al.* 2003; Fulco *et al.* 2003; McBurney *et al.* 2003), suggesting a critical role of sirtuin in human health.

Sirtinol is essential for the shoot and root growth, lateral root growth, and meristem maintenance by regulating expression of crucial cell regulators of the stem, lateral root, and meristem (Singh *et al.* 2017).

Sirtuins in Plants

Information on plant sirtuin enzymes is relatively limited although in the mammalian system it has been extensively studied. The genomic sequence of *Oryza sativa* indicates two putative sirtuin proteins (Pandey *et al.* 2002; Huang *et al.* 2007; Hollender and Liu 2008; Busconi *et al.* 2009; Greiss and Gartner 2009; Aquea *et al.* 2010). One is the SRT1 protein which is a SIRT6/SIRT7-like cluster belonging to class IV, and another one is the SRT2 protein which is a SIRT4 like cluster belonging to class II of the SIR2 family (Pandey *et al.* 2002; Huang *et al.* 2007; Hollender and Liu 2008; Busconi *et al.* 2009; Greiss and Gartner 2009; Aquea *et al.* 2010). Down-regulation of *OsSRT1* increased the acetylation level of histone H3K9 on transposable elements and hypersensitive response-related genes (Huang *et al.* 2007). The absence of *OsSRT1* (a SIR2 homolog) resulted in the hyperacetylation of H3K9 (Lysine-9 of H3), decreased levels of demethylation in H3K9, increased production of H₂O₂, DNA fragmentation, and cell death (Huang *et al.* 2007). *OsSRT1* is essential for genomic stability and prevents cell damage thereby maintaining cell growth and development in rice (Huang *et al.* 2007).

Arabidopsis thaliana contains two types of sirtuins, both showing differential expression profiles. AtSRT1 is expressed predominantly in reproductive tissues while AtSRT2 is expressed in every cell (Schmid *et al.* 2005; Hollender and Liu 2008). AtSRT2 negatively regulates basal defense in Arabidopsis and is predominantly localized inside the nucleus (Wang *et al.* 2010). PAD4, EDS5, and SID2 are SA biosynthesis related enzymes responsible for the synthesis of SA in response to pathogen infection (Shah 2003). Inhibition of PAD4 (Phytoalexins deficient 4), EDS5 (Enhance disease susceptibility 5), and SID2 (Salicylic acid induction-deficient 2) are responsible for compromised basal immunity in the AtSRT2 mutant. König and colleagues (2014) showed, AtSRT2 predominantly localized in the inner membrane of mitochondria where

it interacts with various enzymes involved in metabolism (König *et al.* 2014). Hyperacetylation of ATP synthase and the ATP/ADP carrier in the absence of AtSRT2 further supports the role of AtSRT2 in fine-tuning energy metabolism (König *et al.* 2014).

AtSRT2 negatively regulates the expression of PR1 (Wang *et al.* 2010). The level of histone acetylation regulates the expression profile of PR1 in *PR1* locus of Arabidopsis and tobacco (Butterbrodt *et al.* 2006). AtHD1, an Arabidopsis histone deacetylase enzyme homolog to yeast RPD3 is nuclear protein critical for plants growth and developments (Fong *et al.* 2006).

Non-Histone Protein De/acetylation

The role of deacetylase enzymes in histone modification is well studied and important in modifying the state of chromatin and thereby regulating the expression of genes essential for cell physiology. De/acetylation an essential post-translational modification of proteins widespread in eukaryotes (Landry *et al.* 2000; Li *et al.* 2018). Protein lysine acetylation is a reversible post-translational modification important for many biological processes in organisms (Landry *et al.* 2000; Fischle *et al.* 2001; Li *et al.* 2018). Proteomic analysis of rice anther reveals 1354 lysine acetylation sites in 676 proteins important for plant reproductive developments (Li *et al.* 2018). Lysine acetylation is prevalent in a eukaryotic cell for various cellular functions.

Tumor suppressor p53 was the first non-histone protein substrate reported for sirtuin (Gu and Roeder 1997). The p300/CBP transcriptional co-activator proteins play a central role in the proliferation, differentiation, and apoptosis of cells. Histone acetyltransferase endows p300/CBP with the capacity to influence the chromatin acetylation state (Chan and La Thangue 2001). P300/CBP mediated acetylation of p53 is critical for p53-dependent functions (Luo *et al.* 2004). HDAC1 deacetylate p53 both *in vivo* and *in-vitro* (Luo *et al.* 2004). Apart from HDAC1, SIRT1,

a member of Class III HDAC deacetylate p53 thereby inhibiting its ability to activate p21, which is a cell cycle inhibitor (Luo *et al.* 2004). Inactivation of p21 results in the re-entry of the cell to the cell cycle process after successful DNA repairs. Transcriptional factors such as STAT3 (Signal transducer and activator of transcription 3), c-MYC, E2F/Rb, Smad7 (Smad family member 7), and NF- κ B are non-histone and subjected for de/acetylation (Patel *et al.* 2004; Glozak *et al.* 2005; Yuan *et al.* 2005). Similarly, α -tubulin the best-characterized cytoskeleton protein is the substrate of HDAC6 and SIRT2 deacetylase enzymes (North *et al.* 2003; Zhang *et al.* 2003).

Studies show 3,600 acetylation sites in 1,750 human proteins by high-resolution mass spectrophotometry indicating the importance of the de/acetylation process in nuclear and cytoplasmic functions (Choudhary *et al.* 2009; Johnson and Kornbluth 2012). To date, more than 100 other acetylated proteins have been identified in animal, bacteria, and yeast, which include a large number of DNA associated proteins, transcription factors, and nuclear receptors (Yang and Seto 2007). Arabidopsis contains more than 125 different acetylated proteins involved in a wide range of metabolic pathways (Finkemeier *et al.* 2011; Wu *et al.* 2011). Non-histone proteins involved in apoptosis, actin nucleation, cell cycle regulation, and chromatin remodeling are significant in cancer etiology (Choudhary *et al.* 2009). Acetylated non-histone proteins involved in the biosynthesis of lipopeptides and polypeptides including surfactin, fengycin, putative peptide, bacillibactin and bacilysin (Liu *et al.* 2016b). Acetyl-CoA and NAD⁺ are important factors of protein acetylation that regulates several enzymes activities (Xing and Poirier 2012).

Table 1: List of the non-histone target proteins for de/acetylation in human (Glozak *et al.* 2005; Kim *et al.* 2016)

	Protein
Acetylation increases DNA binding affinity	p53
	SRY
	STAT3
	GATA1
	GATA2
	E2F1
Acetylation decreases DNA binding affinity	YY1
	HMG-A1
	HMG-N2
	p65
Acetylation increases transcriptional activation	p53
	HMG-A1
	STAT3
	AR
	ER α (basal)
	GATA1
	GATA2
	GATA3
	EKLF
	MyoD
	E2F1
Acetylation decreases transcriptional activation	ER α (ligand-dependent)
	HIF1 α
Acetylation increases protein stability	p53
	c-MYC
	AR
	ER α
	E2F1
	Smad7
Acetylation decreases protein stability	HIF1 α
Acetylation promotes protein-protein interaction	STAT3
	AR
	EKLF
	Importin α
Acetylation disrupts protein-protein interaction	NF- κ B
	Ku70
	Hsp90

Table 2: Some of the putative non-histone target proteins in the plant for de/acetylation (König *et al.* 2014)

	Protein
1	gamma subunit of Mt ATP synthase
2	ATPase, F1 complex, delta/epsilon subunit
3	ADP/ATP carrier 1
4	ADP/ATP carrier 2
5	ADP/ATP carrier 3
6	ATP synthase subunit 1
7	Mitochondrial heat shock protein 70-1
8	Mitochondrial HSO70-2
9	Di- and tricarboxylate transporter

Hypothesis

Hypothesis I: SIP-428, a homolog of Silent Information Regulator 2 (SIR2), is NAD⁺ dependent deacetylase enzyme.

Hypothesis II: SIP-428 play an important role in the plant immune system.

Hypothesis III: SIP-428 is involved in the SABP2 signaling pathway.

Hypothesis III: SIP-428 is localized in mitochondria.

CHAPTER 2

MATERIALS AND METHODS

Plant Material

Tobacco plants, wild-type *Nicotiana tabacum* cv. *Xanthi-nc NN* (XNN) and *Nicotiana benthamiana*, transgenic lines #1-2 (SABP2-silenced) (Kumar and Klessig 2003), SIP-428-silenced (this study), and SIP-428 overexpression in the *N. tabacum* cv. *Xanthi-nc NN* (this study) background was used in this study. Similarly, a mutant line of *Arabidopsis thaliana* (SALK_131994C) and a wild-type (Col-0) from ABRC were also used. All the Arabidopsis and tobacco plants were grown from seeds in a controlled environment. The Arabidopsis and tobacco seeds were sown on autoclaved soil (Fafard F-15, Agawam, MA) in 4 x 4-inch square plastic pots in a plant growth chamber (PGW 36, Conviron, Canada) set at 22°C and a 16-hour light cycle maintained with a light intensity of about 200 $\mu\text{mol m}^{-2} \text{sec}^{-1}$. About 7-10 days later, individual seedlings (with two cotyledons) were transferred into 4 x 4-inch pots and grown for 3 to 4 weeks. Each young plant was then transferred to a single 7" pot (1 plant per pot) and grown for 2-3 weeks before using them for the experiments. Jack's Professional 20-10-20 Peat Lite water-soluble fertilizer was applied three days after transferring to the pot (with 100 ppm of N₂ final concentration).

Chemicals/Reagents

Sodium dodecyl sulfate (SDS), ECL western blotting substrate, magnesium chloride (MgCl₂), sodium chloride (NaCl), sodium phosphate monobasic (NaH₂PO₄), sodium phosphate dibasic (Na₂HPO₄), imidazole, methanol, ethanol, Tween-20, Triton X-100, N,N-Bis (2-(2-hydroxyethyl) glycine (Bicine), magnesium chloride (MgCl₂), sodium chloride (NaCl), sodium

phosphate monobasic ($\text{Na}_2\text{H}_2\text{PO}_4$), sodium phosphate dibasic (Na_2HPO_4), β -estradiol, bovine serum albumin (BSA), tetramethylethylenediamine (TEMED), ammonium persulfate (APS) were purchased from Thermo Scientific. Mouse monoclonal anti-poly-Histidine antibody, mouse anti myc monoclonal antibody, rabbit polyclonal anti GFP antibody. Goat anti-Mouse and monoclonal anti-rabbit, IgG γ chain specific secondary antibodies conjugated to HRP were purchased from Sigma. β -mercaptoethanol (β -ME), acetosyringone (3'5'-dimethoxy-4'-hydroxyacetophenine) were purchased from Sigma Aldrich. Agar from Acros Organics, sucrose from Bioworld, and polyvinylidene fluoride membrane (PVDF) from Millipore. Coomassie brilliant blue R-250, ponceau-stain, phenylmethylsulfonyl fluoride (PMSF), 30% acrylamide, and gel loading dye were purchased from Bio-Rad. Taq DNA polymerase and platinum pfx DNA polymerase from Invitrogen, CA. QIAprep Spin Miniprep Kit, Qiagen Plasmid Midi Kit, and Gel extraction kit were purchased from Qiagen, CA. RNase free DNase from Promega. DNA ladder from NEB. Low molecular weight (LMW) protein ladder Mono Q column purchased from GE Healthcare, Piscataway, NJ. Tobacco mosaic virus (TMV) was available in-house.

Inducible overexpression plasmid (pER8) was obtained from Dr. Nam Hai Chua, Rockefeller University, NY. Gateway cloning system was used for RNAi silencing using pDONR221 as the entry vector (plasmid), and pHELLSGATE8 was used as the destination vector (obtained from CSIRO, Australia). TOPO plasmid was purchased from Thermo Fisher, and pSITE-2CA plasmid was from TAIR.

Other Materials

Spectrophotometer (evolution), French press, ND-1000 Nanodrop spectrophotometer, Pierce® GST Spin column, ultrasonicator were from Fisher Scientific. FastPrep-24 Instrument from MP Biomedicals. HDAC Glo™ assay kit and SIRT Glo™ assay kit was purchased from Promega. HiTrap desalting column and Mono-Q column was purchased from GE Healthcare. SYNERGY HT Multi-Mode Microplate Reader (BioTek), LI-COR C-DIGIT western blot imager (LI-COR), UV transilluminator (UVP Bioimaging Systems). pH meter from Beckman. Centrifuge (Beckman, model J2-21 or Sorvall RC5B) and ultracentrifuge (Sorvall ultra speed T-865) purchased from Sorvall (Beckman). 1 ml syringes (BD Syringes), cheesecloth, and miracloth were purchased from Calbiochem. Mastercycler from Eppendorf. Other regular laboratory accessories (e.g., pipettes, microcentrifuge) were used for this research.

Oligonucleotides (Primers)

All primers used in this study were synthesized by Eurofins MWG (Huntsville, AL). Lyophilized primers were resuspended to a final concentration of 10 µM by using autoclaved nuclease-free water and stored at -20°C for further use. Primers used for RNAi silencing of SIP-428 and its homologs as well as overexpress SIP-428 listed on the table below:

Table 3: List of primers used for this study

Primer	Sequence	Purpose
T7	TAATACGACTCACTATAGGG	Sequence verification (SIP-428 protein)
M13 Forward	GTAAAACGACGGCCAG	Sequence verification (SIP-428 protein)
M13 Reverse	CAGGAAACAGCTATGAC	Sequence verification (SIP-428 protein)
DK502	AGAGCTCCTAGAGAGCAGGGATACTCA	Cloning into pET28(a) (for both full length and without signal peptide)
DK503	TGGGAGCGATCCACTTGAAT	mRNA expression (Arabidopsis)
DK504	GCATCGCTCTGTTTTGCAAC	mRNA expression (Arabidopsis)

DK505	GAGTTACGCTGGATGGAGGA	mRNA expression (Arabidopsis)
DK506	TCAGGCCTTTGTTTCATGCC	mRNA expression (Arabidopsis)
attb2-428	GGGGACCACTTTGTACAAGAAAGCTGGGTACTAGAG AGCAGGGATACTCAAGGA	Cloning full length SIP-428 into pDONR221
DK662	GGGGACAAGTTTGTACAAAAAAGCAGGCTATATGTC CATGTCTCTTCGACTTTG	Cloning full length SIP-428 into pDONR221
DK663	GGGGACAAGTTTGTACAAAAAAGCAGGCTATCGAAA GTTTGGATTATGACAGCC	Silencing Primer (gateway cloning)
DK664	GGGGACCACTTTGTACAAGAAAGCTGGGTTTTACAAT TGCAGTCGCAGC	Silencing Primer (gateway cloning)
DK665	GACACGAGCTGACGATCTTG	Screening Primer (Silencing and homolog silencing lines)
DK666	TCGAGTGTGTGGGGGTATTT	Screening Primer (Silencing and homolog silencing lines)
DK667	GGGGACAAGTTTGTACAAAAAAGCAGGCTATAGTAC CAAGCTTGTGTATTGACG	Homolog Silencing (gateway cloning)
DK668	GGGGACCACTTTGTACAAGAAAGCTGGGTTAGCAGT GAAACGTCTCCAGC	Homolog Silencing (gateway cloning)
DK669	CATATGATGTCCATGTCTCTTCGACTTTGTTGC	Cloning into pET28(a) with signal peptide
DK676	CTCCACTGACGTAAGGGATGAC	Sequence verification in pHELLSGATE8 (35S CaMV)
DK677	AAGGAAGTTCATTTCAATTTGGAGAG	Sequence verification in pHELLSGATE8 (35S CaMV)
DK682	CCTAGGTATGTCCATGTCTCTTCGACTTTG	Cloning into pER8 (SIP-428 overexpression)
DK683	ACTAGTCTAGAGAGCAGGGATACTCAAGGA	Cloning into pER8 (SIP-428 over expression)
DK690	CATATGGATAATTCCCCTTCGAATTTTTTGA	Cloning into pET28(a) without signal peptide
DK699	ATTTGGAGAGGACACGCTGA	pER8 forward primer
DK 701	GATGATACGGACGAAAGCTG	pER8 reverse primer

Bioinformatics Analysis

The full-length cDNA sequence and corresponding translated amino acid sequence of SIP-428 were analyzed using NCBI BLAST (Basic Local Alignment Search Tool) (<http://blast.ncbi.nlm.nih.gov/Blast.cgi>) and ExPASy Bioinformatics Resource Portal (<https://www.expasy.org/tools/>). The NCBI database was used to predict the conserved domain of SIP-428 (<https://blast.ncbi.nlm.nih.gov/Blast.cgi?PAGE=Proteins>). To analyze and compare with known tobacco genes, the nucleotide sequence the *SIP-428* was used to query in Solanaceae database (<https://solgenomics.net/tools/blast>). Multiple sequence alignments of full -length SIP-

428 and *Arabidopsis thaliana* were done using multi-sequence alignments of amino acids (ClustalW2; <https://www.ebi.ac.uk/Tools/msa/clustalo/>). Pymol, Swiss modeling (<https://swissmodel.expasy.org/interactive>), ITASSER (<https://zhanglab.ccmb.med.umich.edu/I-TASSER/>), and (PS) 2: Protein Structure Prediction Server (<http://ps2.life.nctu.edu.tw/index.php>) online tool was used to generate the 3D protein structure model of SIP-428. Secondary structure was predicted using the Chou-Fasman, GOR, and Neural Network online tool (<http://cib.cf.ocha.ac.jp/bitool/MIX/>). Rampage online portal was used to generate a Ramachandran plot (<http://mordred.bioc.cam.ac.uk/~rapper/rampage.php>).

The freely available online signal-peptide prediction tools, Protein Prowler (http://bioinf.scmb.uq.edu.au:8080/pprowler_webapp_1-2/), MultiLoc (<http://abi.inf.uni-tuebingen.de/Services/MultiLoc/>), TargetP 1.1 (<http://www.cbs.dtu.dk/services/TargetP/>), ChloroP (<http://www.cbs.dtu.dk/services/ChloroP/>), LOCALIZER (<http://localizer.csiro.au/>), TPpred 2.0 (<https://tppred2.biocomp.unibo.it/welcome/default/index>), and BaCellLo (<http://gpcr.biocomp.unibo.it/bacello/pred.htm>) were used to predict the presence of signal peptide and putative subcellular localization of SIP-428.

Expression of The Full-length SIP-428 Protein in *E. coli*

Cloning of SIP-428

The full-length coding region of SIP-428 was amplified from cDNA and cloned into a TOPO plasmid by using T4 DNA ligase enzyme. Cloning reaction mixture was transformed into competent Top 10 *E. coli* cells. The cDNA was synthesized from the leaf disk sample of wild-type tobacco plant (XNN) by RT PCR method as described below:

Isolation and Purification of total RNA: A total of 3 to 4 leaf disks from wild-type XNN were collected with a cork borer# 5 and frozen in liquid nitrogen. Frozen leaf disks were homogenized using a mechanical grinder. After grinding, 500 μ l of trizol reagent was immediately added to samples and mixed until it dissolved. Additional 500 μ l of trizol was added to samples to make the final volume of 1 ml. Resuspended samples transferred into 2 ml screw-cap tubes containing 0.2 ml of 2 mm zirconia beads. Samples were homogenized for 45 seconds at 4.5 power setting using FastPrep according to manufacturer's instruction with slight modification (Kasuga and Bui 2011).

Two hundred microliters of chloroform were added to homogenized samples and samples were mixed by inverting tubes vigorously for 15 seconds before incubating at room temperature (RT) for 3 minutes. Samples were centrifuged at 12,000 x g for 15 minutes at 4°C, and the aqueous phase was transferred to a new sterile 1.5 ml eppendorf tube. Five hundred microliters of isopropanol were added to the sample and incubated for 10 minutes at RT after mixing uniformly. Each sample was then centrifuged at 12000 x g for 10 minutes at 4°C, and the supernatant discarded. Ice-cold ethanol (75%) was added to resulting pellet which was resuspended by vortexing. Each sample was then centrifuged at 7500 x g for 5 minutes at 4°C, the supernatant discarded, and the tube with the pellet was air-dried for 10 minutes. Air-dried pellets were resuspended in 43 μ l of DEPC water (Appendix B), and seven microliters of DNase mix (2 μ l DNase + 5 μ l DNase buffer) was added to the mixture and incubated at 37°C for 20 minutes. The excess DNase was removed from pellets by treating it with a trizol reagent, chloroform, isopropanol, and chloroform with half the volume as described above. The resulting pellets were collected and air-dried for 10 minutes at RT. The air-dried pellets were resuspended using 20 μ l of DEPC water and incubated for 5-10 minutes at 55°C to ensure the complete

solubilization of pellet. The concentration of RNA was measured, and one microgram of RNA used for cDNA synthesis.

Synthesis of cDNA from RNA: Reverse transcriptase was used to synthesize complementary DNA (cDNA) from total RNA. Two-Step processes were used. In the first step, two microliters of oligo-dT (0.5µg/ml) were added to 8 µl (1 µg) of total RNA, and the mixture was incubated at 75°C for 10 min in a thermocycler. Samples were cooled to 4°C and 10 µl of RT mixture that consisted of 1 µl reverse transcriptase (RT) (MMLV), 4 µl 5X RT buffer, 1 µl RNAsin (RNAase inhibitor), 1 µl 10 mM dNTP, and 3 µl DEPC treated water was added. Samples were vortexed and then incubated for 60 minutes at 42°C followed by 70°C for 10 minutes in the thermocycler. The cDNA samples were then stored at -20°C for further experiments.

Reverse Transcriptase-Polymerase Chain Reaction (RT-PCR): The cDNA from wild-type XNN plants was used for RT-PCR. A 10 µl PCR reaction mixture contained 6.4 µl of DEPC water, 1 µl 10x dNTP, 1 µl 10 x Taq polymerase buffer, 0.2 µl Taq polymerase, 0.2 µl of 10 µM forward primer, 0.2 µl of 10 µM reverse primer (Table 4) and 1 µl of cDNA sample.

Table 4: List of primers used for screening of SIP-428 silenced and homolog silenced lines

Gene Names	Forward Primer	Reverse Primer
EF1 α	GTGAGCGTGGTATCACCATT	ACTTGGGGGTAGTGGCAT
SIP-428	CATATGGATAATTCCCCTTCGAATTTTTTGA	AGAGCTCCTAGAGAGCAGGGATACTCA

Transformation of Chemically Competent *E. coli* Cells

One vial of 100 µl of chemically competent cells (Top 10 *E. coli*) was thawed on ice. Two microliters of cloning reaction mixture were gently added into a vial of chemically competent cells and incubated on ice for 5 minutes, and heat shocked for 40 seconds at 42°C

(water bath). Immediately after heat shock, a sample was placed on ice for 5 minutes. Seven hundred fifty microliters of sterile super optimal broth with catabolite repression (SOC) medium (Appendix B) was added to the vial under the sterile condition. The sample was incubated in a 37°C shaker incubator at 250 rpm for 1 hour. Then, 50 µl and 150 µl aliquots of transformed bacterial cells were plated on LB plates containing 50 µg/ml of kanamycin. The plates were incubated overnight at 37°C.

Screening of Transformed Cells using Colony PCR

Colony PCR was performed on transformed cells to screen for the presence of TOPO-SIP-428 plasmid. The colony was picked and streaked on a fresh LB agar plate containing 50µg/ml kanamycin. The colony PCR mix contained 10 µl of transformed bacterial suspension in sterile water, 2 µl of PCR buffer (10x), 2 µl of dNTP (10x), 0.2 µl of Taq polymerase, 0.2 µl of vector-specific M13 forward primer, 0.2 µl of gene-specific reverse primer (DK 502) and 4.2 µl of sterile water to make a final volume of 20 µl. Thirty cycles of PCR reaction was done using a thermocycler with 94°C denaturation temperature for 30 seconds, 55°C annealing temperature for 30 seconds, 72°C extension temperature for 2 minutes, and a final extension temperature of 72°C for 7 minutes after 30 cycles. PCR amplified product was analyzed on 1.0% agarose gel.

Agarose Gel Electrophoresis

Agarose gel (1.0%) was prepared by mixing 0.5 g of agarose powder with 50 ml 1x TAE buffer (Appendix B) that was heated to dissolve agarose. After 10-15 minutes of cooling in 55°C water bath, 2.5 µl (250 µg/ml) of ethidium bromide was added to the agarose. Then, the solution was poured onto an agarose gel tray. A mixture of 8 µl of PCR product and 2 µl of 6X DNA

loading dye (Appendix B) was loaded in the wells of the agarose gel. The gel was run for 20-30 minutes at 80 volts and visualized using a UV transilluminator.

Isolation of TOPO-SIP-428 Plasmid DNA

Five positive cells (TOPO-SIP-428) were each inoculated into a 5 ml sterile LB broth with 50 µg/ml of kanamycin and incubated overnight at 37°C in a shaker (250 rpm). TOPO-SIP-428 plasmid DNA was isolated and purified using a QIAprep Spin MiniPrep Kit (Qiagen) according to manufacturer's instruction. Purified plasmid DNA was quantified using a Nanodrop and stored at -20°C for further use.

DNA Sequencing of Recombinant Plasmids

Eight microliters of purified plasmid DNA (~1000 ng) was sent for DNA sequencing to the DNA Analysis Facility at Yale University. The Sanger Sequencing method was used for sequencing the TOPO-SIP-428 construct. Ten micromols (10 µM) of M13 forward and reverse primers were used to sequence the construct.

Restriction Digestion of TOPO-SIP-428 Plasmid and Destination Plasmid (pET28a (+))

One microgram each of verified construct (TOPO-SIP-428) and pET28a (+) plasmids were digested with NdeI and SacI restriction enzymes using a cut smart buffer (NEB) at RT for 3 hrs. Two microliters of digested products were run in 1.0% agarose gel and observed under UV transilluminator to verify digestion. After verification, the remaining digested construct and destination plasmid was gel extracted and purified as described earlier. The purified product was eluted using 50 µl of warm (55°C) TE buffer, quantified, and stored at -20°C for further use.

Cloning of SIP-428 into Destination Plasmid (pET28a (+))

Digested fragments of SIP-428 from TOPO-SIP-428 constructs and digested pET28a (+) plasmids were ligated using T4 DNA ligase enzyme. The ligation mixture was incubated overnight at RT and transformed into chemically competent Top 10 *E. coli* cell by the heat shock method. Transformed cells were selected in antibiotic selection plates (kanamycin; 50 µg/ml). Colony PCR of transformed cells was performed using a pET28a (+) vector forward primer (T7 promoter) and the gene-specific reverse primer (DK 502) to screen for the positive cells. Plasmid DNA from positive destination cells (pET28a (+)-SIP-428) was extracted and quantified.

One microgram of destination plasmid (pET28a (+)-SIP-428) was transformed into chemically competent *E. coli* protein expression host (BL21-CodonPlus (DE3)-RIL) by the heat shock method (Sambrook and Russell 2006). Transformed expression cells were selected and used for expression of full-length SIP-428 proteins.

Solubility Test of Full-length SIP-428

To determine the suitable incubation temperature and the concentration of IPTG (isopropyl β-D-1-thiogalactopyranoside) that allows expression of soluble full-length SIP-428, an overnight culture from a single colony (pET28a(+)-SIP-428) grown on LB media containing 50 µg/ml kanamycin at 37°C. The overnight culture was diluted ~100 fold into fresh LB media containing 50 µg/ml of kanamycin and incubated at 37°C until OD₆₀₀= 0.6 reached. Expression of full-length SIP-428 was induced by adding a different final concentration of IPTG (10, 100 and 1000 µM) to culture and incubating at 37°C for 3 hours or 17°C for overnight (16 hrs) respectively in a shaker (250 minutes). The bacterial pellet was collected by centrifuging the bacterial culture at 3,800x g for 3 minutes at RT. Pellet was re-suspended in 200 µl of 1X Ni-

NTA lysis buffer (Appendix B) with 1mM PMSF (phenylmethylsulfonyl fluoride). Cells were broken by sonication using an ultrasonicator with 20% amplitude for 15 seconds and 2 minutes of cooling in ice. The process was repeated three times. The supernatant (soluble) and pellet (insoluble) were separated by centrifugation at 17,900x g for 15 minutes at 4°C. The pellet was resuspended in 200 µl of 1X Ni-NTA lysis buffer. Proteins from both soluble and insoluble fractions were processed and separated by SDS-PAGE. Western blot analysis was performed to look into the solubility of full-length SIP-428 using anti His tag antibody.

Sodium Dodecyl Sulfate-Polyacrylamide Gel Electrophoresis (SDS PAGE) and Western Blot

Each sample was mixed with equal volume of 2X SDS sample buffer (1:1) containing 5% of β-mercaptoethanol (β-ME). Samples were incubated in boiling water for 5 minutes and centrifuged at 17,900 x g for 10 minutes at RT. Nine microliters of the supernatant were loaded into a 12% SDS-PAGE gel and run at 20 mA until the tracking dye reached the end of the gel (~1 hour).

Before western blot, precut PVDF membrane was first soaked in 100% methanol briefly for 10 seconds and then rinsed with deionized water for 2 minutes. The membrane was then rinsed with 1X transfer buffer (Appendix B) for 10 minutes. The SDS-PAGE gel and the PVDF membrane were sandwiched between the sponge and 3mm Whatman papers and clamped tightly together after ensuring no air bubbles had been formed between gel and membrane. The protein transfer was carried out at ~94V for 1 hour at 4°C.

After transferring the proteins to the PVDF membrane, the membrane was taken out and soaked in 100% methanol for 10 seconds and air dried. Once membrane was dried, it was again soaked in 100% methanol for 10 seconds and stained with Ponceau stain (Appendix B) for 1-2

minutes at RT. After staining, the membrane was rinsed with deionized water, and the pictures were taken to verify the transfer of protein from gel to the PVDF membrane. The membrane was then washed with 1X PBS buffer 5 minutes each three times. The membrane was incubated in 5 ml blocking buffer (Appendix B) at RT for 1 hour on a shaker then washed with 1X PBS buffer 5 minutes each three times.

The membrane was incubated with anti-His tag monoclonal antibody (1:2000) in 5 ml of blocking buffer at 4°C on a platform shaker for overnight. Next day, the membrane was washed two times for 5 minutes each with 1X PBS buffer first, then with 1X PBS buffer containing 0.03% Tween 20, and finally with 1X PBS buffer. The membrane was then incubated with anti-mouse IgG peroxidase conjugate (1:5000 in 5 ml of blocking buffer) at RT for 1 hour on a shaker. The membrane was then subjected to washing as described earlier. The membrane was then incubated in the ECL substrate per the manufacturer's instructions, and the signal on the membrane was captured using a Li-COR ECL scanner.

Expression and Purification of SIP-428-72 Protein

Cloning and Expression of SIP-428-72

Full-length SIP-428 was cloned and expressed with N-terminal 6x His tag, but soluble protein was not detected. Based on the bioinformatic analysis, 72 amino acid residues of SIP-428 in N-terminal was predicted to be a signal peptide (Figure 4). To express in soluble form SIP-428 without signal peptide (SIP-428-72) was cloned into destination plasmid (pET28a(+)) using NdeI and SacI restriction enzyme as described earlier for full-length SIP-428. Transformation of the verified destination plasmid (pET28a(+)-SIP-428-72) into *E. coli* expression cell (BL21-CodonPlus (DE3)-RIL) was performed as described earlier using a different concentration of

IPTG and incubation temperature. SDS-PAGE and western blot was done to detect soluble SIP-428-72 protein.

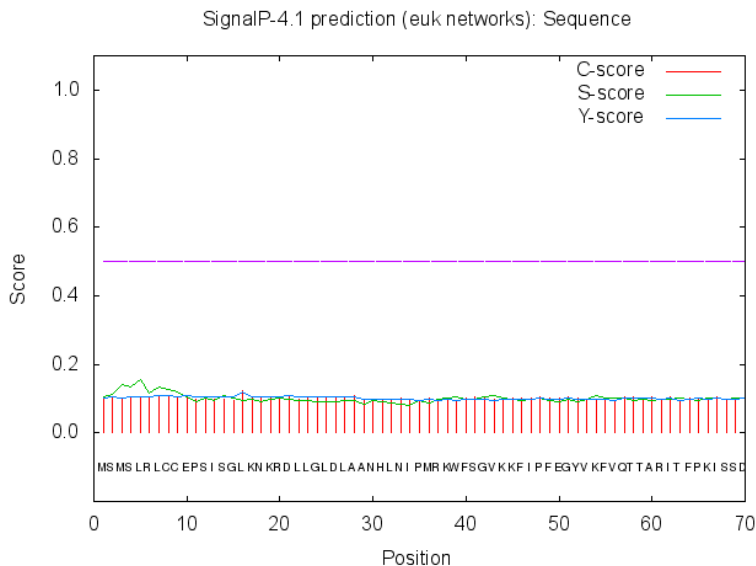


Figure 4: Prediction of SIP-428 signal peptide cleavage site. Even though the predicted signal peptide cleavage site value is below the threshold value (0.45), Signal P online software analysis predict possible 72 amino acid residue to be signal peptide of SIP-428. C-score is a raw cleavage site score, S-score is a signal peptide score, and Y-score is the geometric average of the C-score and the slope of the S-score.

Purification of SIP-428-72 Using Ni-NTA Chromatography

Ni-NTA column chromatography was used to purify the His-tag SIP-428-72 protein with modified purification protocol (Forouhar *et al.* 2005). The transformed bacterial cells containing destination plasmid (pET28a (+)-SIP-428-72) were used for further experiments.

Transformed bacterial cells were grown in the LB plate containing kanamycin 50µg/ml for overnight at 37°C. A single colony from the overnight grown culture was inoculated to 5 ml of LB broth with 50µg/ml kanamycin. The culture was grown for 12-16 hour at 37°C shaker-incubator and then diluted to fresh 50 ml LB broth (in 1:100 ratio) containing appropriate

antibiotics. Bacterial cultures were grown at 37°C (250 rpm) until OD reached to 0.4-0.6. Once the OD reached 0.4-0.6, expression of the SIP-428-72 protein was induced by adding 100 µM of IPTG (final concentration) to culture and incubated at 17°C at 250 rpm overnight. The overnight culture was centrifuged at 3485 x g for 10 minutes at 4°C to pellet the bacteria. The bacterial pellet was then resuspended in 1X Ni-NTA lysis buffer containing protease inhibitors and lysed using french-press as previously described. The cell lysate was incubated on ice for 20 minutes and centrifuged at 17,900 x g for 15 minutes at 4°C to separate soluble and insoluble proteins. Soluble SIP-428-72 protein was purified by using metal affinity chromatography (Ni-NTA).

The soluble protein extract was added to the Ni-NTA resin and incubated at 4°C for overnight with gentle shaking. Next day the flow-through containing unbound proteins was collected, and loosely bound proteins were washed using Ni-NTA wash buffer (Appendix B). Bound proteins were eluted using Ni-NTA elution buffer containing 250 mM imidazole (Appendix B). Purification of SIP-428-72 was assessed using SDS-PAGE and western blot using the monoclonal anti-His tag antibody.

Purification of SIP-428-72 Using Mono-Q

Ni-NTA fractions containing soluble SIP-428-72 were further purified using a Mono-Q anion exchange column. Ni-NTA fractions containing SIP-428-72 were pooled, concentrated, and desalted by using a bicine buffer (Appendix B) in a HiTrap desalting column (column volume 10ml). Desalted fractions were applied to a Mono-Q column (Mono-Q 5/50 GL). Unbound proteins were collected as flow through. Bound proteins were eluted with a linear gradient of 0-250mM sodium chloride in bicine buffer. The presence of SIP-428 was determined by a western blot analysis as described earlier.

Dialysis of SIP-428-72

Mono Q purified fractions (~4ml) were pooled together in a dialysis bag and dialyzed against a bicine buffer at 4°C with gentle stirring. The buffer was changed every 8 hours for three times. Dialyzed proteins were collected and analyzed by SDS-PAGE followed by western blot. Purified dialyzed protein was quantified using absorbance at 280 nm (Nanodrop) and aliquoted in 100µl to each vial and stored at -80°C for further use.

Deacetylase Enzyme Assay

The deacetylase enzyme activity of the purified SIP-428-72 protein was determined using the SIRT Glo™ assay kit according to the manufacturer's instruction. Briefly, the assay buffer, developer, and substrate were equilibrated at RT. The substrate solution was prepared by diluting the stock substrate solution with assay buffer. The SIRT-Glo™ reagent was made by adding the developer reagent to the substrate solution. SIP-428-72 was serially diluted (1 to 8 µg) in a total volume of 100 µl of assay buffer and dispensed in a 96 well plate. Then 100 µl of SIRT-Glo™ reagent was added to serially diluted SIP-428-72 protein. Three replicates of each concentration were used for this enzyme activity. Buffer without SIP-428-72 was used as a negative control. The reaction mixture was incubated at RT for 15 minutes in an orbital shaker at 500 rpm. Three independent experiments were carried out, and steady-state luminescence signal was measured to detect the SIRT deacetylase activity of SIP-428-72 by using a Microplate Reader.

HDAC Deacetylase Enzyme Assay

The deacetylase enzyme activity of the purified SIP-428-72 protein was determined using HDAC Glo™ assay kit (Promega) according to manufacturer instruction. Briefly, the assay buffer, developer reagent, and substrate were equilibrated at RT. The substrate solution was

made by diluting the substrate stock with buffer. The HDAC-Glo™ reagent was made by adding the developer reagent to the substrate solution. SIP-428-72 was serially diluted from 1 to 8 µg with total volume of 100 µl of buffer and dispensed in a 96 well plate. Then 100 µl of HDAC-Glo™ reagent was added to each well of serially diluted SIP-428-72. Three replicates of each concentration were used for this enzyme activity. Buffer without SIP-428-72 was used as a negative control. The reaction mixture was incubated at RT for 15 minutes in an orbital shaker at 500 rpm. Three independent experiments were carried out, and steady-state luminescence signal was measured to detect the HDAC deacetylase activity of SIP-428-72 by using a Microplate Reader.

GST-Pull Down Assay

Mono-Q purified SIP-428 protein was dialyzed in 1X PBS buffer. Full-length SABP2 was cloned into a pDEST15 vector by the gateway cloning method using pDONR221 as an entry plasmid. DNA sequence of pDONR221-SABP2 entry plasmid was verified by the Sanger DNA sequencing method and cloned into destination vector (pDEST15) which expressed a SABP2 protein with N-terminal GST tag. The pDEST15-SABP2 plasmid DNA was then transformed into competent BL21-CodonPlus (DE3)-RIL bacterial strain by the heat shock method. The GST-SABP2 fusion protein was expressed in the pDEST15 vector by inducing with IPTG. After inducing with IPTG, bacterial cells were harvested and resuspended in lysis buffer (1X PBS, 1% Triton X-100, 1X protease inhibitor). Cells were then sonicated three times for 10 seconds each with an amplitude of 20% with 2 minutes of cooling in ice between each sonication. Samples were kept in ice for 15 minutes and then centrifuged at 17,900x g for 15 minutes at 4°C to collect soluble proteins in the supernatant. The supernatant was transferred to a Pierce® GST Spin

column and purified according to the manufacturer's instruction using reduced glutathione. Purified SABP2 with GST tag was used for the GST pull-down assay.

For the GST pull-down assay, purified GST-SABP2 was mixed with pre-equilibrated glutathione-agarose beads (by washing five times in 1X PBS, 1% Tween-20, and protease inhibitor cocktail) and incubated at 4°C for 30 minutes. The beads were then washed with 1X PBS buffer five times to remove unbound proteins and excess GST-SABP2. Approximately 20 µg of purified SIP-428 protein was then added to beads and incubated for 30 minutes at 4°C. Following incubation, beads were washed five times to exclude unbounded SIP-428 proteins as described earlier. Beads were then treated with 1X SDS loading buffer for eluting the bound proteins. SDS-PAGE and western blot with anti-GST and anti-His tag antibody was done to detect the interaction between SABP2 and SIP-428.

Verification of SIP-428 Homolog Mutant

The homologous gene in Arabidopsis (At5g09230) to the tobacco SIP-428 was identified, and its corresponding T-DNA insertion mutants were obtained from the Arabidopsis Biological Resource Center (ABRC) (Haq 2014). Generally, T-DNA insertion causes a loss of function of the corresponding gene. The two T-DNA insertion lines were obtained from ABRC (Table 5) and used in this experiment are SALK_131994C and SALK_149295C.

Table 5: Details of T-DNA insertion lines

Seed Lines	Background	Clone Name	Insertion site	Gene Names	Locus
SALK_131994C	Col-0	pROk2	Intron	SIRTUIN2	AT5G09230
SALK_149295C	Col-0	pROk2	Exon	SIRTUIN2	AT5G09230

Confirmation of T-DNA Insertion

Confirmation of T-DNA insertion was done according to the protocol of the TAIR website. Briefly: 2-4 seeds from each seed line along with wild-type control (Col-0) were sown in a 4'x4' inch flat rack with autoclaved soil and kept in the darkroom at 4°C for 3-4 days. Seeds were then transferred to a growth chamber with 16 hrs of daylight.

Three to four-leaf disk samples (~3-5 mg) were collected from each mutant line and wild-type control in 1.5 ml micro-centrifuge tubes. A 200µl aliquot of extraction buffer (10 fold dilution of Edward's solution (Appendix B) in TE buffer (Appendix B)) was added to each tissue sample and homogenized using FastPrep homogenizer. The homogenized mixture was centrifuged at 17,900x g for 5 minutes at RT and supernatant was collected as the DNA sample. One microliter of the supernatant was used in 20 µl of PCR reaction mixture with a specific primer to analyze T-DNA insertion as described on the TAIR website. The primers used for verifying T-DNA insertion are listed in Table 6.

Table 6: Primer details of Arabidopsis AtSRT2 mutants

Name of Primers	Sequences
SALK_149295C-LP	ATGATCCGGACATTGTGCTAG
SALK_149295C-RP	ATCAGGTGATCTGAAGGCAAG
SALK_131994C-LP	CGCAGAGAGAGAACAAAATCG
SALK_131994C-RP	TTCCACATTCTGTGCTAACCC

Confirmation of SIP-428 Homolog Mutant

RT-PCR was used to analyze the AtSRT2 mutant of the Arabidopsis seed lines as described earlier. The extraction of total RNA from mutant and wild-type control (Col-0) was done by using the trizol method and cDNA was synthesized from RNA to verify the mutant lines. Primer3 software

(<http://www.bioinformatics.nl/cgi-bin/primer3plus/primer3plus.cgi/>) and OligoPerfect™ Designer (<https://tools.thermofisher.com/content.cfm?pageid=9716>) was used to generate primers to analyze the mutant lines as listed in Table 7.

Table 7: List of Arabidopsis AtSRT2 primer

Gene Names	Forward Primer	Reverse Primer	Product Size
ATSRT2	TGGGAGCGATCCACTTGAAT	GCATCGCTCTGTTTTGCAAC	354
ATSRT2	GAGTTACGCTGGATGGAGGA	TCAGGCCTTTGTTTCATGCC	324

Role of SIP-428 in Biotic Stress

Role of SIP-428 in Basal Resistance

To assess the role of SIP-428 in basal resistance, SIP-428 homolog mutants (*atsrt2*) in Arabidopsis (SALK_131994C) were used. A bacterial growth assay was done by measuring the growth of the pathogen in infiltrated leaves (Kiefer and Slusarenko 2003; Chapagai 2014). Three upper leaves of healthy *atsrt2* mutant plants and wild-type control Col-0 (3-4 week) were infiltrated with OD=0.0002 of a virulent plant pathogen, *Pseudomonas syringae* pv. *maculicola* (*Psm*) in 10 mM magnesium chloride (MgCl₂) buffer. The 10 mM MgCl₂ buffer was used as a mock or control. Three days post-infection (3 DPI), four-leaf disks from each plant were taken independently using a cork borer (size # 2) from the infected leaf and homogenized in 1 ml sterile distilled water using FastPrep with 4.5 rates for 20 seconds (3 times) and 1 minutes interval to cool down the sample in ice. A series of 10-fold dilutions in sterile water were made, and 20 µl aliquot from different dilution were plated out on LB agar plate containing 20 µg/ml of rifampicin. Plates were incubated at the 28°C incubator for 32 hrs, the number of colony forming units (CFU) were counted and multiplied by the dilution factor to get CFU/ml. The statistical

analysis was done using student t-test. Three independent experiments were carried out with multiple samples each time showing a similar pattern of results.

Role of SIP-428 in Systemic Acquired Resistance (SAR)

To assess the role of SIP-428 in SAR induction the *atsrt2* mutant and wild-type (Col-0) Arabidopsis plants were used. Bacterial growth was measured in infiltrated leaves by processing the leaf disk samples as described earlier and plated on LB agar medium with selective antibiotic (Kiefer and Slusarenko 2003).

Initially, two lower leaves of healthy *atsrt2* mutant plants and wild-type control plant (Col-0) were treated with OD=0.002 of an avirulent pathogen (*P.s tomato* DC3000 AvrRPT2). At two days post primary infection (2 DPI), three upper untreated leaves were challenged with a virulent plant pathogen *Psm* (OD=0.0002). Ten millimolar (10 mM) magnesium chloride (MgCl₂) was used as a mock control for SAR experimental setup. At 3 DPI post-secondary infection, four leaf disks were collected and processed for bacterial growth assay as described earlier and plated on LB agar plates containing 20 µg/ml of rifampicin. The number of CFU were counted and multiplied by the dilution factor to get CFU/ml. The statistical analysis was done using the student t-test. Three independent experiments were carried out with multiple samples showing a similar pattern of results.

Role of SIP-428 in Abiotic Stress

To assess the role of SIP-428 in abiotic stress, *atsrt2*, and Col-0 seeds were surface sterilized by incubating in 70% ethanol for 5 minutes followed by incubating in sterile wash solution (Appendix B) for 10 minutes. After surface sterilization, seeds were washed with sterile water at least four times and plated on half strength MS media containing 1X Gamborg vitamins

(Appendix B). Plated seeds were then kept in the dark at 4°C for two days before transferring to the tissue culture room with 16 hrs of daylight. After seven to ten-days, seedlings were transferred into half MS media containing various concentrations of stress-inducing chemicals (salt and mannitol). Surface area, root length, and chlorophyll content were measured for both mutants plants and wild-type control plant. Chlorophyll content was measured using methanol extraction method (Porra *et al.* 1989) and PhotoSynQ device as per manufacturer instruction (<https://photosynq.org/>).

Generation of RNAi Lines Silenced in SIP-428 and Homologs of SIP-428

Transgenic tobacco lines using XNN background were generated where expression of SIP-428 and its homolog altered using RNA interference (RNAi). RNA interference or RNAi term was coined by Fire and coworker in 1998 (Fire *et al.* 1998). A Gateway cloning system was used to generate RNAi constructs. RNAi is an important process that is involved in the degradation of mRNA, post-transcriptionally, in a sequence-dependent manner (Fire *et al.* 1998). The RNAi technique is advantageous, as it allows production of a foreign transgene in the host cell that targets specific endogenous gene (mRNA). It does not produce a biologically active foreign protein (Montgomery *et al.* 1998; Dutta *et al.* 2015). The RNAi technique was utilized in many molecular studies to characterize critical genes both *in vitro* (cell cultures) or *in vivo* (model organisms) (Bertil 2006). Gateway cloning primers were designed, with attB1 and attB2 sites (Table 3) that were used for amplifying the conserved region of SIP-428 from a verified plasmid (TOPO-SIP-428-1) that was specific in SIP-428 sequence (Figure 30) or the region that is shared between its homolog (SIP-428 homolog silencing) (Figure 31).

PCR products were then gel purified and cloned into a Gateway entry vector (pDNOR221) by using a BP clonase enzyme. DNA sequence of the entry plasmid was verified by sending plasmid DNA sample for Sanger DNA sequencing. The verified entry plasmid was subcloned into destination plasmid (pHELLSGATE8) by performing LR reaction catalyzed by LR clonase enzyme. The positive destination plasmid with SIP-428 sequence (pHELLSGATE8-SIP-428) was extracted and transformed into competent *Agrobacterium tumefaciens*. Transformed *Agrobacterium* was used for transformation of wild-type tobacco plants (XNN) via the leaf disk method to generate stable transgenic lines (Burow *et al.* 1990).

A pHELLSGATE8-SIP-428 construct was used to express double-stranded RNA (SIP-428 specific sequence) under the control of 35S CaMV promoter in a plant cell (Wielopolska *et al.* 2005). Double strand RNA generated from pHELLSGATE8-SIP-428 was then incorporated into an active RNA-induced silencing complex (RISC). Thus formed guide strand of RNA-RISC complex then base-pairs with the complementary mRNA target sequences resulting in the endonucleolytic cleavage. Endonucleolytic cleavage was induced by argonaute protein (catalytic component of the RISC complex). Cleavage of a targeted sequence of specific mRNA prevents the translation of targeted transcript (gene) (Tang *et al.* 2003; Henderson *et al.* 2006; Axtell 2013; Borges and Martienssen 2015). Transformed plant cells (T1 generation) were selected using 300µg/ml kanamycin and 100µg/ml cefotaxime in selection media.

PCR Amplification of SIP-428 Silencing and Homolog Silencing Fragment

The coding sequence of SIP-428 was used in sol genomics database (https://solgenomics.net/help/gene_search_help.pl) to query conserved sequences of SIP-428 gene in the *Nicotiana tabacum*. A sequence of 304 base pair (bp) was identified as specific for

SIP-428 by BLAST analysis (<https://solgenomics.net/tools/blast/>). Similarly, a sequence of 100 bp was identified to be shared among SIP-428 homolog genes. Primers were designed for the Gateway cloning system as described earlier.

PCR amplification of silencing and homolog silencing fragments with gateway cloning primers (Table 3) were done independently using verified full-length SIP-428 plasmid (TOPO-SIP-428-1). A 30 μ l PCR reaction mixture was made which consisted 22.2 μ l of sterilized water, 3 μ l of PCR buffer (10 X), 0.6 μ l of dNTP (50 X), and 3 μ l of template (1 ng-1 pg / 50 μ l reaction), 0.6 μ l of Advantage HF polymerase (50 x) and 0.6 μ l of forward and reverse primers. Thirty cycles of PCR reaction were carried out with denaturation temperature set at 94°C for 30 seconds, an annealing temperature of 55°C for 30 seconds, an extension temperature of 72°C for 1.5 minutes, and a final extension temperature of 72°C for 7 minutes. PCR product was stored on ice at 4°C for further experiments.

Agarose Gel Electrophoresis and Gel Extraction

Two microliters of PCR product was run on a 0.05 % ethidium bromide (EtBr) stained agarose gel and detected by UV-transilluminator to verify amplification of the desired product. After verification the remaining 48 μ l of PCR product was run on agarose gel with 0.05% Ethidium bromide (EtBr) and gel purified. The purified product was eluted using 50 μ l of warm TE buffer (55°C) and quantified.

Cloning of SIP-428 (Silencing and Homolog Silencing) into pDONR221

Purified gel extracted PCR product was used for a BP cloning reaction with BP clonase enzyme. The reaction mixture consisted of 1 μ l of the entry plasmid (150 ng of pDONR221), 1 μ l of BP clonase enzyme, 150 ng of the purified SIP-428 fragment and TE buffer was added to

make a final volume of 10 μ l. The reaction was incubated at 37°C for two hours and stopped by adding 1 μ l proteinase K. Two microliters of the reaction mixture was transformed into chemically competent Top 10 *E. coli* cell by the heat shock method. Transformed Top10 *E. coli* cell were selected in LB agar plate containing kanamycin (50 μ g/ml) and incubated at 37°C overnight. Transformed cells were screened by colony PCR as previously described.

Isolation of pDONR221-SIP-428 Plasmid DNA

Five positive clones containing pDONR221-SIP-428 construct for both silencing and homolog silencing were inoculated into 5 ml of fresh LB broth containing 50 μ g/ml of kanamycin and incubated at 37°C overnight at 250 rpm. The pDONR221-SIP-428 plasmid DNA was isolated, purified, quantified, and stored at -20°C for further use. One microgram of plasmid DNA was sequenced by the Sanger DNA sequencing method (DNA Analysis Facility at Yale University) using an M13 forward primer (Table 3).

Cloning of SIP-428 (Silencing and Homolog Silencing) into pHELLSGATE8

Verified entry plasmid containing SIP-428 fragment for silencing and homolog silencing was subcloned into the destination plasmid pHELLSGATE8 by the LR reaction. The reaction mixture consisted of 1 μ l of pHELLSGATE8 (150 ng/ μ l), 1 μ l of LR clonase enzyme, 150 ng of pDONR221-SIP-428 plasmid DNA and 7 μ l of TE buffer (pH 8.0) to make a final volume of 10 μ l reaction. The reaction mixture was incubated at RT overnight and terminated by adding 1 μ l proteinase K (2 μ g/ μ l). Two microliters were transformed into chemically competent Top 10 *E. coli* cells by the heat shock method. Transformed Top10 *E. coli* cells were selected on LB agar plate containing spectinomycin (50 μ g/ml).

Isolation of pHELLSGATE8-SIP-428 Plasmid DNA

Transformed cells were screened for the presence of pHELLSGATE8-SIP-428 plasmid by colony PCR using screening primer (Table 3). Plasmid DNA from positive cells for silencing and homolog silencing were extracted, purified, quantified, and stored at -20°C for further use.

Transformation of pHELLSGATE8-SIP-428 Silencing and Homolog Silencing Plasmid into Competent *Agrobacterium tumefaciens*

Two microliters of plasmid DNA for SIP-428 silencing and SIP-428 homolog silencing was transformed into 20 µl of each electro-competent *Agrobacterium tumefaciens*. The mixture of competent *Agrobacterium* and plasmid DNA (pHELLSGATE8-SIP-428) was transferred to 0.2 cm electroporation cuvette. The cells were electroporated using a pulse of 2.20 kV (kilovolts) for 5.4 milliseconds, and 1 ml of YEB media (Appendix B) was added to the electroporated cells. Cells were transferred into a sterile eppendorf tube and incubated at 28°C for 3-4 hours. Fifty microliters of cells were plated on LB agar plate with 100µg/ml spectinomycin and incubated overnight at 28°C.

Screening of Transformed *Agrobacterium*

Transformed *Agrobacterium tumefaciens* was screened for the presence of pHELLSGATE8-SIP-428 plasmid by colony PCR. Vector-specific forward primer (DK 677: 35S CaMV promoter sequence in Appendix C: A-1) and gene-specific reverse primers (DK 666) were utilized to check for the silencing and homolog silencing construct respectively. A master plate of the transformed *Agrobacterium* was made for further experiment, and 10% glycerol stock was made for future work.

Generation of Inducible SIP-428 Overexpressing Transgenic Lines

Inducible transgenic lines overexpressing SIP-428 were generated using pER8 plasmid. The pER8 plasmid is an estrogen receptor-based chemical inducible system comprising of a chimeric transcriptional activator XVE (LexA-VP16-ER), assembled by fusing the DNA binding domain of the bacterial repressor LexA, an acidic transactivating domain of VP16, and a regulatory region of the human estrogen receptor (Zuo *et al.* 2000). A c-myc tag was added for easy detection. The transactivating activity of the chimeric XVE factor whose expression is controlled by the strong constitutive promoter G10-90 regulated by estrogen (Guo *et al.* 2003; Zuo *et al.* 2000). It is highly desirable to express genes controllably in plants research and biotechnological applications (Zuo *et al.* 2000). Use of an inducible system allows flexibility for studying the functions of genes whose expression is developmental specific or tissue specific (Zuo *et al.* 2000).

Cloning of SIP-428 into pER8 Plasmid

Full length of SIP-428 along with stop codon was used. AvrII and SpeI restriction enzymes sites were incorporated on N and C terminal, respectively, of the primers specific for amplifying SIP-428 (Table 3). SIP-428 overexpression fragment was amplified from a verified plasmid (TOPO-SIP-428-1) by PCR amplification method. The amplified product was gel extracted, purified, and quantified.

The SIP-428 fragment was cloned into a pGEMT-Easy vector (50 ng/μl) using T4 DNA ligase (3 Weiss units/μl). The ligation mixture was incubated at 28°C for 1 hour and transformed into the chemically competent Top 10 *E. coli* cells by the heat shock method. Transformed cells

were selected using 100 µg/ml of ampicillin. Transformed cells were screened by colony PCR using T7 promoter forward primer (Table 3) and gene-specific reverse primer (DK 502).

Plasmid DNA from positive cells was extracted and quantified. One microgram of plasmid DNA was sequenced using the Sanger DNA sequencing method (DNA Analysis Facility at Yale University). One microgram of the verified entry plasmid (pGEMT-SIP-428) and pER8 plasmid were digested using AvrII and SpeI restriction enzymes separately. The Digested fragment and plasmid DNA was gel extracted, purified, quantified, and stored at -20°C independently for further use.

The digested SIP-428 fragment from pGEMT-SIP-428 construct was ligated with the digested pER8 plasmid using T4 DNA ligase enzyme and transformed into chemically competent Top 10 *E. coli* cells by the heat shock method. Transformed cells were selected on LB agar plate containing 100 µg/ml of spectinomycin. Colony PCR of transformed clones using pER8 plasmid forward primer (Table 3) and the gene-specific reverse primer (DK 502) were performed. Plasmid DNA (pER8-SIP-428) from positive clones was extracted and quantified. One microgram of plasmid DNA was sequenced by the Sanger DNA sequencing method (DNA Analysis Facility at Yale University).

Preparation of Competent *Agrobacterium tumefaciens* LBA4404

The *LBA4404* strain of *Agrobacterium* was streaked from -80°C stocks onto an LB agar plate containing rifampicin (20 µg/ml) and incubated at 28°C for 48 hrs. A single colony from bacterial culture was added to 5 ml of LB broth with 20 µg/ml of rifampicin and grown at 28°C (250 rpm) overnight. The overnight culture was subcultured into 100 ml of LB broth (1:100 dilution) and incubated at 28°C shaker incubator (250 rpm) until a 1.0 OD was reached. Cells

were centrifuged at 2000x g for 10 minutes at 4°C. The supernatant was discarded, and the pellet was resuspended in 5 ml of ice-cold 20 mM calcium chloride solution. Cells were again centrifuged at 2000x g for 5 minutes at 4°C. Resulting pellets were resuspended in 1 ml of ice-cold 20 mM calcium chloride, then 100 µl were aliquoted into sterile 1.5 ml Eppendorf tubes containing 11 µl of 100% sterile glycerol and snap frozen in liquid nitrogen. Glycerol stock of chemically competent *Agrobacterium* was stored at -80°C for further use.

Transformation of the pER8-SIP-428 Plasmid into Competent *Agrobacterium*

Two microliters of verified plasmid for overexpression (pER8-SIP-428) was transformed into 100 µl of chemically-competent *Agrobacterium* by the heat shock method. Transformed cells were selected in LB agar plates containing 100 µg/ml spectinomycin and streptomycin. Transformed *Agrobacterium* was used for both transient expression and generation of stable SIP-428 overexpressing transgenic lines.

Transient Expression of SIP-428 in *Nicotiana benthamiana*

Expression of SIP-428 protein with the c-myc tag was tested by transiently expressing verified clones (pER8-SIP-428) in *N. benthamiana*. Transformed *Agrobacterium* was inoculated into 5 ml of LB broth containing 100 µg/ml spectinomycin and streptomycin and incubated overnight at 28°C (250 rpm). Saturated overnight culture was sub-cultured in 20 ml LB broth (1:100 ratio) with 100 µg/ml spectinomycin and streptomycin, 20 µM acetosyringone, 500 µl of 10 mM MES (pH 5.5), and incubated overnight at 28°C (250 rpm). After overnight incubation, the bacterial culture was harvested by centrifugation at 2000x g for 10 minutes at 4°C. The bacterial pellet was resuspended and washed twice with infiltration buffer (Appendix B). Bacterial cells were resuspended in infiltration buffer containing 150 µM acetosyringone to a

final OD of 0.6. The conical flask containing bacterial culture was incubated at RT (250 rpm) for 2-4 hrs at dark. The bacterial suspension was infiltrated on the abaxial side of the *N. benthamiana* leaves by 1 ml of a needleless syringe. Infiltrated plants were kept in a growth chamber shelf with continuous light (150-200 $\mu\text{E}/\text{m}^2/\text{sec}$) for 24 hrs. After 24 hrs, each leaf infiltrated with pER8 -SIP-428 were sprayed with 50 μM β -estradiol in 0.01% Tween-20 solution in a chemical hood to induce SIP-428 expression. After induction, infiltrated plants were returned to the shelf with continuous light. After 24 hrs, leaf disks samples (cork borer# 6) were collected to detect SIP-428 expression.

Collected leaf disk samples were snap frozen in liquid N_2 and homogenized using a mechanical homogenizer. After grinding, 100 μl of 1X SDS sample buffer containing β -mercaptoethanol was added to sample, resuspended, and incubated in boiling water for 5 minutes followed by centrifugation at 17,900 x g for 10 minutes in RT. Nine microliters of samples were run in SDS-PAGE gel along with positive control (pER8-SABP2). SDS-PAGE and western blot using anti-myc antibody was done to detect SIP-428 expression.

Generation of Stable Transgenic Tobacco Lines with Verified pER8-SIP-428 and pHELLSGATE8-SIP-428 Plasmid in Agrobacterium

Plant transformation was done by the leaf disk method (Figure 5). Verified *Agrobacterium* cells for SIP-428 silencing, homolog silencing, and overexpressing were grown in LB media with 100 $\mu\text{g}/\text{ml}$ of spectinomycin and streptomycin at 28°C (250 rpm) for two days. Cultures were diluted in 1:1 ratio using fresh LB. Twenty milliliters of each diluted cultures were transferred independently into 50 ml sterile Falcon tube.

Four whole young leaves from wild-type tobacco plants (XNN) were collected. Surface sterilization of leaves was done by submerging leaves in a solution containing 20% (v/v) commercial bleach and 0.1% Tween-20 for 5-10 minutes. Leaves were then rinsed three times with sterile water to remove the traces of bleach solutions. About 50 leaf disks were collected for each construct from the surface-sterilized leaves using a sterile cork borer# 5. These 50 leaf disks were submerged into each *Agrobacterium* cultures (SIP-428 silencing, homolog silencing, and overexpressing) and incubated at RT for 30 minutes with continuous shaking (~250 rpm).

After incubation, leaf disks were blotted with a sterile paper towel to remove excess media and then leaf disks were placed on plates with shoot inducing media (SIM) (Appendix B) with no antibiotics in an inverted position. These plates were incubated at 23°C in the dark for two days. After two days the disks were taken out from SIM media and submerged in 20 ml of MS media containing carbenicillin (100 mg/ml) and 3% sucrose with continuous shaking for 2 hours at RT. These leaf disks were then placed on SIM containing carbenicillin (100 µg/ml) and hygromycin (20 µg/ml) for pER8-SIP-428 or kanamycin (300 µg/ml) for pHELLSGATE8-SIP-428 (silencing and homolog silencing) for selection. The plates were incubated at 23°C with 16 hrs of daylight and allowed to grow until callus was formed. Once a shoot in SIM media was long enough (roughly 2 inches in length), shoots were transferred into a root-inducing media (RIM) (Appendix B) with a selective antibiotic (20 µg/ml of hygromycin for pER8-SIP-428 and 200 µg/ml of kanamycin for pHELLSGATE8-SIP-428 (silencing and homolog silencing)) for selection. Rooted plants were transferred to the soil as shown in Figure 5.

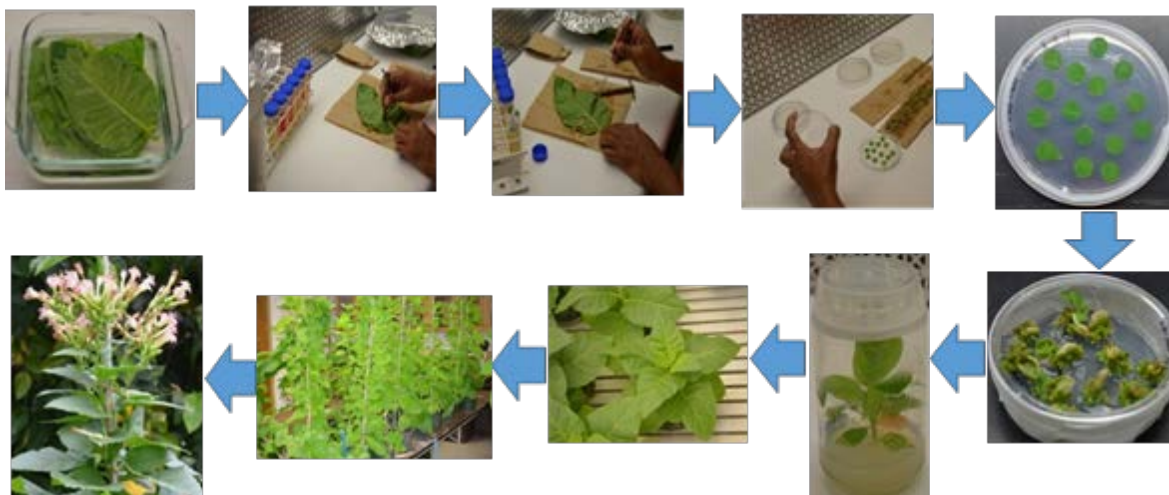


Figure 5: Generation of stable SIP-428 transgenic tobacco lines by leaf disk method.

Screening of SIP-428 Silenced and Homolog Silenced Transgenic Lines

SIP-428 silenced, and homolog silenced lines were screened by RT-PCR (Reverse Transcriptase PCR) which involve the isolation of total RNA from each independent transgenic lines followed by the synthesis of cDNA. Expression of SIP-428 in each transgenic silenced line was detected by PCR amplification method using the primer as listed in Table 4.

Screening of T2 and T3 generation of SIP-428 silenced lines were done similarly as that of T1 generation. The T2 generation plants were germinated in half MS plate with 200 $\mu\text{g/ml}$ of kanamycin using the seeds from verified T1 generation lines. Seeds from XNN control (wild-type) and SIP-428 silenced lines were surface-sterilized by incubating in 70% ethanol for 5 minutes followed by incubation in wash solution (Appendix B) for 20 minutes with intermittent shaking at RT.

After surface sterilization, seeds were washed with sterile water at least four times and plated on half strength MS media containing 1X Gamborg vitamins. For T2/T3 SIP-428 silenced

lines, half strength MS media with 1X Gamborg vitamins and 200 $\mu\text{g/ml}$ of kanamycin was used for selection. Plated seeds were kept in the dark at 4°C for two days and then transferred to the light shelves in the tissue culture room with 16 hrs of daylight. Seedlings (~10-15 days old) were then transferred to 4'X 4' flat rack with autoclaved soil and covered with a transparent cover to maintain humidity. Three to five days later covers were removed, and seedlings were allowed to grow up to 5-6 leaf stage.

Leaf disk samples collected from each transgenic line along with 2-3 wild-type controls and total RNA was extracted. The cDNA was synthesized from total RNA by RT-PCR. The reduction in the degree of SIP-428 expression in a T2 generation lines was analyzed by PCR amplification of SIP-428 using cDNA of T2 generation lines. Seeds from the T2 generation of SIP-428 silenced lines were collected. As the degrees of SIP-428 silencing in T2 generation lines were a variable, seeds from T2 generation lines were collected to germinate T3 generation lines. T3 generation of SIP-428 silenced lines were used for the further experiment.

Screening of SIP-428 Overexpressing Transgenic Lines

SIP-428 overexpressing transgenic lines were screened by inducing leaf disk samples with 50 μM of β -estradiol in 0.01% Tween-20 solution. Two leaf disks were collected with cork borer# 6, and leaf disks were induced with 50 μM of β -estradiol for 24 hr with continuous light. After induction leaf disks samples were grounded with a mechanical grinder and processed with 100 μl of 1X SDS. Western blot analysis using an anti-myc tag antibody was done to screen the positive t1 generation of SIP-428 overexpressing lines. Positive lines were grown to collect the seeds for a T2 generation.

Seeds from T1 generation lines were grown on soil for germination. Seedlings were transferred to 4'x4' flat rack and grown until the 4-5 leaf stage. The screening of T2 generation of SIP-428 overexpressing lines using leaf disk was done as described earlier for T1 generation using anti-myc tagged antibody. Positive lines of T2 generation of SIP-428 overexpressing lines were used for further experiments.

Role of SIP-428 in Biotic Stress

Role of SIP-428 in Basal Resistance

To understand the role of SIP-428 in basal resistance, the T3 generation of SIP-428 silenced, and T2 generation of SIP-428 overexpressing lines was used along with wild-type control (XNN) in the bacterial growth assays. The same methodologies used as in the Arabidopsis model system, but *P. syringae* pv *tabaci* (*Pst*) was used in place of *Psm* as a virulent pathogen in a 4-6 week of healthy plants. Three days post-infection (3 DPI), five leaf disk samples were taken using cork borer# 4 from the infected leaf of each line. Leaf disk samples were homogenized separately in 1 ml sterile water using FastPrep with 4.5 rates for 20 seconds (3 times) with 2 minutes of cooling in ice. The homogenized samples were serially diluted in a series of 10 fold dilutions in sterile water, and a 20 µl aliquot from each different dilution were plated on LB agar plate with 20 µg/ml of rifampicin antibiotic. Plates were incubated at 28°C for 32 hrs. The number of *Pst* CFU counted and multiplied by the dilution factor to get CFU/ml. Three independent experiments were carried out with multiple samples each time showing a similar pattern of the results. Statistical analysis was done using the student t-test (P<0.05).

Role of SIP-428 in SAR

To assess the role of SIP-428 in SAR induction, the T3 generation of SIP-428 silenced, and T2 generation of SIP-428 overexpressing lines was used along with wild-type control (XNN). TMV virus method was used with slight modification (Forouhar *et al.* 2005; Park *et al.* 2007). Three lower leaves of 4-6 week healthy plants were treated with 10 µg/ml concentration of TMV virus in 25mM Phosphate buffer (pH 7.2) using carborundum (abrasive powder). Seven days later, 3-4 upper uninfected leaves were treated with 1 µg/ml concentration of TMV virus. Five days after the secondary infection, the size of TMV necrotic lesion in upper treated leaves (secondary infection) of plants was measured with a caliper.

Subcellular Localization of SIP-428

The gateway cloning system was used to generate pSITE-2CA plasmid expressing SIP-428 with GFP tag in the N-terminus. The full-length SIP-428 coding sequence along with attB site was PCR amplified using gateway cloning primer (DK662 and attB2-428: Table 3). PCR amplification was conducted using Platinum Pfx DNA polymerase.

PCR products containing full-length SIP-428 were gel extracted, purified, and quantified. Purified SIP-428 was cloned into a pDONR221 plasmid by BP reaction. Two microliters of BP reaction mixture was transformed into 100 µl of chemically competent Top 10 *E. coli* cell by heat shock method and screened by colony PCR. Vector-specific (DK 551) and gene-specific (DK 662) primers were used for colony PCR. Plasmid DNA from positive entry clones was isolated and sequenced by Sanger DNA sequencing method (DNA Analysis Facility at Yale University).

SIP-428 was subcloned into a destination plasmid (pSITE-2CA) by an LR reaction. LR reaction mixture was incubated overnight at RT, and 2 μ l of LR reaction mixture was transformed into chemically competent Top 10 *E. coli* cells by the heat shock method. Transformed cells were screened by colony PCR using vector-specific (DK 677) and gene-specific (DK 502) primers. Plasmid DNA from the positive destination clones (pSITE-2CA-SIP-428) was extracted, purified, and transformed into competent *Agrobacterium tumefaciens* by the heat shock method.

Time Course Expression of SIP-428

Transformed *Agrobacterium* with pSITE-2CA-428 construct was used for transient expression in *N. benthamiana* as described earlier. Two leaf disk samples with cork borer #6 were collected from the infiltrated leaf at different time point post-infection to evaluate the expression level of SIP-428. SDS-PAGE and western blot analysis using anti-GFP primary antibody was done to detect the expression level of SIP-428 in *N. benthamiana*.

Confocal Microscopy

Confocal microscopy of SIP-428 was performed using a Leica TCS SP8 confocal microscope. Based on the time course expression of SIP-428, leaf disk samples from *N. benthamiana* infiltrated with pSITE-2CA-SIP-428 were collected and observed under the confocal microscope from the abaxial side.

Green-fluorescent protein (GFP) from jellyfish *Aequorea victoria* can be expressed under the control of a strong constitutive promoter to express stable recombinant GFP protein without exogenous substrate and cofactors (Sheen *et al.* 1995). GFP emits bright green fluorescence that is visible when excited with UV or blue light, even in the presence of red chlorophyll

autofluorescence from chloroplasts, using a fluorescence microscope (Jones *et al.* 2013). A GFP expression system could be used for monitoring gene expression, co-transfection, transformation, protein trafficking, and localization in higher plants (Sheen *et al.* 1995).

The GFP was excited using 488 nm laser light and image was acquired and exported as TIFF files. Image analysis was conducted using Photoshop and Imaris software (BITPLANE an Oxford Instrument company)

Subcellular Fractionation

Transient expression of SIP-428 with N-terminal GFP tag (pSITE-2CA-428), and N-terminal myc tag (pER8-SIP-428) was done in *N. benthamiana*. For the pER8-SIP-428 transfected plant, the expression of SIP-428 was induced by treating the plants with 50 μ M β -estradiol. Treated leaf samples were collected after 24 hrs for subcellular fractionation. Two leaf disks with cork borer # 6 were taken as a total protein sample which was flash frozen in liquid N₂ and stored at -80°C for further use.

All experiments were carried out at 4°C. Leaves from the infiltrated plants were harvested, weighed, washed in deionized water and deveined before cell fractionation. Leaves equivalent to 2-2.5 gm were homogenized in 10 mL grinding buffer (Appendix B) using an ice-cold sterile mortar and pestle. The homogenate was filtered through 4 layers of cheesecloth and one layer of miracloth. The resulting homogenate was centrifuged at 100 x g for 2 minutes to remove the unbroken cells.

The supernatant was transferred to new tubes and centrifuged at 600 x g for 10 minutes to sediment nuclei. The nuclei pellet was resuspended in 1-2 ml of grinding buffer and again

centrifuged at 600x g for 10 minutes. Washing of nuclei fraction using grinding buffer was repeated three times before collecting nuclei fraction for further experiments. Supernatant from nuclei fraction (not from the wash) was transferred to new tubes and centrifuged at 2420 x g (SS 34 rotor, Sorvall) for 1 minute to pellet chloroplasts. The supernatant was transferred to a new tube while the pellet was washed three times using grinding buffer as described earlier.

The supernatant from the chloroplast fraction was centrifuged at 16,000 x g for 10 minutes to pellet mitochondria. The supernatant was transferred to an ultracentrifuge tube, and the pellet was gently resuspended in grinding buffer using a nylon paintbrush to minimize mechanical breakage of mitochondria. Mitochondrial pellet was washed three times using grinding buffer, and mitochondrial pellet was processed for further experiments.

The supernatant in the ultracentrifuge tube was centrifuged at 100,000 x g for 1 hr at 4°C to separate the soluble cytosol from the plasma membrane, microsomal fraction and large polyribosome. After ultracentrifugation, the supernatant was transferred to a fresh ultracentrifuge tube while the pellet was resuspended in 700 µl of grinding buffer. The resuspended pellet was gently added to sucrose gradient (18%, 25%, 35%, 40% and 50% of sucrose in grinding buffer) to recover intact plasma membrane. Both the plasma membrane fraction in a sucrose gradient and cytosol in new ultracentrifuge tube were centrifuged at 100,000 x g for one and half hours at 4°C.

After centrifugation, 1 ml of cytosol was taken for further analysis while plasma membranes, which was in the junction between 40% and 50% sucrose, were collected and resuspended in 8-10 ml of grinding buffer to wash the sucrose. Resuspended plasma membrane from sucrose gradient was centrifuged at 100,000 x g for 1 hour, and resulting pellet was

resuspended in 200 μ l of grinding buffer which was used for the further experiment (Chaumont *et al.* 1995; Singer 1972; Yang and Murphy 2013).

SDS PAGE Electrophoresis and Western Blot Analysis

Leaf disk samples which served as the total sample were processed with 100 μ l of 1X SDS dye. A 50 μ l aliquot of each subcellular fractions were processed with 50 μ l of 2X SDS dye with β -mercaptoethanol (1:1 ratio). Nine microliters of all samples were run in 12% SDS-PAGE gel. A gel was stained with Coomassie blue for 1-2 hr in RT followed by destaining for 1 hr in RT. Pictures were taken, and proteins were quantified using Image studio software.

Quantification of protein was required to have equal loading control for western blot analysis. An equal amount of protein was loaded in each lane of 12% SDS-PAGE gel, and western blot was done using anti-GFP and anti-myc antibodies for GFP-SIP-428 and myc-SIP-428 proteins respectively.

Statistical Analysis

Statistical analysis was carried out using the two-tailed Student t-test to determine the significance of mean differences. Value (difference) equal to or less than the *p*-value of 0.05 was considered as the significant.

CHAPTER 3

RESULTS

Bioinformatics Analysis of SIP-428

Putative Conserved Domains of SIP-428

Protein BLAST was performed using the standard NCBI protein BLAST to identify putative conserved domains of SIP-428 using “non-redundant protein sequences.” The BLAST result showed that SIP-428 has homology with a SIR2 superfamily of proteins (Figure 6). It showed 45% identity with SIRT4 human deacetylase enzyme.

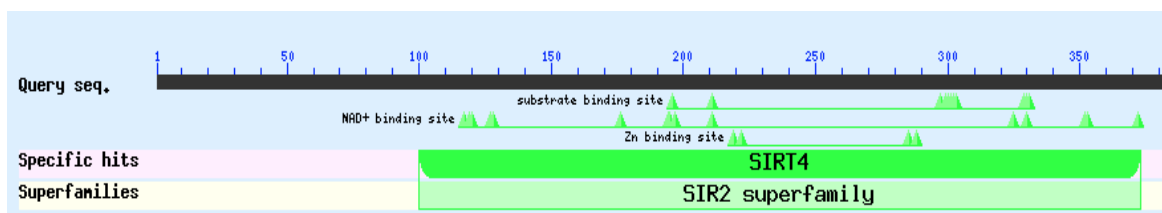


Figure 6: NCBI Protein BLAST analysis of SIP-428. The SIP-428 belongs to SIR2 superfamily with specific hit at human SIRT4 protein.

Amino acid sequence alignment was done to determine the similarities between SIP-428, Human Sirtuin-4 (NP 036372.1) and Arabidopsis sirtuin, AtSRT2 (NP 001078550.1). The sequence showed 45% and 72% identity, respectively (Figure 7). Amino acid residues 100 to 373 of SIP-428, highlighted with a dark background, shows the catalytic domain of SIR2 superfamily enzymes (Figure 6 and 7). This catalytic domain shows four conserved sites involved in zinc metal ion binding (indicated by red arrow), eleven sites involved in NAD⁺ binding (indicated by purple arrow), and five sites involved in substrate binding (indicated by brown arrow) based on similarity with *Archaeoglobus fulgidus* SIR2 homolog and human SIRT2 histone deacetylase structures (Figure 6) (Min *et al.* 2001).

Human-Sirtuin-4	-----MKMSFA--LTFRSA-	12
SIP-428	-MSMSLRLCCEPISISGLKNKRDLLGLDLAANHLNIPMRKWFSGVKKFIPFEGYVKFVQTT	59
AtSRT2	MLSMMNR-----RVFGGVSTDLFPSSRSMYRPLQSGGNLVMFLFKGCRRFVRTT	47
	: * * :	
Human-Sirtuin-4	-----KGRWIANPSQPCSKASIGLFPASPPLDPEKVKELQRFITLSKRLLVMTGAGIS	66
SIP-428	ARITFPKISSDCKDNPSNFLSHKKKVPYSDDPPSMKDVDLSLYEFFDRSTKLVVLTGAGMS	119
AtSRT2	CRVSIPIGGLGNEKAPPRFLRDRKIVPDADPPNEDIHKLYRLFQSSRLTILTGAGVS	107
	: . * ** : * . : . . . * . : : * . : * : * : * : *	
Human-Sirtuin-4	TESGIPDYRSEKVGLYARTDRRPIQHGFVRSAPIRQRYWARNFVGPWFSSHQPNPAHW	126
SIP-428	TESGIPDYRSPNGAY--STGFKPITHQEFLLRSSKARRRYWTRSYAGWRRFTAAQPGSTGHI	177
AtSRT2	TECGIPDYRSPNGAY--SSGFKPITHQEFTRSSRARRRYWARSYAGWRRFTAAQPGPAHT	165
	** . * * * * * : . : . : * * * : * * * : * * * * : * * * * : * * : * : * . *	
Human-Sirtuin-4	ALSTWEKLGKLYWLVTONVDALHTKAGSRRLTELHGCMDRVLCCLDCGEQTPRGVLQERFQ	186
SIP-428	ALSSLEKAGHISFMITQNVDRLLHHRAGSNPL-ELHGTVYIVACTNCGFTLPRFLQDQVK	236
AtSRT2	ALASLEKAGRINFMITQNVDRLLHHRAGSDPL-ELHGTVYIVTVMCLECGFSFPRDLFQDQLK	224
	** : * * * : : : * * * * * * * * * * * * * * * * : * * * * * * * * : * * : * : * : * : * : *	
Human-Sirtuin-4	VLNPTWSAEAHGL-----APDGDVFLSEEQ-VRSFQVPTCVQCGHHLKPD	230
SIP-428	AQNPKWAAAIESLDYD-SRDESFQGMKQRPDGDIEIDEKFWEEEDFYIPDCERCCQGVLLKPD	295
AtSRT2	AINPKWAEAIESIDHGDGPEKSEKQRPDGDIEIDEKFWEEGFHIPPVCEKCKGVLLKPD	284
	. * * . * : . : : * * * * : : * : . . * : * * * * * * * * * * *	
Human-Sirtuin-4	VVF [↓] FGDTVNPDKVDFVHKRVKEADSLLVV [↓] GSSLQVY [↓] SGYR [↓] FILTAW [↓] EKKLP [↓] IAILNIG [↓] P [↓] T	290
SIP-428	VVF [↓] FGDNV [↓] PKARADVAMEAAKGCDAFLV [↓] L [↓] GSSMT [↓] MSAFRL [↓] I [↓] KAAHEAGAATAIVNIG [↓] V [↓] T	355
AtSRT2	VIF [↓] FGDNI [↓] PKERATQAMEVAKQSDAFLV [↓] L [↓] GSSLMT [↓] MSAFRL [↓] CRAAHEAGAMTAIVNIG [↓] ET	344
	* : * * * : . : . : . * . * : * * * * * * * . : * : * * * * * * * * * * *	
Human-Sirtuin-4	RSDDLACLKLN [↓] SRCGELLPLIDPC-----	314
SIP-428	RADDLVPLKINARVGEI [↓] LPRLLNVGSL [↓] SIPAL	387
AtSRT2	RADDIVPLKINARVGEI [↓] LHRVLDVGSLSVPAL	376
	* : * * : . * * : * * * * * * * * * : .	

Figure 7: Multiple protein sequence alignment of SIP-428, AtSRT2 (NP 001078550.1), and Human Sirtuin-4 (NP 036372.1). The star indicates identity; dot indicates conserved substitution; colon indicates semi-conserved substitution between two proteins, and the gaps indicate the dissimilarities between them. Amino acid with dark background represent the SIR2 catalytic domain present in SIP-428 protein.

Protein Structure of SIP-428

Possible three-dimensional structures of SIP-428, AtSRT2, and human mitochondrial sirtuin-4 were generated using the Swiss model online portal and visualized using pymol software as described in material and methods (Figure 8). SIP-428 secondary structure showed eleven α helix and twelve β -sheet region (Figure 9). Ramachandra plot analysis showed 94.2%, 4.5% and 1.4% of the amino acid residues of SIP-428 belong to favored, allowed and outlier

region respectively (Figure 9). Rossmann-fold characteristically binds to NAD⁺ and NADH (Chang *et al.* 2002). Acetylated lysine of proteins also enters the Rossmann fold where the catalytic activity of SIR2 deacetylase enzymes take place in the presence of NAD⁺ (Sanders *et al.* 2010). Figure 8 shows the difference in the structure by an orange arrow.

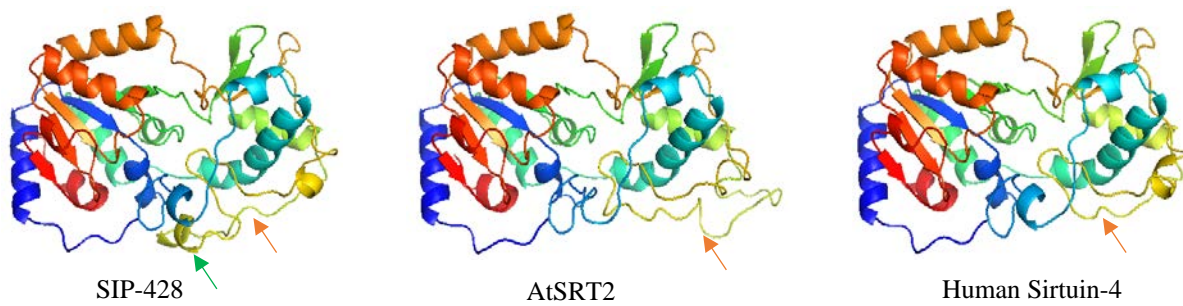
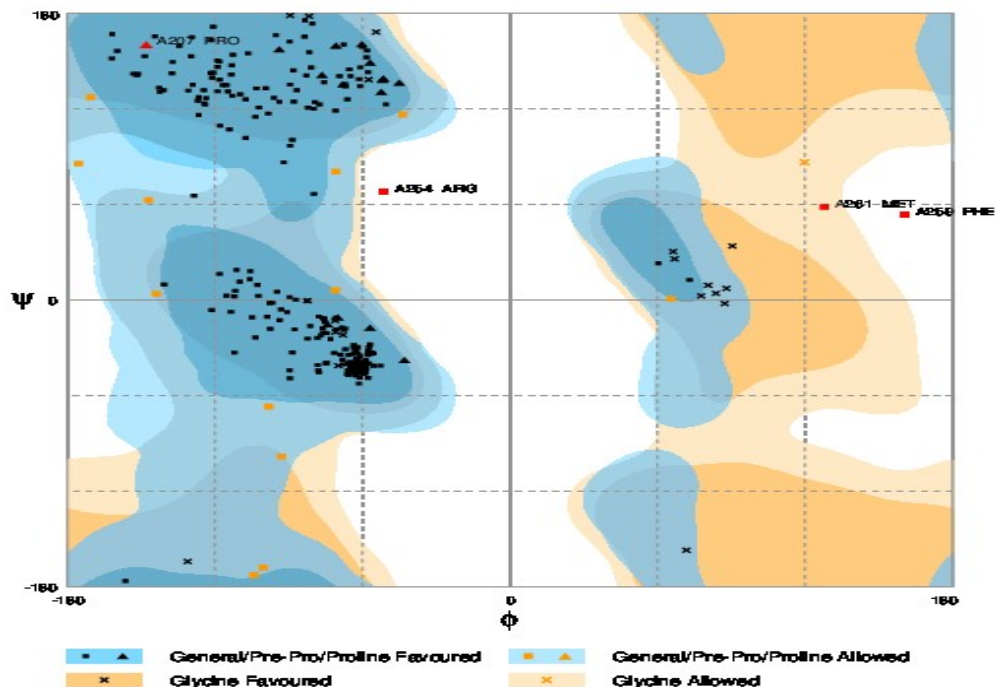
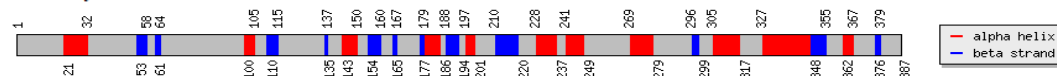


Figure 8: Predicted 3D structure of SIP-428, AtSRT2, and Human sirtuin-4. Predicted tertiary structure of SIP-428 shares a similar arrangement as that of its homolog in Arabidopsis (NP 001078550.1) and human sirtuin-4 (NP 036372.1) with an equal number of α helix and β -sheet region. Orange and green arrows indicate the difference between the predicted 3D structures and α helix that is unique in SIP-428, respectively.

A

Result of comparing Chou-Fasman method, GOR method and Neural Network method

Summary:



B

Figure 9: Bioinformatic analysis of SIP-428. Panel A, the prediction of secondary structure of SIP-428 with 11 alpha helix and 12 β sheet based on Chou-Fasman, GOR and Neural Network method. Panel B, the Ramchandra plot analysis of SIP-428 for structural validation

Expression of Full-length SIP-428 in *E. coli*

To determine the enzymatic activity of SIP-428, full-length SIP-428 was expressed in *E. coli* using pET28a(+) plasmid. IPTG was used to induce the expression of SIP-428 as described previously. Solubility test of the SIP-428 protein was done to determine optimum condition for expression of the soluble SIP-428 protein. The bacterial pellet from bacterial cultures grown at different temperatures (17°C and 37°C) were lysed by sonication. The supernatant (soluble) and pellet (insoluble) fractions were collected and analyzed by SDS-PAGE and western blot with anti His tag antibody using 428T (truncated SIP-428) as a positive control (Figure 10). Results

showed the expression of full-length SIP-428 in the total cell (428RIL) but not in soluble form (supernatant). Although different bacterial expression cell lines were used (BL21 (DE3) and BL21-CodonPlus (DE3)-RIL) soluble form was not detected (Figure 10). These result showed full-length SIP-428 did not express in soluble form.

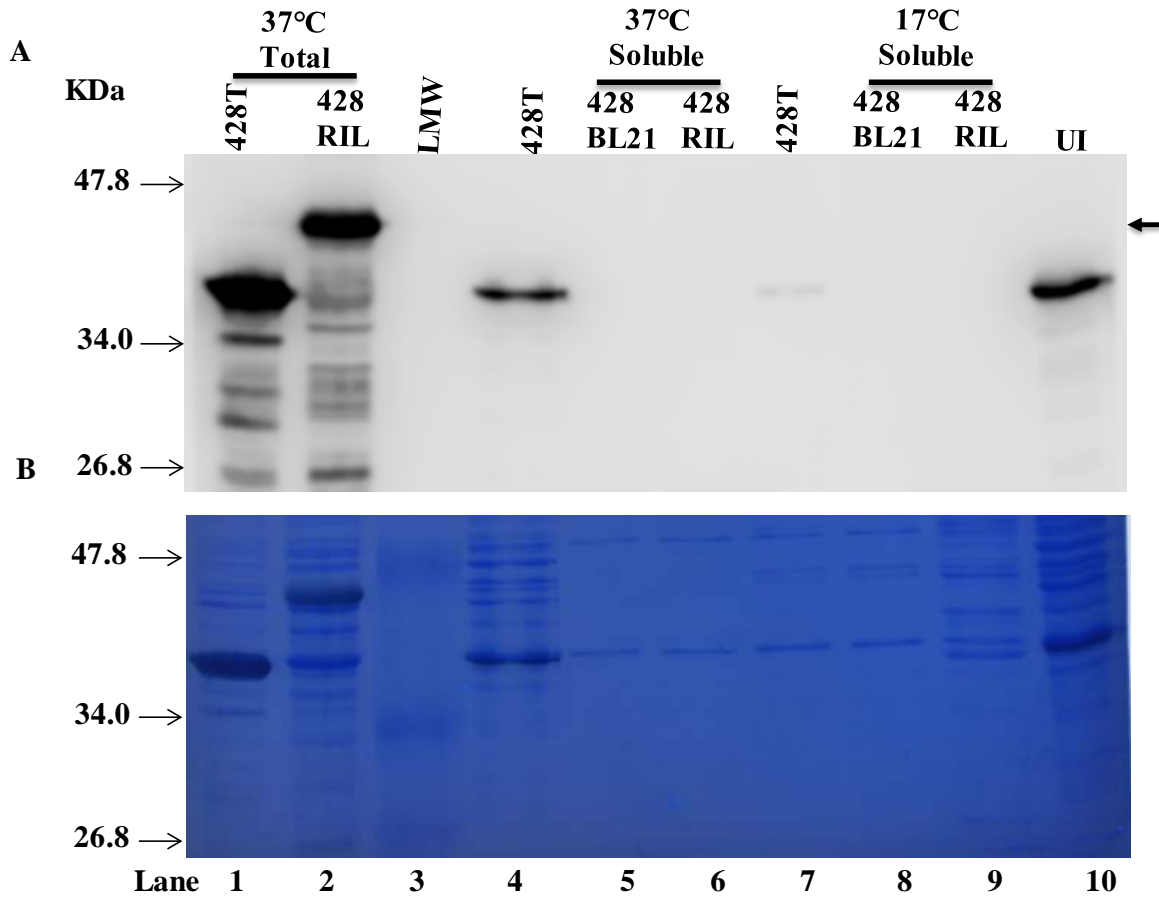


Figure 10: Expression of full-length SIP-428. Panel A. Western blot analysis of SIP-428 using anti-His tag antibody. Panel B. Coomassie blue stained blot of SIP-428 expressed at different temperatures and in different bacterial expression cells. 428T is total protein sample (Lane #1, 2, 4 and 7). Full length SIP-428 was expressed in BL21-CodonPlus (DE3)-RIL and BL21 (DE3) bacterial expression cells represented by 428 RIL and 428 BL21, respectively. Protein ladder (LMW) is in lane# 3). UI is un-induced protein of 428T (Lane# 10).

Expression of SIP-428-72 Protein in *E. coli*

SIP-428 without the putative signal peptide (SIP-428-72) was cloned into pET28a(+) plasmid and transformed into chemically competent Top 10 *E. coli* cells. The transformed cells were screened by colony PCR (Figure 11) which showed successful cloning of SIP-428-72 into pET28a(+) plasmid. The plasmid DNA was isolated from the positive clone and used for further experiments (Figure 12).

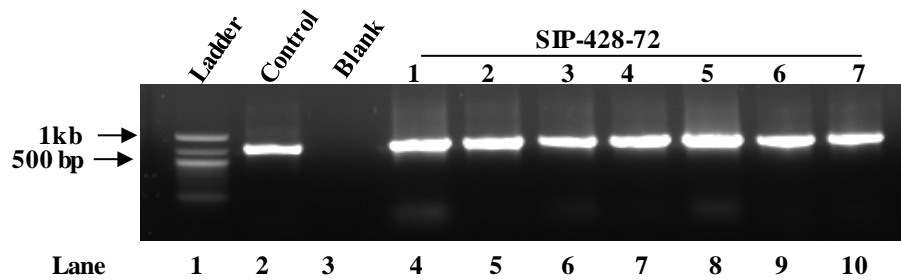


Figure 11: Colony PCR of SIP-428-72 (pET28a (+)-SIP-428-72). Lane# 4-10 shows positive clones and lane#2 shows the positive control. An EtBr stained agarose gel was used to visualize PCR amplification.

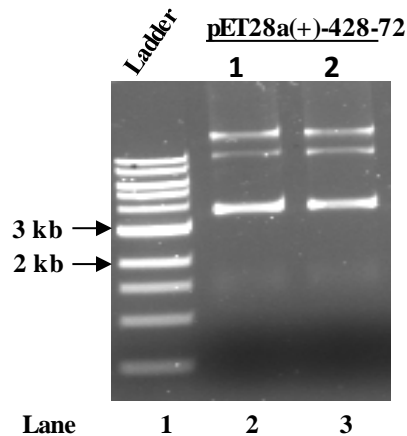


Figure 12: Isolation of plasmid DNA (pET28a (+)-SIP-428-72). Plasmid DNA of SIP-428-72 were isolated from colony 1 and 2 (lane# 2 and 3) and visualized on a 1.0% agarose gel.

Extracted plasmid DNA was transformed into bacterial expression cells to express the recombinant SIP-428-72 protein. SDS-PAGE and western blot using anti His tag antibody was used to analyze the expression of SIP-428-72 as described earlier using a different concentration of IPTG and incubation temperatures. The results showed SIP-428-72 was expressed in soluble form at 17°C incubation after inducing with 0.1mM IPTG (100 μM) (Figure 13). Results also showed the expression of SIP-428-72 in soluble form without induction at 17°C (Figure 13). Large-scale expression of SIP-428-72 was carried out by inducing bacterial culture by 0.1mM IPTG at 17°C incubation temperature for further experiments.

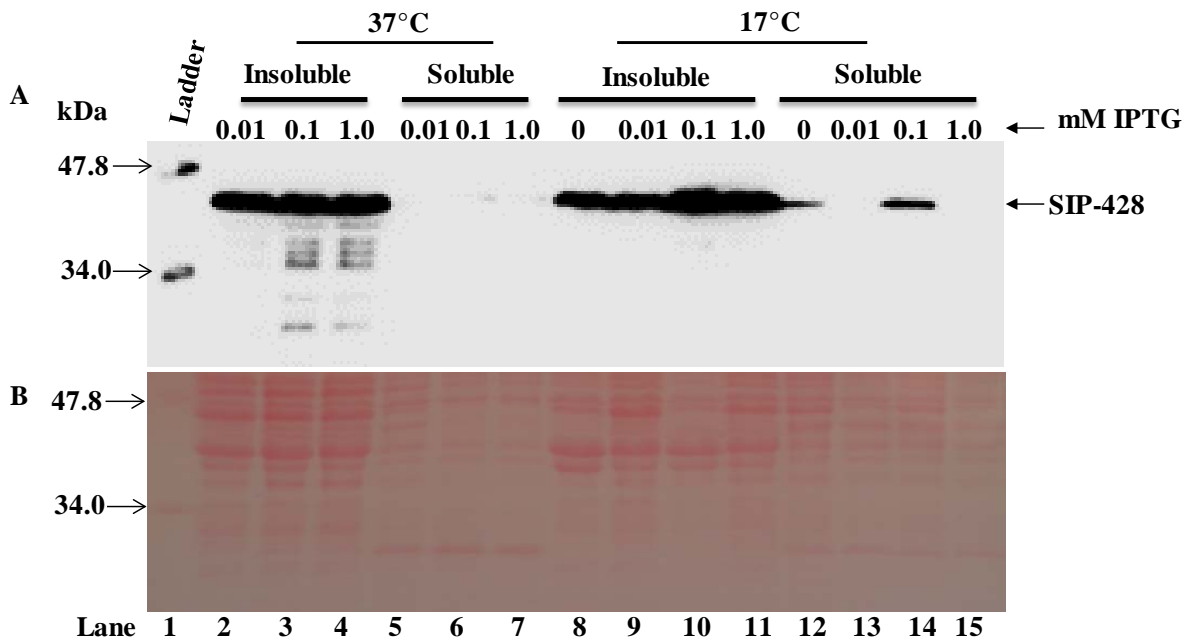


Figure 13: Solubility test of SIP-428-72 protein obtained from 37°C and 17°C growth culture. Panel A, western blot analysis using anti-His tag antibody. Arrow indicate SIP-428 protein. Panel B, ponceau stained blot showing total protein content for both soluble and insoluble fraction of 37°C and 17°C culture. Lane# 1 shows ladder, lane# 2-7 shows protein expressed in 37°C incubation (soluble and insoluble), and lane# 8-15 shows protein expressed in 17°C incubation (soluble and insoluble).

Expression and Purification of SIP-428-72 using Ni-NTA

SIP-428-72 with N-terminal 6x His tag was expressed in *E. coli* and purified using Ni-NTA affinity chromatography. SDS-PAGE followed by western blot analysis was performed to confirm the purification of SIP-428-72. SIP-428-72 protein samples were processed with 2X SDS sample dye and loaded into the SDS-PAGE gel. Unbound and loosely bound proteins were washed with 1X Ni-NTA buffer containing 10 mM of imidazole (lane# 3). Then, the bound proteins were eluted with 1X Ni-NTA elution buffer containing 250 mM imidazole (lane# 4-15). The result showed fraction # 5-11(lane# 6-12) contained a higher amount of SIP-428-72 as an equal volume of each eluted fraction was loaded (Figure 14). Results showed fractions containing SIP-428-72 protein still contained other unwanted proteins. In order to prevent the leaching of SIP-428-72 in flow-through (FL), the bed volume of Ni-NTA was increased and also incubation time of SIP-428-72 with Ni-NTA beads was increased but still, some SIP-428-72 eluted in the flow through that indicate potential weak binding affinity of SIP-428-72 with Ni-NTA beads.

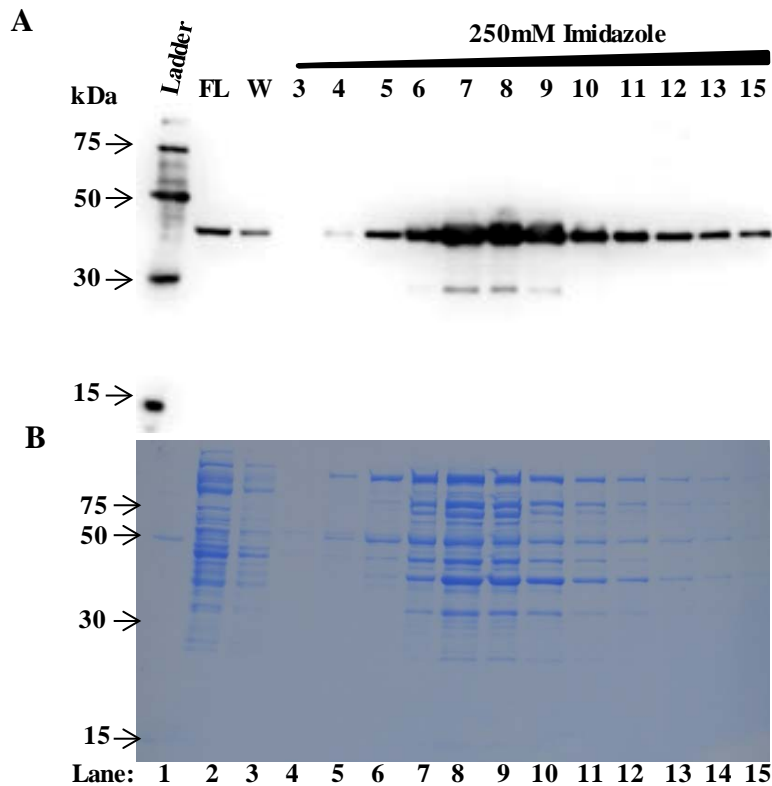


Figure 14: Purification of SIP-428-72 protein using Ni-NTA column chromatography. Panel A, western-blot analysis of purified SIP-428-72 using Ni-NTA affinity column. Panel B, coomassie stained blot. Ladder, flow through (FL), and wash (W) presented in first three lanes# 1-3. Lane # 5-15 showed eluted fraction: 3-15.

Purification of SIP-428-72 Using Mono-Q Ion Exchange Chromatography

Ni-NTA fractions (5-11) containing SIP-428-72 proteins (Figure 14) were pooled together and further purified on a Mono Q column. In the Mono Q column, most proteins were eluted and collected as fractions #1-51 (Figure 15 and 16). Each fraction was tested for the presence of SIP-428-72 by western blot. The result showed SIP-428-72 was detected in fraction # 17-51 (Figure 16). Eluted fractions (17-47) showed other unwanted proteins along with SIP-428-72 (Figure 16) indicating weak binding affinity of SIP-428-72 protein with Mono-Q column as shown in chromatography profile; protein started to elute with a low concentration of NaCl.



Figure 15: Chromatography profile of protein in Mono Q column purification. The absorbance of protein at 280nm (blue line), salt conductivity (brown line), and collected fraction (0.5ml) (red line). Fractions #15-51 were used for SDS gel and western blot analysis.

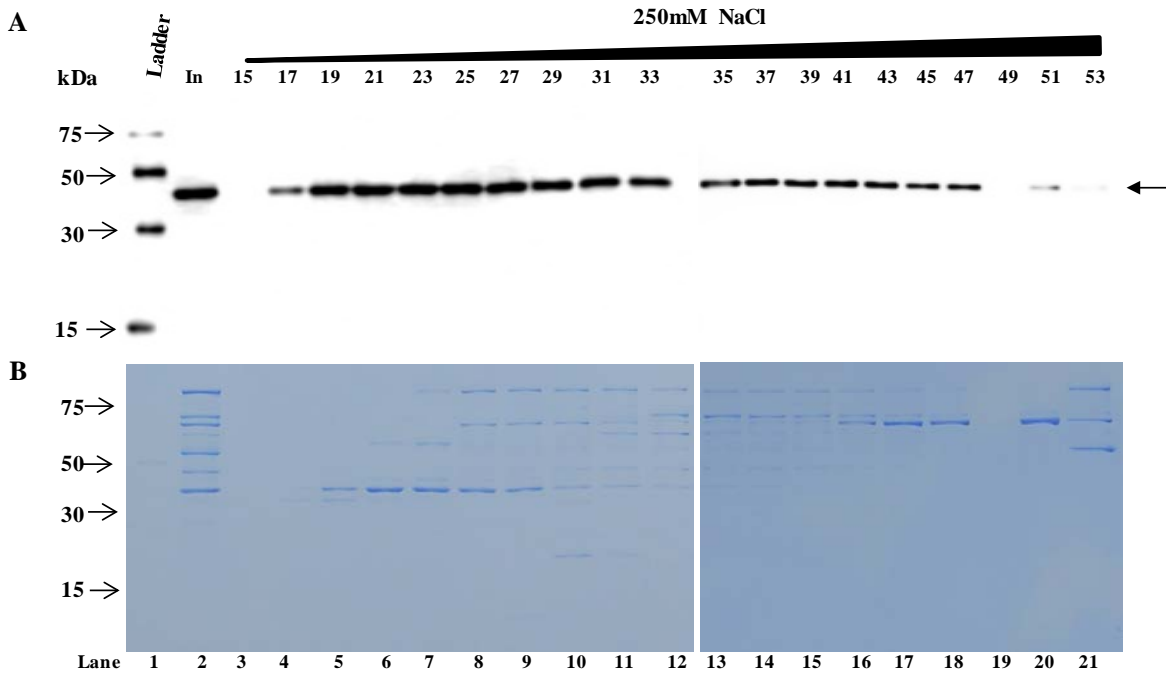


Figure 16: Purification of SIP-428-72 by Mono Q chromatography. Panel A, western blot analysis using anti His tag antibody. Panel B, coomassie stained blot. Figure shows ladder (lane# 1), input sample (lane# 2), and Mono Q eluted fraction 15-51 (lane# 3-20).

The purification of SIP-428-72 in Ni-NTA chromatography and Mono-Q chromatography showed a broad range of SIP-428-72 elution using 250mM Imidazole and 250mM NaCl respectively. Elution of SIP-428-72 in Mono-Q was also tested with increasing the concentration of NaCl up to 500 mM, but still, other unwanted proteins were detected.

Dialysis of SIP-428-72

Mono Q fractions of SIP-428-72 (lane# 5-18) (Figure 16) were pooled together and dialyzed against 500 ml deacetylase buffer with slow stirring at 4°C. The buffer was changed every eight hours for three times. The purified protein was analyzed by SDS-PAGE (Figure 17). The dialyzed SIP-428-72 was quantified by Nanodrop and stored at -80°C for further analysis. Although SIP-428-72 protein was subjected for Ni-NTA and Mono-Q purification, results

showed the presence of background proteins which could be due to the weak binding affinity of SIP-428-72 to Ni-NTA and Mono-Q column (Figure 17).

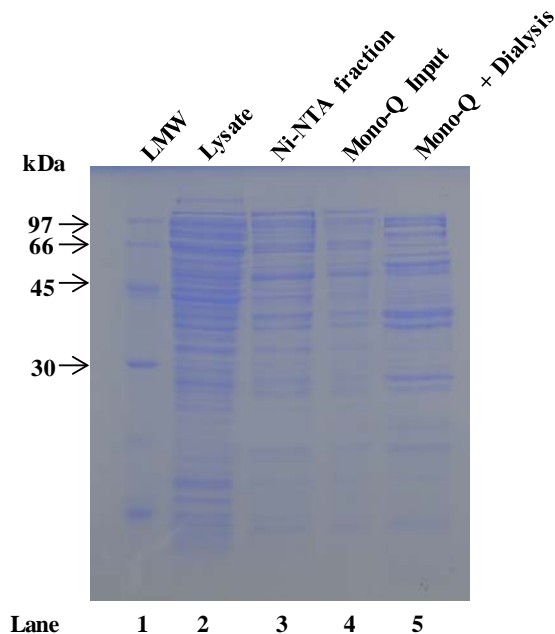


Figure 17: Purification of SIP-428-72 protein from *E.coli*. Lane 1; low molecular weight protein marker (LMW), lane 2; crude SIP-428-72 protein, lane 3; SIP-428-72 after Ni-NTA purification, lane 4; SIP-428-72 Mono-Q purification, and lane 5; dialyzed SIP-428-72 after Mono-Q purification.

Enzyme Assay

SIR2 Deacetylase Enzyme Assay

The deacetylase activity of the purified SIP-428-72 protein was tested with the SIRT Glo™ assay kit. An artificial lysine-acetylated peptide p53 in the kit was used as the substrate in this luminescence-based assay. The result showed SIP-428-72 deacetylated the acetylated p53 peptides in a linear concentration-dependent manner (Figure 18) that indicated SIP-428 exhibits a sirtuin type deacetylase activity. Buffer without SIP-428-72 protein in substrate solution was

used as a negative control for the SIRT Glo™ assay.

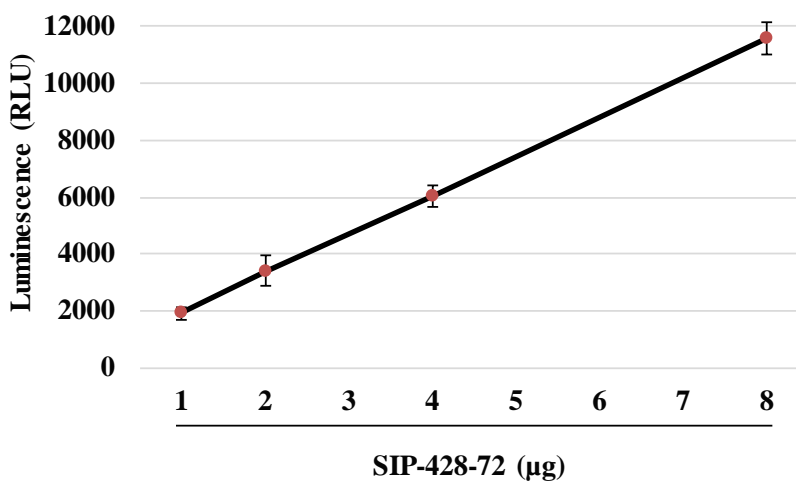


Figure 18: SIR2 deacetylase enzyme activity. The linear range of SIP-428-72 protein (1-8 µg) exhibiting SIR2 deacetylase enzymatic activity on acetylated p53 peptide using SIRT-Glo assay. The relative luminescence unit (RLU) was detected after 2 hr of incubation at RT.

Histone Deacetylase Enzyme Assay

Purified SIP-428-72 protein was used to test the histone deacetylase enzymatic activity with the HDAC Glo™ assay kit. Artificial lysine-acetylated histone 4 peptides in the kit were used as a substrate in the luminescence-based assay. Results showed SIP-428 did not exhibit histone deacetylase activity although the different concentration of SIP-428-72 was used (1-8 µg), (Figure 19). Buffer without the purified SIP-428-72 protein in substrate solution was used as a control for HDAC Glo™ assay.

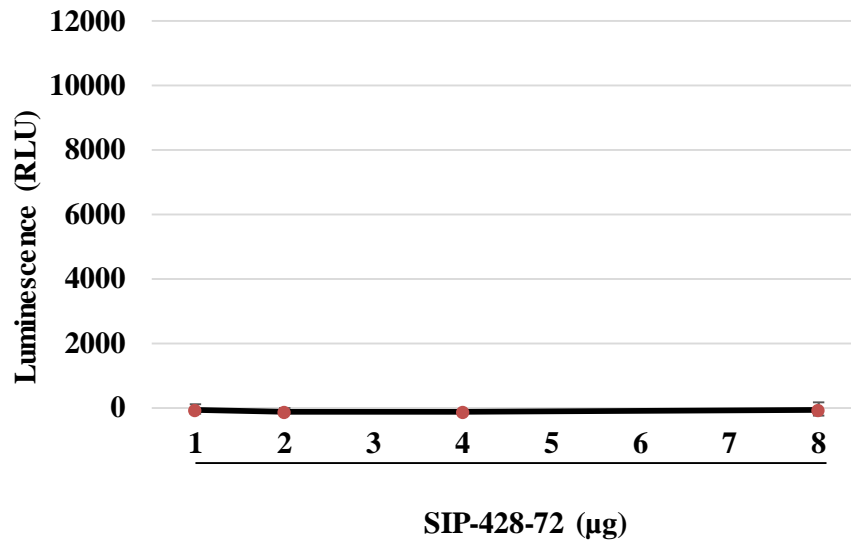


Figure 19: Histone deacetylase enzyme activity. SIP-428-72 protein (1-8 µg) didn't exhibit histone deacetylase enzymatic activity on histone 4 peptide using HDAC-Glo assay. The relative luminescence unit (RLU) was detected after 2 hr of incubation at RT.

GST Pull-Down Assay

The interaction between SABP2 and SIP-428 was observed in the yeast two-hybrid system (Kumar *et al.*, 2018 unpublished). To verify the interaction, a GST-based pull-down assay was performed using GST agarose beads. The full-length SABP2 was sub-cloned into a pDEST15 bacterial expression vector, and SABP2 was expressed as GST-fusion proteins in *E. coli* earlier. SIP-428-72 protein was expressed with a 6x His tag. A GST pull-down assay was performed as described earlier using GST agarose beads. After incubation, the GST agarose beads were washed, the proteins were eluted, and interacting proteins were analyzed by western blot (Figure 20). In western blot using anti His antibody, the signal was detected in SIP-428-72 input and GST bead. Since SIP-428-72 only has 6xHis-tag, it could not have bound to GST beads by itself unless it was interacting with SABP2 protein (has GST tag). SABP2 could bind to GST beads (Figure 20). Western blot using anti-GST antibody showed a signal in SABP2 input

and GST bead indicating the binding of GST fused SABP2 with GST beads as well as SIP-428-72 proteins (Figure 20). These results confirmed the interaction between SABP2 and SIP-428-72.

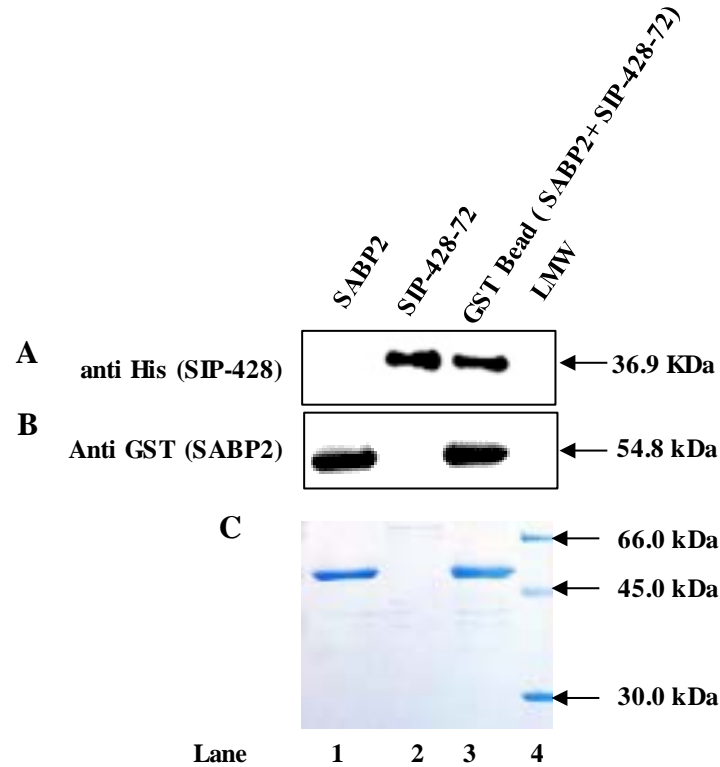


Figure 20: Figure: Glutathione-S-transferase (GST) pull-down assay. Panel A, the western blot using anti His antibody. Panel B, western blot using anti GST antibody. Panel C the coomassie stained blot. Lane 1; SABP2 protein input, lane 2; SIP-428-72 protein input, lane 3; GST bead with interacting proteins (SABP2 and SIP-428-72), and lane 4; low molecular weight protein marker.

Screening of SIP-428 Homolog Mutant

T-DNA Insertion Confirmation

Arabidopsis mutants (*atsrt2*) from the selected lines (SALK-149295C and SALK-131994C) were tested for T-DNA insertion. The wild-type Col-0 being the parental background for the mutants was used as a control. For Col-0, primer pairs RP and LP were used for the

detection of AtSRT2 and, for both the mutants, LB and RP primer pairs were used to examine the T-DNA insertion. The expected size of the PCR-amplified fragments was 410-710 bp for the mutants and 900-1100 bp for Col-0. Results showed the presence of T-DNA in SALK-149295C (lane# 2 and 3) and SALK-131994C (lane# 5 and 6) (Figure 21). As a T-DNA insertion was present in both the mutant lines (SALK-149295C and SALK-131994C), the SALK-131994C mutant lines were used for further experiments.

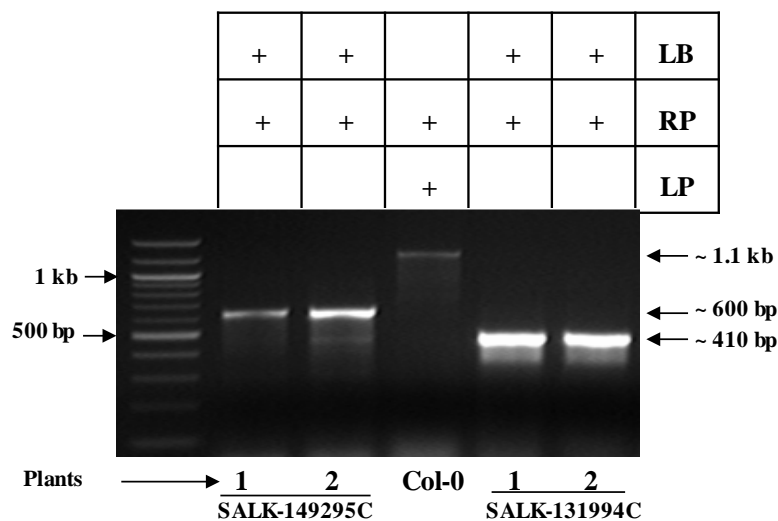


Figure 21: Confirmation of T-DNA insertion in AtSRT2 mutant *Arabidopsis thaliana*. PCR products were visualized on 1.0% agarose gel.

Confirmation of *atsrt2* Mutant

Total RNA was extracted from fully-grown Col-0 and *atsrt2* mutant plants (4 weeks). RT-PCR was used to detect the expression of *AtSRT2*. The expression of tubulin was used as a loading control (Figure 22). Results showed that the *atsrt2* mutant was an did not express *AtSRT2* mRNA. Verified *atsrt2* mutant plants were used for further experiments.

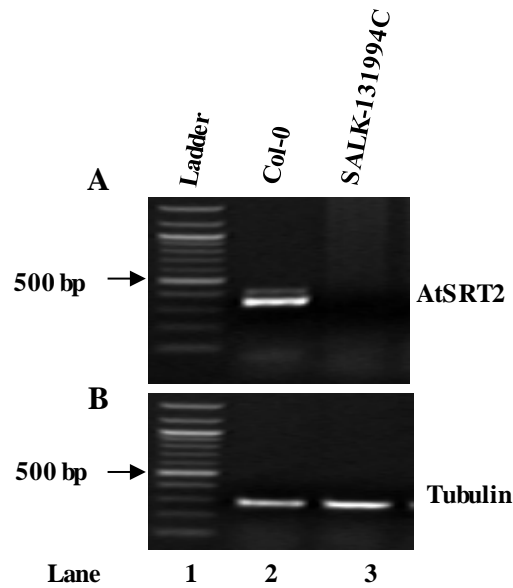


Figure 22: Confirmation of AtSRT2 mutant plant (*atsrt2*). Panel A, the expression of AtSRT2. Panel B, the expression of tubulin, which was used as an internal standard. Lane# 3 (A) shows the absence of AtSRT2 expression in *atsrt2* mutant line while AtSRT2 expression was detected in Col-0 (lane# 2).

Role of AtSRT2 in Biotic Stress

Arabidopsis Mutant of SIP-428 and Basal Resistance

The role of SIP-428 in basal resistance was investigated by the bacterial growth assay. The result showed that the *atsrt2* mutant plants were significantly more resistant to pathogen infection compared to the wild-type control (Figure 23 and 24). Mutant plants allow significantly reduced growth (CFU) of *Pseudomonas syringae* pv *maculicola* (*Psm*) (6.5×10^4) compared to the wild-type (5.3×10^6) at three days post-infection (DPI) (Table 8 and 9, Figure 23 and 24, $p < 0.05$). Normalization of CFU was done to make the equal mass/surface area of infected tissue and volume of sterile water (1ml) used to grind the samples.

Table 8: The bacterial growth of *Pseudomonas syringae* pv *maculicola* (CFU/ml) on three days post-infection (3DPI).

	Average	Standard Deviation
Col-0	5250000	1443375
<i>atsrt2</i>	65000	11726

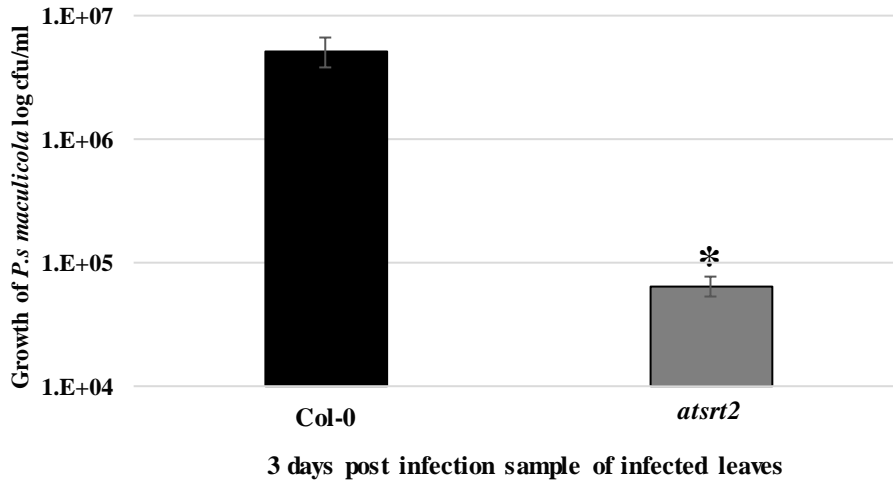


Figure 23: Bacterial growth assay in Arabidopsis wild-type Col-0 and *atsrt2*. Figure shows CFU of *Psm* in *atsrt2* mutant and the wild-type Col-0 at 3 days post infection (DPI). Student t test was used for statistical analysis ($P < 0.05$) with multiple samples.

Table 9: The bacterial growth of *Pseudomonas syringae* pv *maculicola* (CFU/ml) on three days post-infection (3DPI)

	Average	Standard deviation
Col-0	3750000	1440486
<i>atsrt2</i>	55000	18516

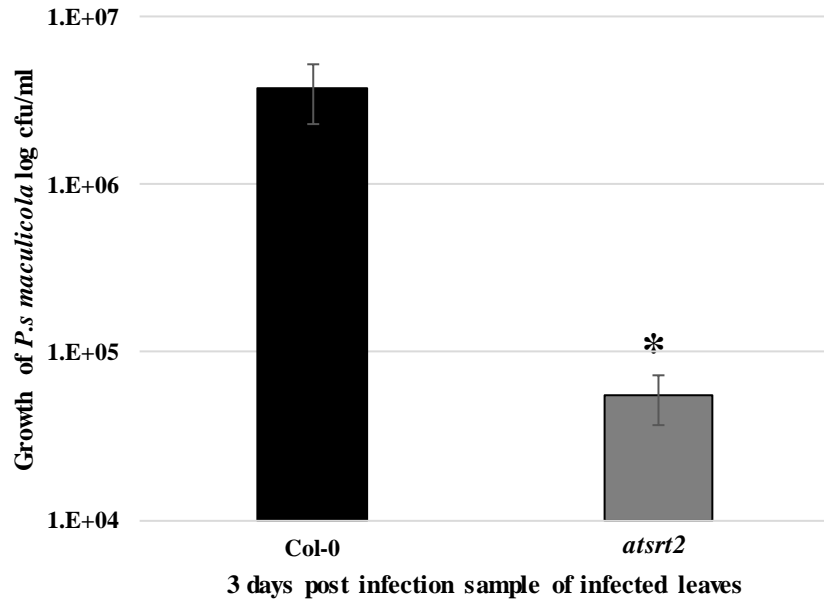


Figure 24: Bacterial growth assay in Arabidopsis wild-type Col-0 and *atsrt2*. Figure shows CFU of *Psm* in *atsrt2* mutant and the wild-type Col-0 at 3 days post infection (DPI). Student t test was used for statistical analysis ($P < 0.05$) with multiple samples.

Arabidopsis Mutant of SIP-428 and SAR

The role of AtSRT2 in SAR was investigated by the bacterial growth assay. Plants exhibiting SAR were expected to show significantly fewer CFUs compared to the primary infection (or that of the mock-treated plant) since SAR of plants were already activated by primary infections using avirulent pathogen *Pseudomonas syringae* pv *tomato strain DC3000 avrRpt2* (*Pst DC3000 AvrRpt2*). However, if the plant did not exhibit SAR, the difference in CFUs would not be significant since the primary infections did not induce the SAR. The result of this experiment showed wild-type Col-0 plants allowed the growth of *Pseudomonas syringae* pv *maculicola* (*Psm*) to 3.2×10^7 CFU while the SAR induced Col-0 plant only allowed the *Psm* growth to 2.4×10^5 CFU (Table 10 and 11). The significant decrease in the growth of the pathogen indicated induction of SAR upon primary infection with *Pst DC3000 AvrRpt2*.

Similarly, *atsrt2* mutant plants also showed a clear SAR response at three days post-infection as it allowed the growth of *Psm* to 6.4×10^6 CFU while the SAR induced *atsrt2* mutant plant only allowed the *Psm* growth to 2.8×10^5 CFU (Table 10 and 11). Results showed AtSRT2 in Arabidopsis likely not affect SAR (Figure 25 and 26). Student t-test was used for statistical analysis ($p < 0.05$).

Table 10: The bacterial growth of *Pseudomonas syringae* pv *maculicola* (CFU/ml) on three days post-infection (3DPI) on Col-0 and *atsrt2* mutant plants.

	Col-0 Mock	Col-0 Treated	<i>atsrt2</i> -Mock	<i>atsrt2</i> -Treated
Average	32500000	237500	6375000	283333
Standard deviation	1.44E+07	94648	3637192	230940

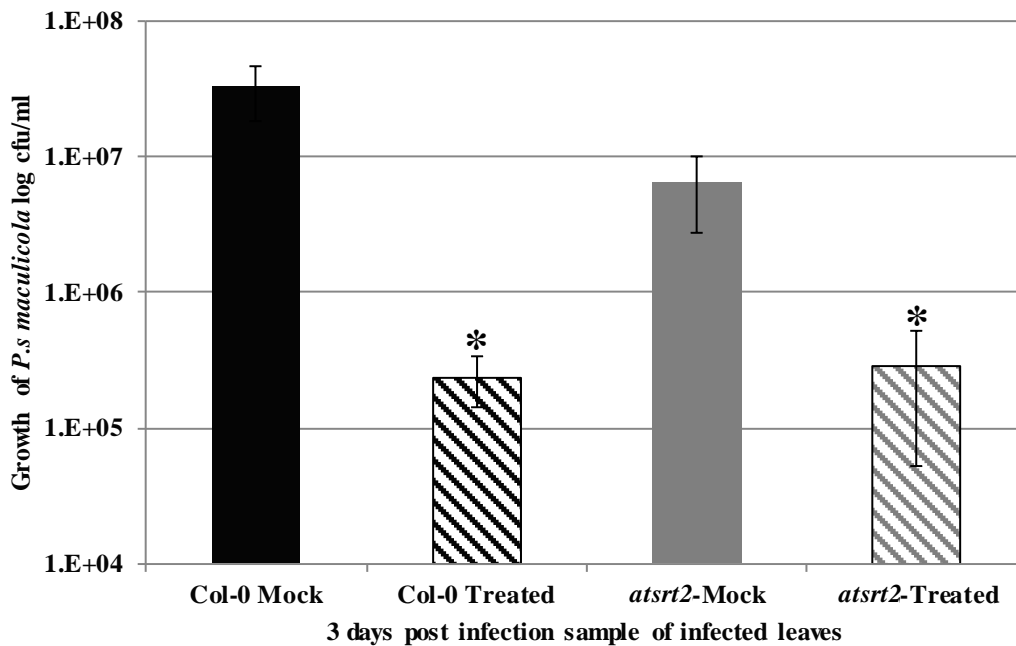


Figure 25: SAR in arabidopsis wild-type Col-0, and *atsrt2* mutant. Figure shows significantly reduced number of CFU in the avirulent treated plants (both Col-0 and *atsrt2* mutant plants) as compared to mock treated ($P < 0.05$).

Table 11: The bacterial growth of *Pseudomonas syringae* pv *maculicola* (CFU/ml) on three days post-infection (3DPI) on Col-0 and *atsrt2* mutant plants.

	Col-0-Mock	Col-0-Treated	<i>atsrt2</i> -Mock	<i>atsrt2</i> -Treated
Average	7666666	666666	2083333	275000
Standard deviation	1.75E+06	297769	1068488	52440

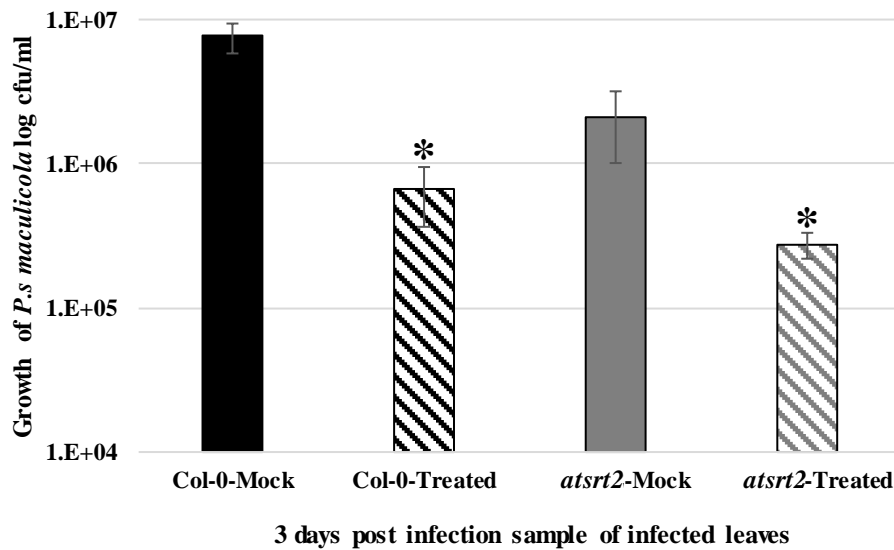


Figure 26: SAR in arabidopsis wild-type Col-0, and *atsrt2* mutant. Figure shows significantly reduced number of CFU in the avirulent treated plants (both Col-0 and *atsrt2* mutant plants) as compared to mock treated ($P < 0.05$). *atsrt2* mutant plants show reduced growth of *Psm* (CFU) as compare to wild type mock treated plant.

Role of AtSRT2 in Abiotic Stress

The role of SIP-428 homolog in abiotic stress was investigated using salt (NaCl) and mannitol to mimic salinity and drought stress respectively. Surface area and root length of both wild-type and Arabidopsis mutant plants were measured using Image J software

(<https://imagej.net/Welcome>). Although the difference was observed between wild-type and

mutant plants until day 21 of exposure to both the stress (0, 75, 100, and 150 mM of NaCl and mannitol) (Figure 27 and 28), it was not significant one ($P < 0.05$). Multiple experiments showed a similar pattern of results.

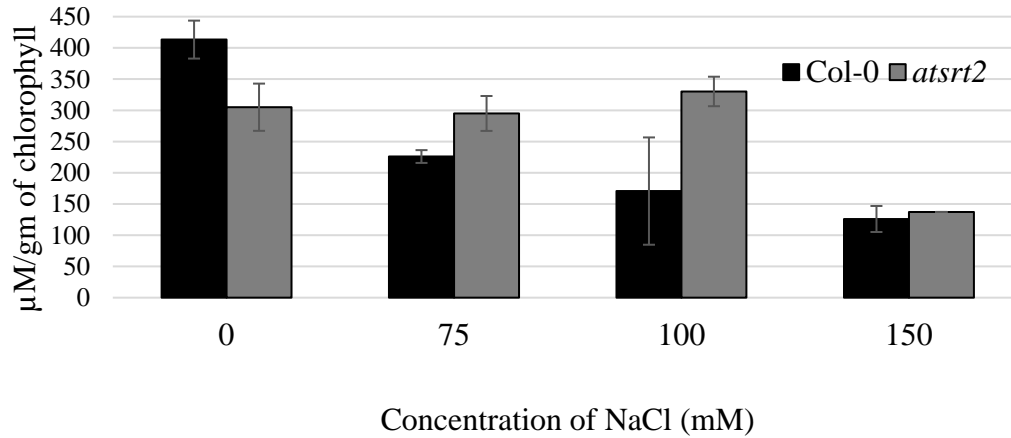


Figure 27: Effect of salinity on chlorophyll content in wild-type (Col-0) and *atsrt2* mutant plant. Bar diagram represent the average of chlorophyll content with Standard deviation for Col-0 (black) and *atsrt2* (gray) ($P < 0.05$).

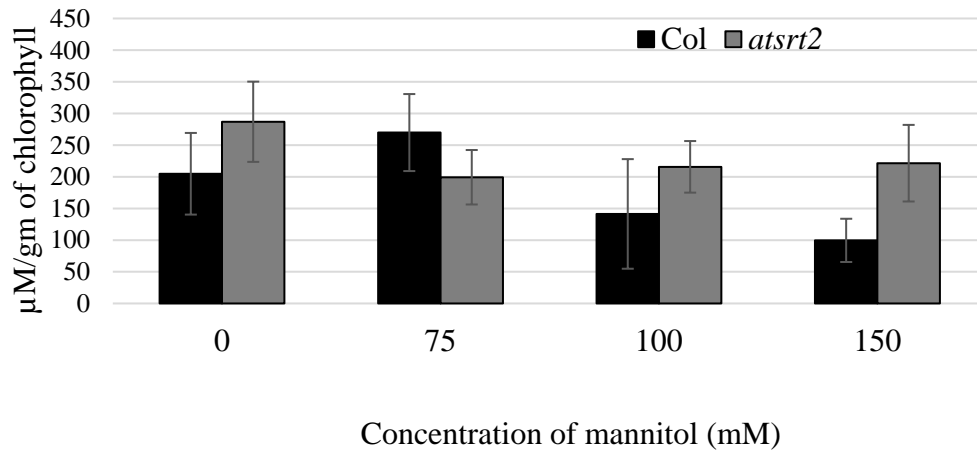


Figure 28: Effect of osmotic stress on chlorophyll content in wild-type (Col-0) and *atsrt2* mutant plants. Bar diagram represent the average of chlorophyll content with Standard deviation for Col-0 (black) and *atsrt2* (gray) ($P < 0.05$).

Generation of SIP-428 Silenced, and Homolog Silenced Tobacco Lines

To investigate the possible roles of SIP-428 in biotic stress, transgenic tobacco lines silenced in the expression of SIP-428 and its homolog were generated, respectively. The leaf disk method was used to generate stable transgenic tobacco lines. The pDONR221 gateway cloning based plasmid was used as the entry plasmid and a pHELLSGATE8 plasmid as the destination plasmid (Figure 29). The pHELLSGATE8 plasmid with SIP-428 fragments was transformed into competent *Agrobacterium tumefaciens* cells by the heat shock method. Transformed *Agrobacterium* was used for further experiments.

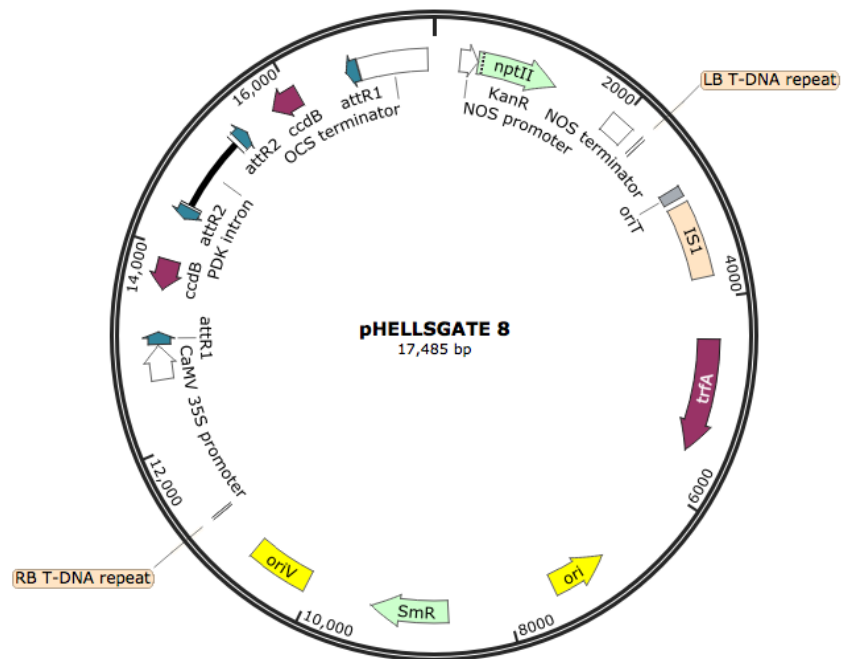


Figure 29: Vector map of pHELLSGATE8 vector (Wielopolska et al. 2005). The pHELLSGATE8 was used as RNAi destination vector to generate SIP-428 silenced and homolog silenced tobacco lines.

PCR Amplification of SIP-428 Silencing and Homolog Silencing Fragment

To generate silencing and homolog silencing constructs, selected fragments of SIP-428 coding sequences for silencing (Figure 30) and homolog silencing (Figure 31) were amplified from a verified plasmid (TOPO-SIP-428-1) using gateway cloning primers flanked with attB1 and attB2 sites (DK 663 and 664 for silencing and DK 667 and 668 for homolog silencing: Table 3) for PCR amplification as described earlier. Selected fragments were successfully amplified as shown in Figure 34. The resulting fragments were used for further experiments.

5'ATGTCCATGTCTCTTCGACTTTGTTGCGAACCTCAATTTCTGGCTTAAAGAATAAAAGAGATTTGCTGGGCTTAGATTTGGCAGCTAAT
CATTGAATATCCCAATGAGGAAATGGTTTAGTGGAGTAAAAAGTTTCATTCCTTTGAGGGATATGTTAAGTTTGTGCAAACAACAGCA
AGAATAACATTTCCAAAGATCTCATCAGATTGTAAGATAATCCCTTCGAATTTTTGAGTCACAAAAAGAAGGTTCTTATTCCGGATC
CCCCTAGCATGAAAGATGTGGACAGTTTGTATGAATCTTTGATAGGAGTACCAAGCTTGTATTGACGGGAGCTGGCATGAGCACA
GAGAGTGGAAATCCGGATTACAGGAGCCCAAATGGAGCATATAGTACTGGTTTCAAACCAATTACCCATCAGGAGTTTCTCCGATCAAG
CAAGGCTCGAAGGCGTTATTGGACACGGAGTTATGCTGGCTGGAGACGTTTCACTGCAGCTCAACCTAGTACAGGTCATATAGCTCTATC
ATCTCTTGAGAAAGCAGGCCATATAAGTTTTATGATTACACAGAATGTGGACAGGCTGCATCATCGGGCTGGCAGCAATCCACTTGAATT
GCATGGGACCGTCTACATTGTTGCTGTACAAATTGGTTTTACTCTACCTCGAGAAGTGTTCAGATCAAGTGAAGGCTCAAATCCT
AAGTGGGCAGCAGCTATCGAAAGTTTGGATTATGACAGCCGATCAGACGAGAGCTTTGGTATGAAGCAAAGGCCTGATGGGGATATT
GAGATCGATGAGAAATCTGGGAGGAGGATTCTACATTCCTGATTGTGAGAGGTGCCAAGGAGTTCTCAAACCTGACGTTGCTTCT
TTGGGGATAATGTCCCTAAAGCTAGAGCTGATGTTGCCATGGAAGCTGCAAAGGGATGTGATGCCTTCCTGTACTTGGTTCATCTAT
GATGACCATGTCTGCTTCCGGCTTATCAAAGCTGCGCACGAGGCAGGCGCTGCGACTGCAATTGTAATATTGGGGTGACACGAGCT
GACGATCTGTACCTTGAATAAATGCTCGAGTTGGAGAGATACTCCAAGATTGCTTAATGTTGGATCCTTGAGTATCCCTGCTCTCT
AG 3'

Figure 30: SIP-428 cDNA nucleotide sequence showing 302 bp long fragment (738-1039) selected for silencing (underlined and bold).

5'ATGTCCATGTCTCTTCGACTTTGTTGCGAACCCCTCAATTTCTGGCTTAAAGAATAAAAGAGATTTGCTGGGCTTAGATTTGGCAGCTAAT
 CATTGAATATCCCAATGAGGAAATGGTTTAGTGGAGTAAAAAAGTTTCATTCCTTTGAGGGATATGTTAAGTTTGTGCAAACAACAGCA
 AGAATAACATTTCCAAAGATCTCATCAGATTGTAAAGATAATCCCTTCGAATTTTTGAGTCACAAAAAGAAGGTTCTTATTCCGGATC
 CCCCTAGCATGAAAGATGTGGACAGTTTGTATGAATCTTTGATAGGAGTACCAAGCTTGTATTGACGGGAGCTGGCATGAGCACA
 GAGAGTGAATCCGGATTACAGGAGCCCAAATGGAGCATATAGTACTGGTTTCAAACCAATTACCCATCAGGAGTTTCTCCGATCAAG
 CAAGGCTCGAAGGCGTTATTGGACACGGAGTTATGCTGGCTGGAGACGTTTCACTGCAGCTCAACCTAGTACAGGTCATATAGCTCTATC
 ATCTCTTGAGAAAGCAGGCCATATAAGTTTTATGATTACACAGAATGTGGACAGGCTGCATCATCGGGCTGGCAGCAATCCACTTGAATT
 GCATGGGACCGTCTACATTGTTGCTGTACAAATTGTGGTTTTACTCTACCTCGAGAAGTGTTCAGATCAAGTGAAGGCTCAAATCCT
 AAGTGGGCAGCAGCTATCGAAAGTTTGGATTATGACAGCCGATCAGACGAGAGCTTTGGTATGAAGCAAAGGCTGATGGGGATATTG
 AGATCGATGAGAAATTCTGGGAGGAGGATTTCTACATTCCTGATTGTGAGAGGTGCCAAGGAGTTCTCAAACCTGACGTTGTCTCTTTG
 GGGATAATGTCCCTAAAGCTAGAGCTGATGTTGCCATGGAAGCTGCAAAGGGATGTGATGCCTTCCTGTACTTGGTTCATCTATGATGA
 CCATGTCTGCTTTCCGGCTTATCAAAGCTGCGCACGAGGCAGGCGCTGCGACTGCAATTGTAATATTGGGGT**GACACGAGCTGACGAT**
CTTGACCTTTGAAAATTAATGCTCGAGTTGGAGAGATACTTCCAAGATTGCTTAATGTTGGATCCTTGAGTATCCCTGCTCTAG 3'

Figure 31: SIP-428 cDNA nucleotide sequence showing 100 bp long sequence (1062-1161) selected for homolog silencing (underlined and bold).

The silencing and homolog silencing fragment were selected by BLAST analysis in the sol genomic database (Figure 32 and 33). Figure 32 showed the 302 nucleotide sequence selected from SIP-428 (Figure 30) was unique to SIP-428 (SGN-U449398, annotated gene name in sol genomic database). Figure 33 showed the 100 nucleotide sequence selected from SIP-428 (Figure 31) was shared among SIP-428 homologs (SGN-U449398, SGN-U462112, and SGN-U456934).

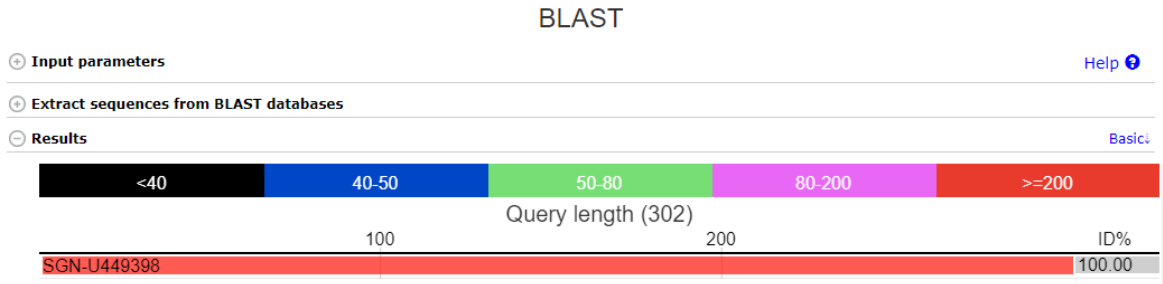


Figure 32: Sol genomic blast analysis of SIP-428 silence fragment. Figure shows unique nucleotide sequence of SIP-428 (SGN-U449398) that is not shared among its homologs.

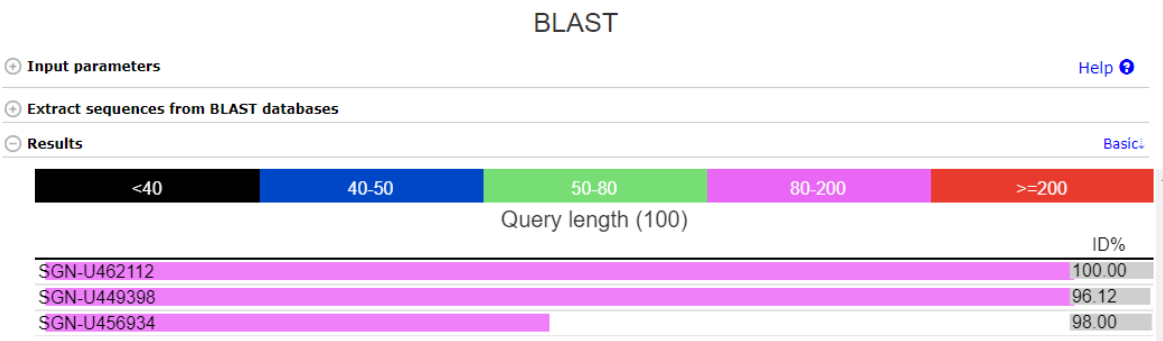


Figure 33: Sol genomic blast analysis of SIP-428 homolog silence fragment. Figure shows unique nucleotide sequence of SIP-428 (SGN-U449398) that is shared among its homologs (SGN-U449398 and SGN-U456934).

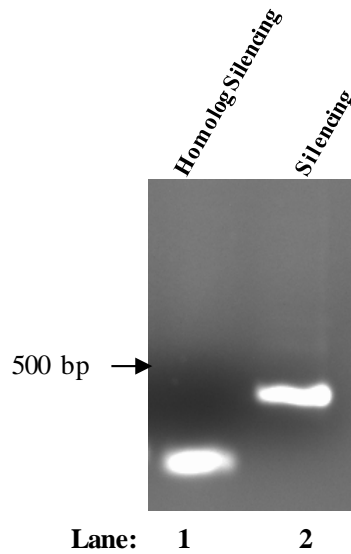


Figure 34: PCR amplification of SIP-428. Lane# 1 and 2 showed the PCR product of SIP-428 fragment for homolog silencing and silencing respectively. Amplified fragments visualized on a 1.5% agarose gel

Cloning of SIP-428 into pDONR221 by BP Reaction

PCR amplified fragments were gel extracted and purified. The purified fragment was cloned into pDONR221 by BP reaction and transformed into chemically competent Top 10 *E. coli* cells by the heat shock method.

Isolation of pDONR221-SIP-428 Plasmid DNA

Transformed cells were selected on LB plates containing 100µg/ml kanamycin. The presence of SIP-428 fragment for silencing and homolog silencing in the entry plasmid (pDONR221-SIP-428) was verified by colony PCR (M13 and DK 664 for SIP-428 silencing, M13 and DK 668 for SIP-428 homolog silencing). Results showed the presence of SIP-428 fragment in the silencing (Figure 35A) and homolog silencing (Figure 35B) entry plasmid respectively.

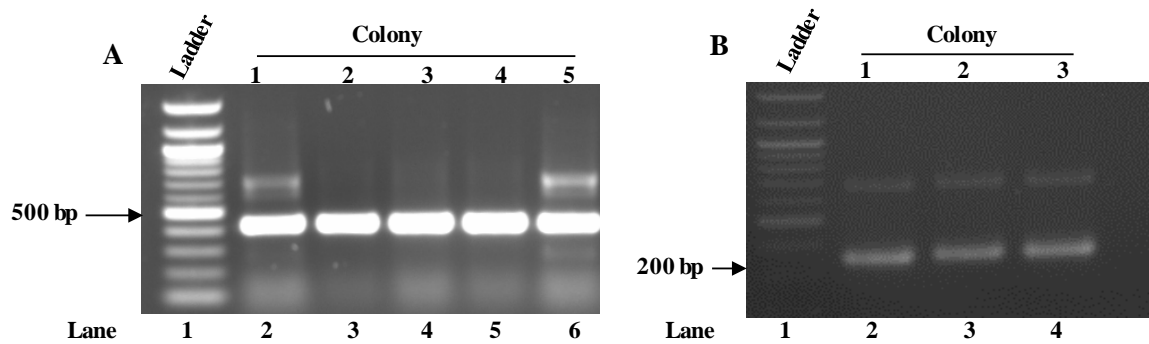


Figure 35: Colony PCR of pDONR221 entry plasmid. The SIP-428 fragment for silencing in entry plasmid (lane# 2-6: 402 bp) (A). The SIP-428 fragment for homolog silencing in entry plasmid (lane# 2-4: 202 bp) (B).

Sequencing of Entry Plasmid (pDONR221)

Plasmids DNA from positive entry clones for both silencing and homolog silencing were isolated, purified and quantified. The DNA sequence of entry plasmid (pDONR221-SIP-428) was verified by sequencing and aligned with SIP-428 cDNA sequence (Figure 36). Verified entry plasmid (pDONR221-SIP-428) was used for further experiments.

A

```

SIP-428 -----AACCAGCTTTCTGTAC 18
PH8-silencing-Clone-1 ATCTAATTTAATATATTGATATTTATATCATTTCGTTCTCGTTTCAGCTTTCTGTAC 120
                        .. *****

SIP-428 AAGTGGTCTCGAGGAATTCGGTACCCAGCTTGGTAAGGAAATAATTATTTCTTTTT 78
PH8-silencing-Clone-1 AAGTGGTCTCGAGGAATTCGGTACCCAGCTTGGTAAGGAAATAATTATTTCTTTTT 180
*****

SIP-428 CCTTTAGTATAAAATAGTTAAGTGATGTTAATTAGTATGATTATAATAATATAGTTGTT 138
PH8-silencing-Clone-1 CCTTTAGTATAAAATAGTTAAGTGATGTTAATTAGTATGATTATAATAATATAGTTGTT 240
*****

SIP-428 ATAATTGTGAAAAATAATTTATAAATATATTGTTTACATAAACACATAGTAATGTAAA 198
PH8-silencing-Clone-1 ATAATTGTGAAAAATAATTTATAAATATATTGTTTACATAAACACATAGTAATGTAAA 300
*****

SIP-428 AAAATATGACAAGTGATGTGTAAGACGAAGAAGATAAAAGTTGAGAGTAAGTATATTATT 258
PH8-silencing-Clone-1 AAAATATGACAAGTGATGTGTAAGACGAAGAAGATAAAAGTTGAGAGTAAGTATATTATT 360
*****

SIP-428 TTTAATGAATTTGATCGAACATGTAAGATGATATACTAGCATTAAATATTGTTTAAATCA 318
PH8-silencing-Clone-1 TTTAATGAATTTGATCGAACATGTAAGATGATATACTAGCATTAAATATTGTTTAAATCA 420
*****

SIP-428 TAATAGTAATTTCTAGCTGGTTTGATGAATTAATATCAATGATAAAAATACTATAGTAAA 378
PH8-silencing-Clone-1 TAATAGTAATTTCTAGCTGGTTTGATGAATTAATATCAATGATAAAAATACTATAGTAAA 480
*****

SIP-428 ATAAGAATAAATAAATTAATAATATTTTTTTATGATTAATAGTTTATTATATAATTAA 438
PH8-silencing-Clone-1 ATAAGAATAAATAAATTAATAATATTTTTTTATGATTAATAGTTTATTATATAATTAA 540
*****

SIP-428 ATATCTATACCATTACTAATAATTTTTAGTTTAAAAGTT 498
PH8-silencing-Clone-1 ATATCTATACCATTACTAATAATTTTTAGTTTAAAAGTT 600
*****

```

B

```

pH8Homologsilencecolony1 GTTTGTACANAAGCAGGCTATAGTACCAAGCTTGTGTATTGACGGGAGC 50
SBIP-428 -----AGTACCAAGCTTGTGTATTGACGGGAGC 29
                        *****

pH8Homologsilencecolony1 TGGCATGAGCACAGAGAGTGGAAATCCGGATTACAGGAGCCCAAATGGAG 100
SIP-428 TGGCATGAGCACAGAGAGTGGAAATCCGGATTACAGGAGCCCAAATGGAG 79
*****

pH8Homologsilencecolony1 CATATAGTACTGGTTTCAAACCAATTACCCATCAGGAGTTTCTCCGATCA 150
SIP-428 CATATAGTACTGGTTTCAAACCAATTACCCATCAGGAGTTTCTCCGATCA 129
*****

pH8Homologsilencecolony1 AGCAAGGCTCGAAGGCGTTATTGGACACGGAGTTATGCTGGCTGGAGACG 200
SIP-428 AGCAAGGCTCGAAGGCGTTATTGGACACGGAGTTATGCTGGCTGGAGACG 179
*****

pH8Homologsilencecolony1 TTTCAGTCTAACCAGCTTCTTGTACAAAGTGGTCTAGAGGATCCAAG 250
SIP-428 TTTCAGTCT----- 187
*****

```

Figure 36: Sequence alignment of entry plasmid (pDONR221) with the SIP-428 cDNA sequence. The sequence alignment of the SIP-428 fragment for silencing construct (A). The sequence alignment of the SIP-428 fragment for homolog silencing construct (B). Matching sequences were indicated with a star below the sequence.

Cloning of SIP-428 (Silencing and Homolog Silencing) into pHELLSGATE8

SIP-428 was subcloned into the destination plasmid pHELLSGATE8 from the verified entry plasmid by LR reaction. It allowed transfer of DNA sequences flanked by attL1 and attL2 from entry plasmid into destination vector pHELLSGATE8 with attR1 and attR2 sites. After the LR reaction, two microliters of LR reaction mixture was transformed into chemically competent Top 10 *E. coli* cells by the heat shock method.

Transformed cells were selected by growing in LB agar plate with 100µg/ml of spectinomycin. Colony PCR was done to screen the presence of SIP-428 fragment for silencing and homolog silencing in destination plasmid (pHELLSGATE8). The result showed a presence of SIP-428 fragments in the destination plasmid (Figure 37).

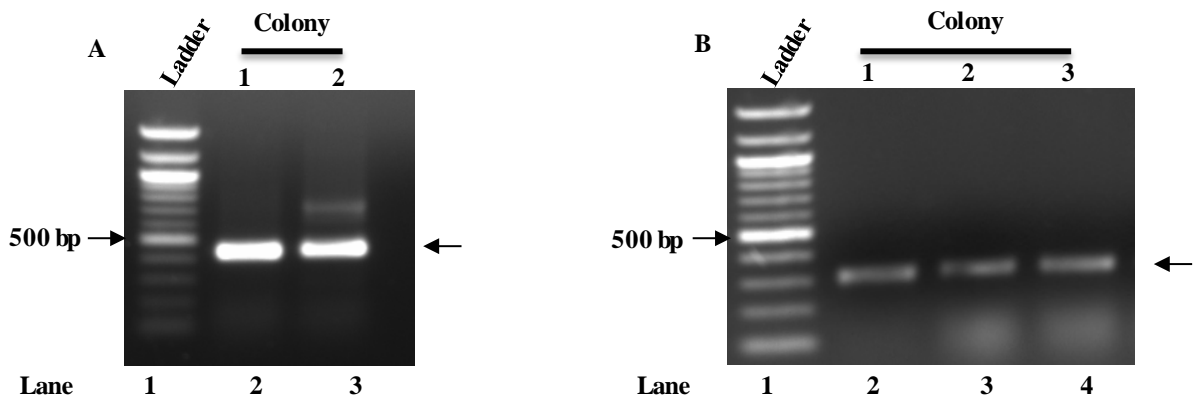


Figure 37: Colony PCR of destination plasmid (pHELLSGATE8). A, the presence of SIP-428 fragment for silencing construct (lane# 2-3). B, the presence of SIP-428 fragment for homolog silencing construct (lane# 2-4).

Isolation of pHELLSGATE8-SIP-428 Plasmid DNA

Plasmid DNA was extracted and purified from positive destination clone (silencing and homolog silencing). Verified destination plasmid was transformed into electrocompetent

Agrobacterium cells, and selected in LB agar plate with 100 µg/ml of spectinomycin.

Transformed Agrobacterium was screened by colony PCR (Figure 38) and used for generating stable RNAi lines.

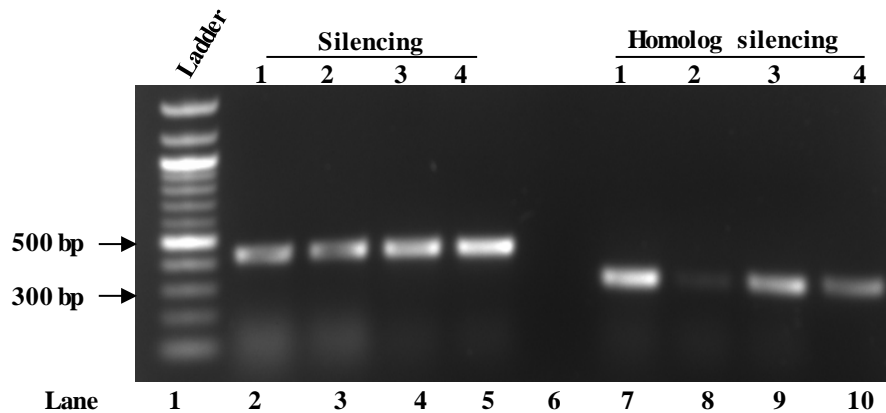


Figure 38: Colony PCR of transformed Agrobacterium. The amplification of SIP-428 fragment for silencing (lane# 2-5) and homolog silencing (lane# 7-10) in the transformed Agrobacterium respectively.

Screening of SIP-428 Silenced and Homolog Silenced Transgenic Lines

Transformation of the plants to generate stable transgenic lines were carried out using the leaf disk method. Transformed plants were grown in half MS media with kanamycin and cefotaxime antibiotics for the selection. Leaf disks (tissue samples) were collected from each transformed plant to determine the relative expression level of SIP-428 as compared to a wild-type plant (XNN). Expression of SIP-428 in wild-type considered as 100%. Total RNA extracted from the leaf tissue collected from each transformed lines were used for cDNA synthesis. The RT-PCR screening was done using the screening primer (Table 3) to select T1 generation of SIP-428 silenced, and homolog silenced lines. Results from RT-PCR screening showed SIP-428 silenced, and homolog silenced lines (Figure 39). Densitometric analysis was done to analyze the

degree of SIP-428 silencing as compared to the wild-type controls using actin as an internal standard (Figure 40). Positives transgenic lines were transferred to soil and grown to collect the seeds for a T2 generation.

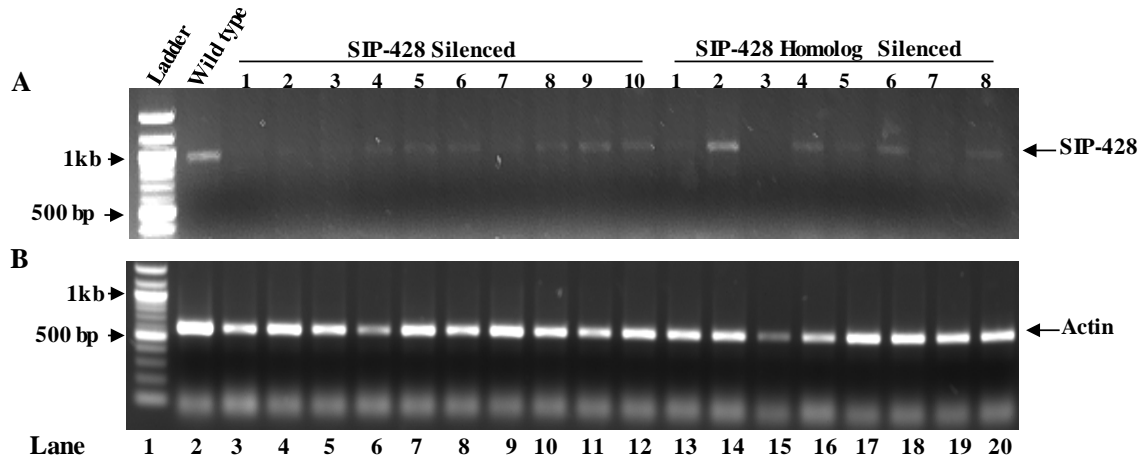


Figure 39: RT-PCR screening of SIP-428 silenced and homolog silenced lines. Panel A, RT-PCR results for silenced and homolog silenced plants and their relative level of expression of SIP-428 as compared to wild-type control with 100% expression level of SIP-428. Panel B, the expression of actin that serve as internal standard used for calibrating SIP-428 silencing level. Arrow indicates the expression of SIP-428 and actin with appropriate size.

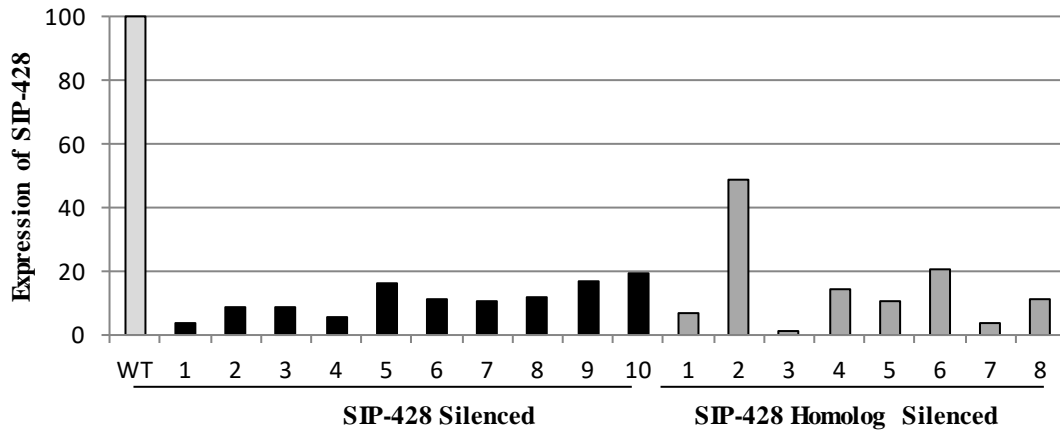


Figure 40: Densitometric analysis of the relative expression level of SIP-428 using UVB software. Expression of SIP-428 in wild-type control (WT) considered as 100%. T1 generation of transgenic lines shows a variable level (degree) of SIP-428 expression level as compared to wild-type control.

Based on the densitometric analysis T1 generation of SIP-428 silenced and homolog silenced lines shows more than 70% reduction in the expression of SIP-428 except line 2 of SIP-428 homolog silenced lines which exhibit around 50% reduction in the SIP-428 expression. T1 generation of the SIP-428 silenced lines (1, 2, 3, and 7) and homolog silenced lines (1, 2, 3, and 7) were kept to generate seeds for a T2 generation. SIP-428 homolog silenced lines 2 was also selected to be used as a control for the future experiment. Seeds from T1 generation lines were processed and sown in half MS media with kanamycin. Young T2 generation plants (2 weeks from sowing seeds to half MS media) were transferred to soil. Two to three weeks later leaf disk samples were collected and processed for total RNA extraction followed by cDNA synthesis. The expression of SIP-428 was detected by RT-PCR to screen the T2 generation of SIP-428 silenced lines (Figure 41 and 42).

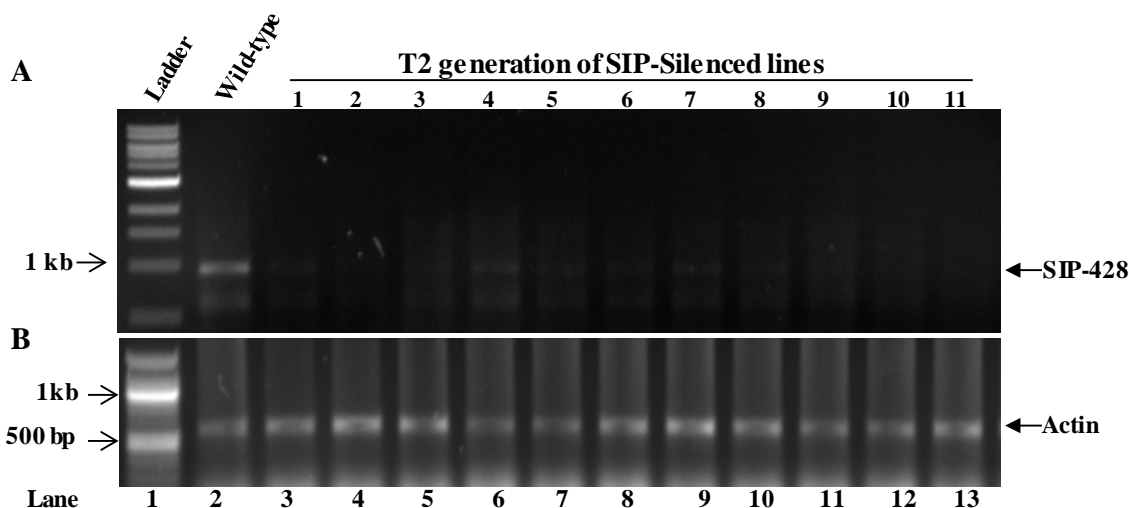


Figure 41: RT-PCR screening of T2 generation of SIP-428 silenced lines. Panel A RT-PCR results for silenced plants and their relative level of expression of SIP-428 (lane# 3-13) compared to wild-type control with 100% expression level of SIP-428 (lane# 2). Panel B the expression of actin that served as internal standard for calibrating SIP-428 silencing level. Arrow indicates the expression of SIP-428 and actin with appropriate size

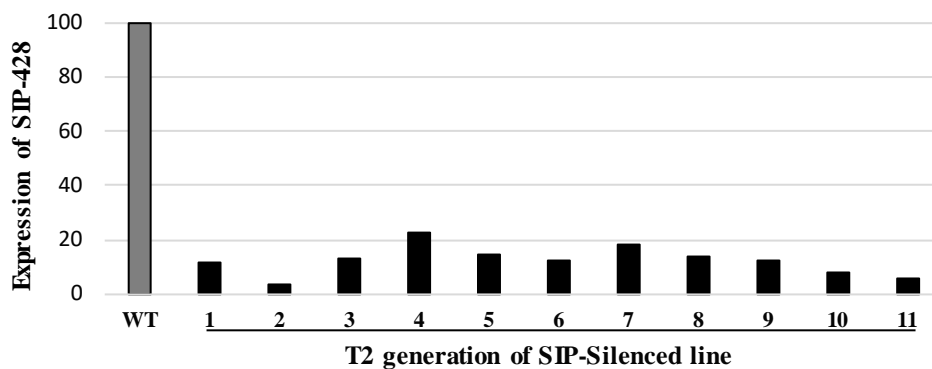


Figure 42: Densitometric analysis of the relative expression level of SIP-428 using UVB software. Expression of SIP-428 in wild-type control (WT) considered as 100%. T2 generation of transgenic lines shows a variable level of SIP-428 expression level as compared to wild-type control.

T2 generation of SIP-428 silenced lines showed a variable degree of SIP-428 expression level, so we decided to work on the T3 generation of SIP-428 silenced and homolog silenced

lines. Seeds from T2 generation (line 2, 3, 10, and 11) collected and used for further experiments. As we focused on SIP-428 but not on its homolog, we decided to use SIP-428 silenced lines only for further experiments. Seeds from single T2 generation plants (MS1-2: label created for the silenced line) were used for further experiments. Seeds were grown and screened in a similar methodology for the T1 generation. Results showed that T3 generation of SIP-428 silenced lines exhibit more than 90% reduction in the SIP-428 expression compare to wild-type (Figure 43 and 44). Verified T3 generation of SIP-428 silenced lines were used for further experiments.

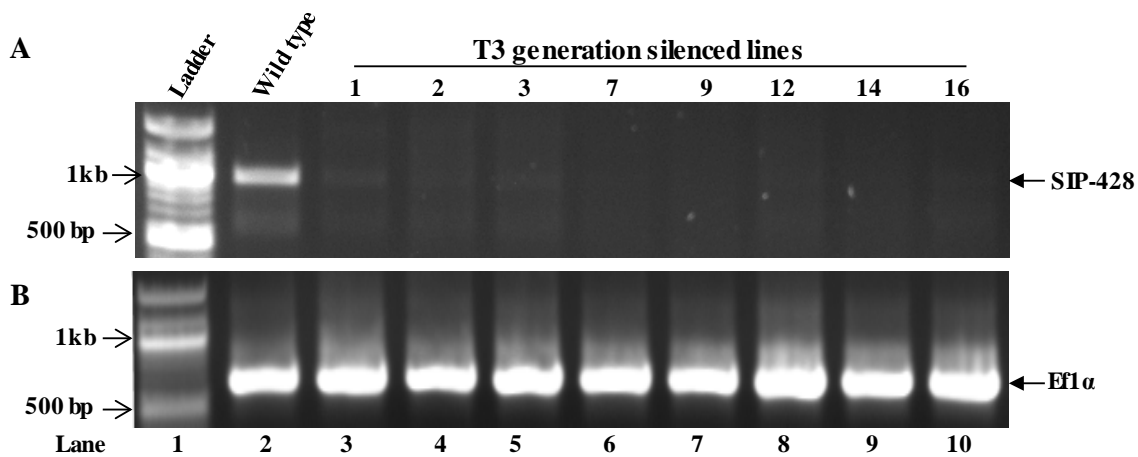


Figure 43: RT-PCR screening of T3 generation of SIP-428 silenced plants. Panel A, RT-PCR results for silenced plants and their relative level of expression of SIP-428 (lane# 3-10) compared to wild-type control with 100% expression level of SIP-428 (lane# 2). Panel B, the expression of Efl α that served as an internal standard for calibrating SIP-428 silencing level. Arrow indicates the expression of SIP-428 and Efl α with the appropriate size.

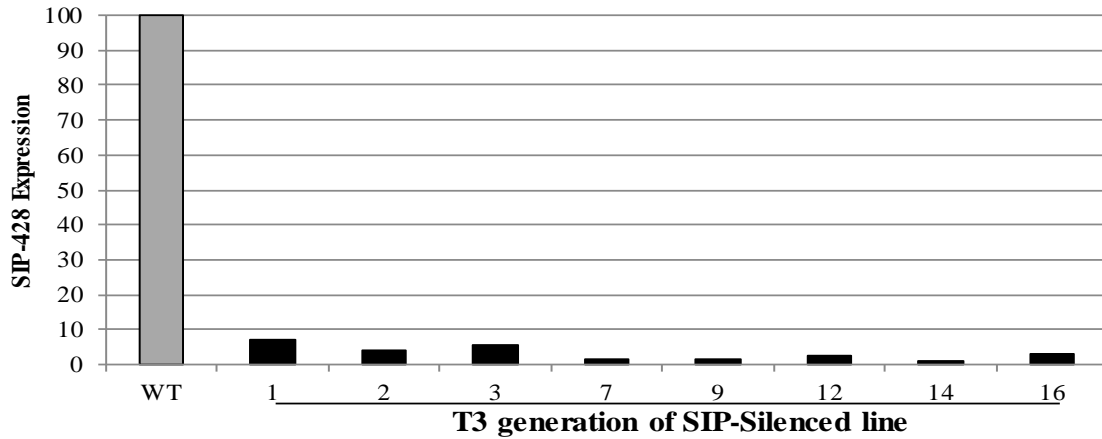


Figure 44: Densitometric analysis of the relative expression level of SIP-428 using UVB software. Expression of SIP-428 in wild-type control (WT) considered as 100%. T3 generation of transgenic lines showed a consistent level (degree) of SIP-428 expression level as compared to wild-type control.

Role of SIP-428 in SABP2 Expression

The expression level of SABP2 in a verified T3 generation of SIP-428 silenced lines were determined by RT-PCR (Figure 45) to test the role of SIP-428 in SABP2 expression. Results showed no difference in expression level of SABP2 in SIP-428 silenced lines.

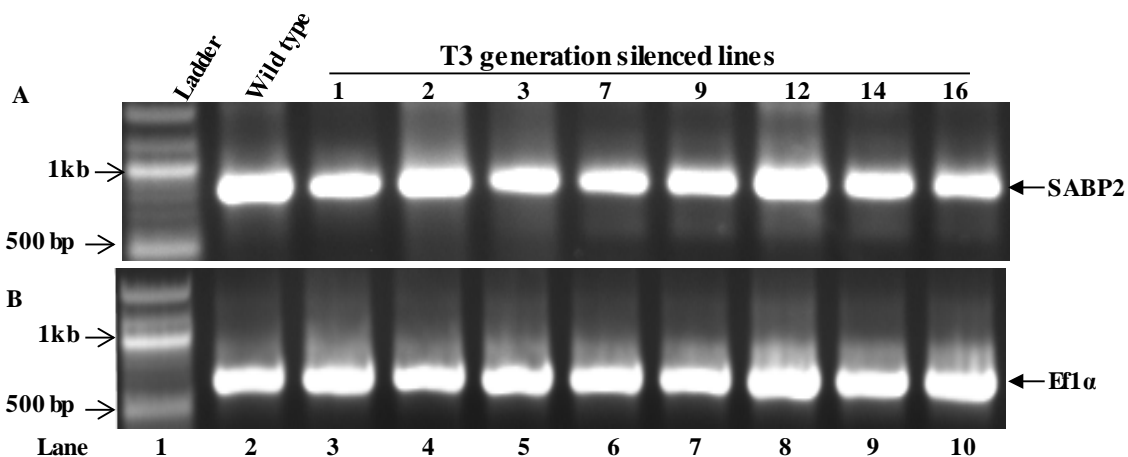


Figure 45: Expression of SABP2 in the T3 generation of SIP-428 silenced line. Panel A, relative expression level of SABP2 in SIP-428 silenced lines (lane# 3-10) compared to wild-type control (lane# 2). Panel B, the expression level of Efl α which served as the internal standard.

Role of SIP-428 in Biotic Stress Using Silenced Lines

SIP-428 Negatively Regulates Basal Resistance

Role of SIP-428 in basal resistance was investigated by bacterial growth assay on SIP-428 silenced plants. *Pseudomonas syringae* pv *tabaci* (*Pst*) is a virulent tobacco pathogen. Results of this experiment showed that SIP-428 silenced plants had significantly reduced *Pst* growth (CFU) as compared to the wild-type control on 3 DPI (Table 12 and 13 Figure 46 and 47). At 3 DPI wild-type XNN allowed growth of *Pst* to 6.1×10^9 CFU while SIP-428 silenced lines allowed growth of *Pst* to 2.1×10^9 CFU. Results from this experiment showed that SIP-428 silenced lines were significantly more resistant to pathogen infections as compared to wild-type controls ($P < 0.05$). These results indicated SIP-428 might negatively regulate basal resistance in plants.

Table 12: The bacterial growth of *Pseudomonas syringae* pv *tabaci* (CFU/ml) on three days post-infection (3DPI) of wild-type (WT) and SIP-428 silenced lines.

	Wild-type	SIP-428 Silenced
Average	4033333333	1500000000
Standard deviation	2250462915	141421356

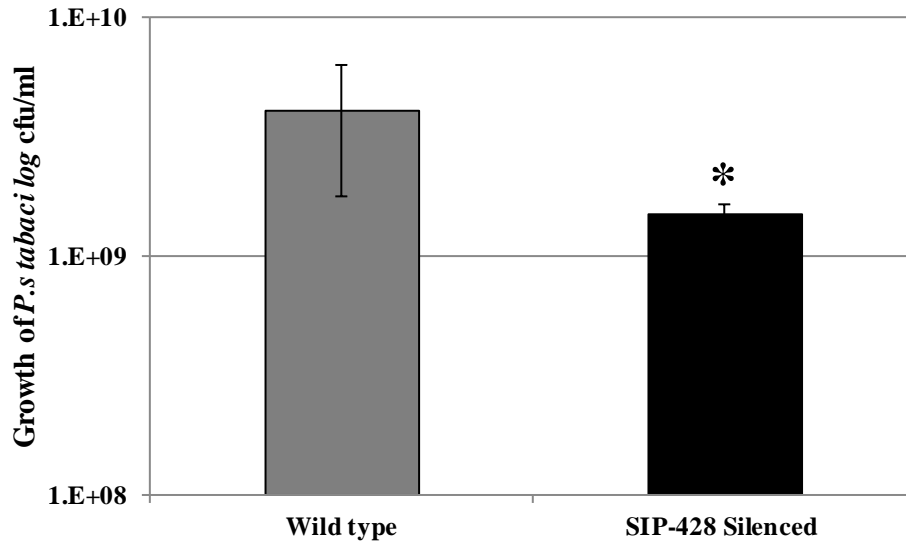


Figure 46: Bacterial growth assay of SIP-428 silenced lines and wild-type (WT). Bar diagram show average CFUs of *Pst* in SIP-428 silenced lines (black) and the wild type (gray) at 3DPI with standard deviation ($P < 0.05$).

Table 13: The bacterial growth of *Pseudomonas syringae* pv *tabaci* (CFU/ml) on three days post-infection (3DPI) of wild-type (WT) and SIP-428 silenced lines.

	Wild-type	SIP-428 silenced
Average	4833333333	2000000000
Standard deviation	1576740661	707106781

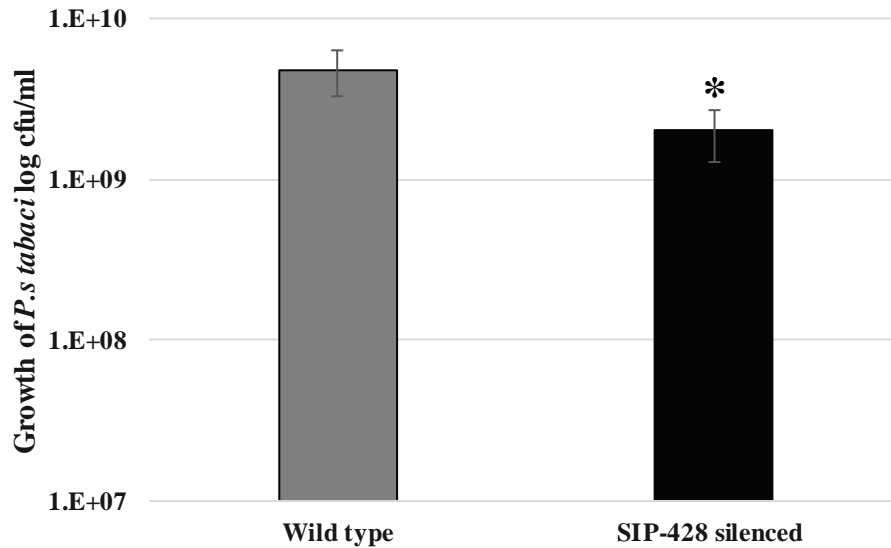


Figure 47: Bacterial growth assay of SIP-428 silenced lines and wild-type (WT). Bar diagram show average CFUs of *Pst* in SIP-428 silenced lines (black) and the wild type (gray) at 3DPI with standard deviation ($P < 0.05$).

SIP-428 Negatively Regulates SAR

The role of SIP-428 in SAR was investigated by infecting SIP-428 silenced lines and wild-type (WT) with tobacco mosaic virus (TMV). T3 generation lines of SIP-428 silenced lines were used after RT-PCR screening along with wild-type as a control. Induction of SAR resulted in a decreased size of TMV necrotic lesions in a secondary infection (Table 14 and 15). High concentration of TMV virus was used for primary infection, and tenfold diluted TMV virus used for secondary infection. Results of this experiment showed that in SAR induced wild-type plant, the size of TMV necrotic lesion in a secondary infection was 1.85 ± 0.52 mm while the size of TMV necrotic lesion in SAR induced SIP-428 silenced lines was significantly reduced to 0.78 ± 0.35 mm ($P < 0.05$) (Table 14 and 15 and Figure 48 and 49). These results indicated SIP-428 silenced lines showed significantly higher SAR response as compared to wild-type control.

Table 14: Average size of TMV necrotic lesion (mm).

	Wild-type	SIP-428 Silenced lines		
		#1	#2	#3
Average (mm)	1.85	0.79	0.82	0.66
STD	0.52	0.35	0.41	0.31

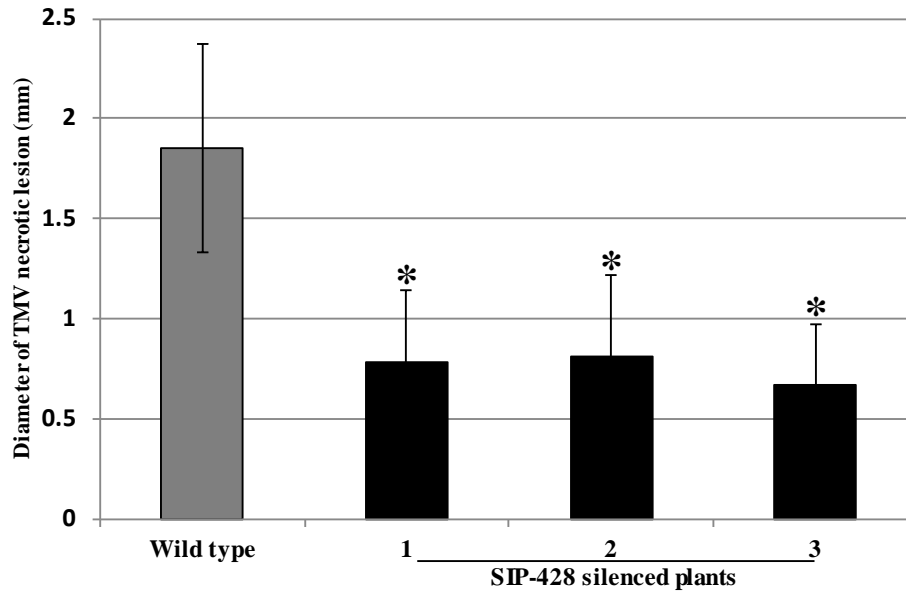


Figure 48: Systemic acquired resistance in SIP-428 silenced lines. Bar diagram shows the average diameter of TMV lesion size with standard deviation in wild-type (gray), and SIP-428 silenced plants (black). Three independent SIP-428 silenced lines (1, 2, and 3) and multiple wild-type controls were used ($P < 0.05$).

Table 15: Average size of TMV necrotic lesion (mm).

	Wild-type	SIP-428 silenced lines	
		#1	#2
Average (mm)	1.91	0.69	0.73
STD	0.23	0.31	0.33

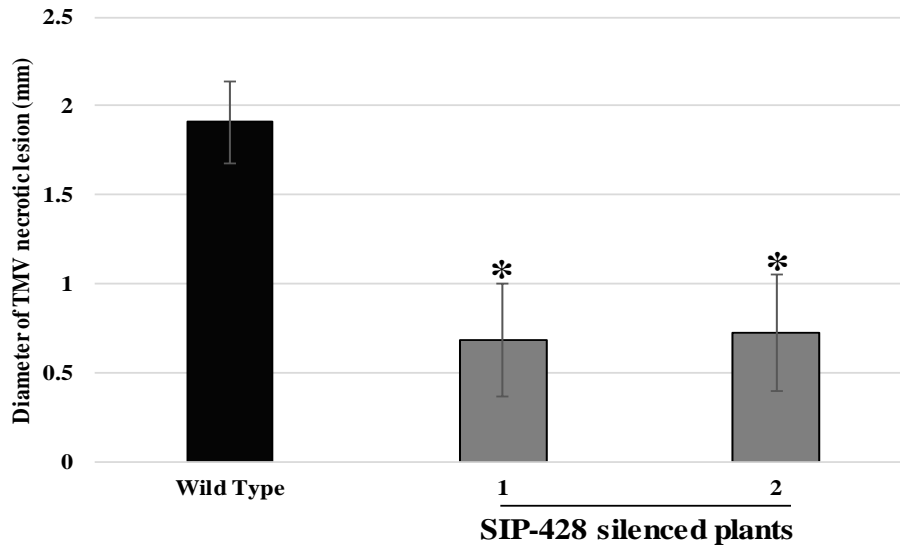


Figure 49: Systemic acquired resistance in SIP-428 silenced lines. The figure shows the average diameter of TMV lesion size with standard deviation in wild-type, and SIP-428 silenced plants. Three independent SIP-428 silenced lines (1 and 2) and multiple wild-type controls were used (t-test, $P < 0.05$).

Role of SIP-428 in SABP2 Dependent Signaling Pathway

To understand the role of SIP-428 in SABP2 signaling pathway 2,2,2,2'-tetra-fluoroacetophenone (tetra FA), a synthetic SA analog that inhibits the methylsterase activity of SABP2 was used in bacterial growth assay (Park *et al.* 2007). Verified T3 generation SIP-428 silenced lines (SIP-428-1-2 or MS1-2), and wild-type controls were used. SIP-428 silenced lines treated with tetra FA act as SIP-428 silenced lines without SABP2 activity. The growth of *Pseudomonas syringae* pv *tabaci* (*Pst*) was measured at three days post-infection (3 DPI).

Plants were divided into three groups. Plants without any treatment were labeled as 'untreated,' plants treated with a buffer but without tetra FA was labeled as 'mock,' and plants treated with tetra FA were labeled as 'Tetra FA treated.' No difference was observed in the

growth of *Pst*(CFUs) between untreated (wild-type 1.4×10^8 CFU and SIP-428 silenced lines 5.7×10^7 CFU) and mock groups of the plants (wild-type 1.2×10^8 CFU and SIP-428 silenced lines 4.5×10^7 CFU) which indicated buffer did not affect plant immune system (Table 16 and Figure 50). Susceptibility of wild-type plants treated with tetra FA (wild-type 7×10^8 CFU) was similar to the previous finding where SABP2 silenced lines were compromised in basal resistance and SAR (Kumar and Klessig 2003; Forouhar *et al.* 2005; Park *et al.* 2009).

Treatment of SIP-428 silenced lines with tetra FA did not affect basal resistance exhibited by SIP-428 silenced lines as number of *Pst* growth (CFU) in tetra FA treated SIP-428 silenced lines did not change as compared to untreated or mock-treated SIP-428 silenced lines (SIP-428 silenced line treated with tetra FA 5.4×10^7 CFU) (Table 16 and Figure 50). Results showed the methylsterase activity of SABP2 did not affect SIP-428 silenced plants in response to the pathogen infection. Taken together with results it showed that SIP-428 most likely acts upstream of SABP2 in the SA signaling pathway.

Table 16: The bacterial growth of *Pseudomonas syringae* pv *tabaci* (CFU/ml) on three days post-infection (3DPI) of wild-type (WT) and SIP-428 silenced lines (untreated, mock and tetra FA treated group).

	XNN untreated	428T3-Untreated	XNN Mock	428T3-Mock	XNN Tetra FA Treated	428T3-Tetra FA Treated
Average	137500000	57187500	116666666.7	45000000	700000000	54375000
STD	25000000	19003494.74	28867513.46	3779644.73	61871843.35	11490485.19

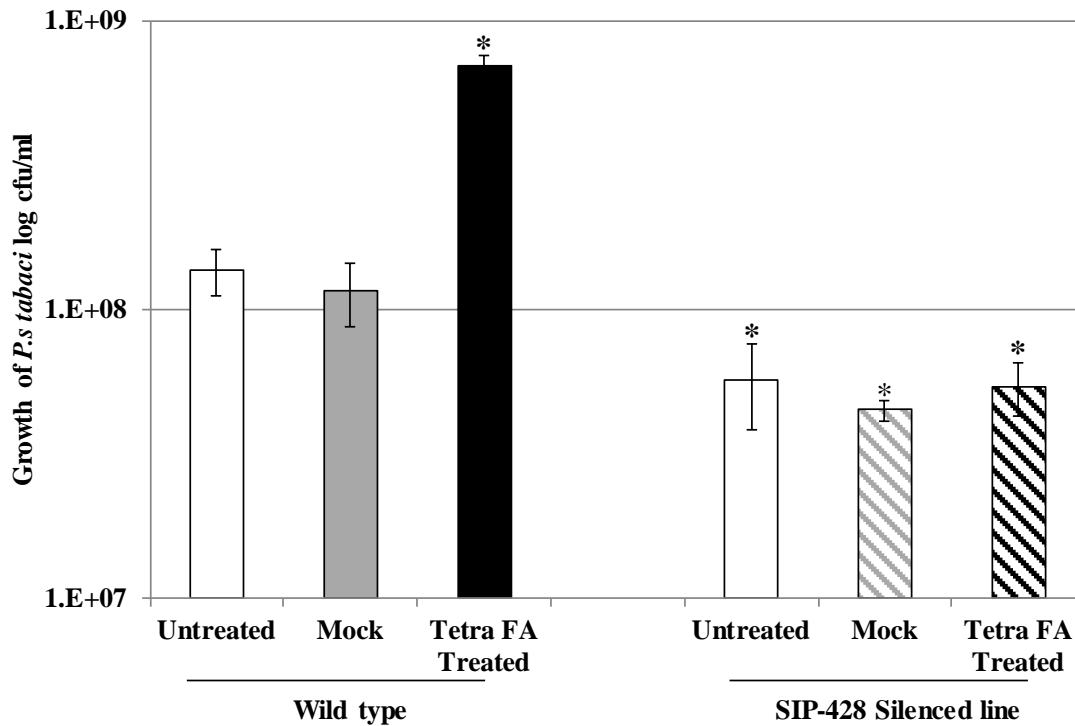


Figure 50: SIP-428 regulate the SABP2 signaling pathway. The *Pst* growth (log CFU/ml) in wild-type control and SIP-428 silenced lines. Wild-type plant treated with tetra FA shows a significantly increased number of CFU as compared to untreated and mock groups of plants. SIP-428 silenced lines showed a significantly reduced number of CFU/ml with and without tetra FA treatment ($p < 0.05$). White, gray and black bar diagram represent untreated, mock and Tetra FA treated group of the plants.

Generation of Inducible SIP-428 Overexpressing Transgenic Lines

An inducible transgenic line overexpressing SIP-428 was generated using the pER8 system with a myc tag to test the role of SIP-428 in biotic and abiotic stress. The pGEMT-Easy plasmid and pER8 plasmid were used as the entry and destination plasmid respectively.

PCR Amplification of SIP-428 Coding Sequence

SIP-428 overexpressing construct was generated by amplifying the full-length coding sequences of SIP-428 (Figure 51) from a verified plasmid (TOPO-SIP-428-1) using DK 682 and

DK 683 primers. Full-length SIP-428 was PCR amplified, gel extracted and purified (Figure 52A).

```
5' ATGTCCATGTCTCTTCGACTTTGTTGCGAACCCCTCAATTTCTGGCTTAAAGAATAAAAGAGATTTGCT
GGGCTTAGATTTGGCAGCTAATCATTTGAATATCCCAATGAGGAAATGGTTTAGTGGAGTAAAAAAGT
TCATTCCCTTTGAGGGATATGTAAAGTTTGTGCAAACAACAGCAAGAATAACATTTCCAAAGATCTCAT
CAGATTGTAAAGATAATTCCCCTTCGAATTTTTGAGTCACAAAAAGAAGGTTCCCTTATTCGGATCCCC
CTAGCATGAAAGATGTGGACAGTTTGTATGAATCTTTGATAGGAGTACCAAGCTTGTGTATTGACG
GGAGCTGGCATGAGCACAGAGAGTGGAAATCCGGATTACAGGAGCCCAAATGGAGCATATAGTACTG
GTTTCAAACCAATTACCCATCAGGAGTTTCTCCGATCAAGCAAGGCTCGAAGGCTTATTGGACACGG
AGTTATGCTGGCTGGAGACGTTTCACTGCAGCTCAACCTAGTACAGGTCATATAGCTCTATCATCTCTT
GAGAAAGCAGGCCATATAAGTTTTATGATTACACAGAATGTGGACAGGCTGCATCATCGGGCTGGCAG
CAATCCACTTGAATTGCATGGGACCGTCTACATTGTTGCCTGTACAAATTGTGGTTTTACTCTACCTCG
AGAAGTGTTC AAGATCAAGTGAAGGCTCAAAATCCTAAGTGGGCAGCAGCTATCGAAAGTTTGGATT
ATGACAGCCGATCAGACGAGAGCTTTGGTATGAAGCAAAGGCCTGATGGGGATATTGAGATCGATGA
GAAATTCTGGGAGGAGGATTTCTACATTCCTGATTGTGAGAGGTGCCAAGGAGTTCTCAAACCTGACG
TTGTCTTCTTTGGGGATAATGTCCCTAAAGCTAGAGCTGATGTTGCCATGGAAGCTGCAAAGGGATGT
GATGCCTTCTTGTACTTGGTTCATCTATGATGACCATGTCTGCTTCCGGCTTATCAAAGCTGCGCAC
GAGGCAGGCGCTGCGACTGCAATTGTAAATATTGGGGTGACACGAGCTGACGATCTTGTACCTTTGAA
AATTAATGCTCGAGTTGGAGAGATACTTCCAAGATTGCTTAATGTTGGATCCTTGAGTATCCCTGCTCT
CTAG3'
```

Figure 51: Verified nucleotides sequence of full-length SIP-428 cDNA. The 1164 nucleotide coding sequence was selected for overexpression.

Cloning of SIP-428 into pGEMT Plasmid

The purified full-length SIP-428 fragment was ligated with a pGEMT-Easy plasmid (would be referred to as pGEMT onward) and transformed into chemically competent Top 10 *E. coli* cells by the heat shock method. Transformed cells were selected in 100 µg/ml ampicillin and screened for the presence of SIP-428 by colony PCR using T7 forward primer and DK 683 reverse primer. The result showed the presence of SIP-428 in the pGEMT plasmid (Figure 52B).

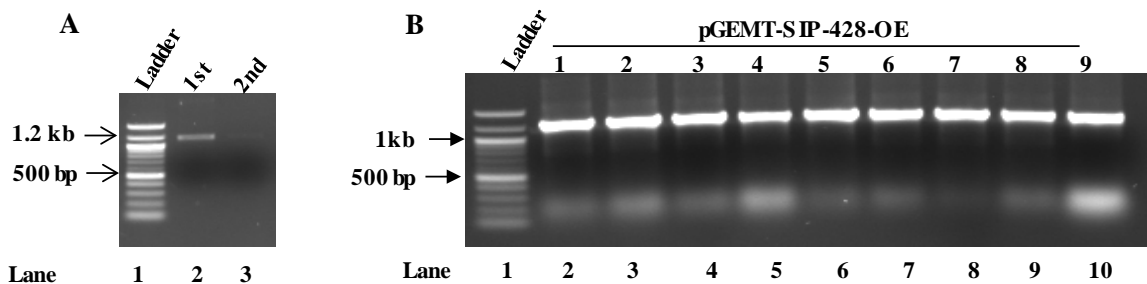


Figure 52: Generation of entry plasmid for SIP-428 overexpression. The first and second gel elution of PCR product of 428-OE with *AvrII* and *SpeI* restriction enzyme site (A). Colony PCR products with the SIP-428 insert in a pGEMT plasmid (B). All the transformed clones (B: lane# 2-10) showed the presence of SIP-428-OE fragment.

Sequencing of Recombinant pGEMT-SIP-428-OE Plasmid

Plasmid DNA from positive transformed cells was extracted (Figure 53), quantified, and sequenced. The sequence of entry clones was aligned with verified SIP-428 cDNA template. Results showed a complete matching sequence of SIP-428 overexpression fragment in the entry plasmid (pGEMT-SIP-428-OE) when aligned with a verified SIP-428 cDNA template (Figure 54).

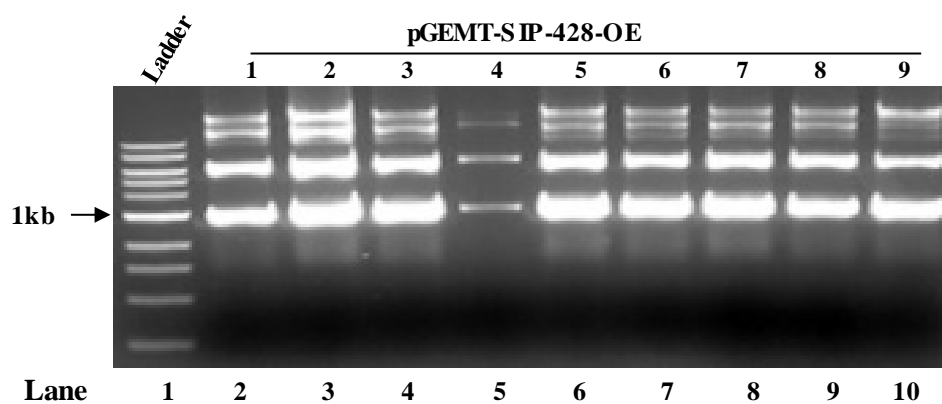


Figure 53: Isolation of plasmid DNA from the positive entry clones. The plasmid DNA (pGEMT-SIP-428-OE: lane# 2-10) visualized on 1.0% agarose gel with an EtBr.

Clone-sequence SIP-428	AGCCTACTAAGGGACTAGTCCTGCAGGTTTAAACGAATTTCGCCCTTCTTAGGTATGTCC -----ATGTCC *****	60 6
Clone-sequence SIP-428	ATGTCTCTCGACTTTGTGCGAACCCCTCAATTTCTGGCTTAAAGAATAAAAGAGATTG ATGTCTCTCGACTTTGTGCGAACCCCTCAATTTCTGGCTTAAAGAATAAAAGAGATTG *****	120 66
Clone-sequence SIP-428	CTGGGCTTAGATTGGCAGCTAATCATTGAATATCCCAATGAGGAAATGGTTTAGTGGA CTGGGCTTAGATTGGCAGCTAATCATTGAATATCCCAATGAGGAAATGGTTTAGTGGA *****	180 126
Clone-sequence SIP-428	GTAAAAAGTTTCATTCCTTTGAGGGATATGTTAAGTTGTGCAAACAACAGCAAGAATA GTAAAAAGTTTCATTCCTTTGAGGGATATGTTAAGTTGTGCAAACAACAGCAAGAATA *****	240 186
Clone-sequence SIP-428	ACATTTCCAAAGATCTCATCAGATTGTAAGATAAATCCCCTTCGAATTTTTTGAGTCAC ACATTTCCAAAGATCTCATCAGATTGTAAGATAAATCCCCTTCGAATTTTTTGAGTCAC *****	300 246
Clone-sequence SIP-428	AAAAAGAAGGTTCTTATTCGGATCCCCTAGCATGAAAGATGTGGACAGTTTGTATGAA AAAAAGAAGGTTCTTATTCGGATCCCCTAGCATGAAAGATGTGGACAGTTTGTATGAA *****	360 306
Clone-sequence SIP-428	TTCTTTGATAGGAGTACCAAGCTGTTGTATTGACGGGAGCTGGCATGAGCACAGAGAGT TTCTTTGATAGGAGTACCAAGCTGTTGTATTGACGGGAGCTGGCATGAGCACAGAGAGT *****	420 366
Clone-sequence SIP-428	GGAATTCGGATTACAGGAGCCCAAATGGAGCATATAGTACTGGTTTCAAACCAATTACC GGAATTCGGATTACAGGAGCCCAAATGGAGCATATAGTACTGGTTTCAAACCAATTACC *****	480 426
Clone-sequence SIP-428	CATCAGGAGTTTCTCCGATCAAGCAAGGCTCGAAGGCGTTATTGGACACGGAGTTATGCT CATCAGGAGTTTCTCCGATCAAGCAAGGCTCGAAGGCGTTATTGGACACGGAGTTATGCT *****	540 486
Clone-sequence SIP-428	GGTGGAGACGTTTCACTGCAGCTCAACCTAGTACAGGTCATATAGCTCTATCATCTCTT GGTGGAGACGTTTCACTGCAGCTCAACCTAGTACAGGTCATATAGCTCTATCATCTCTT *****	600 546
Clone-sequence SIP-428	GAGAAAGCAGGCCATATAAGTTTATGATTACACAGAATGTGGACAGGCTGCATCATCGG GAGAAAGCAGGCCATATAAGTTTATGATTACACAGAATGTGGACAGGCTGCATCATCGG *****	660 606
Clone-sequence SIP-428	GCTGGCAGCAATCCACTTGAATTGCATGGGACCGTCTACATTGTTGCCTGTACAAATTGT GCTGGCAGCAATCCACTTGAATTGCATGGGACCGTCTACATTGTTGCCTGTACAAATTGT *****	720 666
Clone-sequence SIP-428	GGTTTTACTCTACCTCGAGAAGTCTTCAAGATCAAGTGAAGGCTCAAATCCTAAGTGG GGTTTTACTCTACCTCGAGAAGTCTTCAAGATCAAGTGAAGGCTCAAATCCTAAGTGG *****	780 726
Clone-sequence SIP-428	GCAGCAGCTATCGAAAGTTGGATTATGACAGCCGATCAGACGAGAGCTTTGGTATGAAG GCAGCAGCTATCGAAAGTTGGATTATGACAGCCGATCAGACGAGAGCTTTGGTATGAAG *****	840 786
Clone-sequence SIP-428	CAAAGGCCTGATGGGGATATTGAGATCGATGAGAAATCTGGGAGGAGGATTTCTACATT CAAAGGCCTGATGGGGATATTGAGATCGATGAGAAATCTGGGAGGAGGATTTCTACATT *****	900 846
Clone-sequence SIP-428	CCTGATTGTGAGAGGTGCCAAGGAGTTCTCAAACCTGACGTTGTCTTCTTTGGGGATAAT CCTGATTGTGAGAGGTGCCAAGGAGTTCTCAAACCTGACGTTGTCTTCTTTGGGGATAAT *****	960 906
Clone-sequence SIP-428	GTCCCTAAAGCTAGAGCTGATGTTGCCATGGAAGCTGCAAAGGATGTGATGCCTTCCTT GTCCCTAAAGCTAGAGCTGATGTTGCCATGGAAGCTGCAAAGGATGTGATGCCTTCCTT *****	1020 966

Clone-sequence SIP-428	GTACTTGTTTCATCTATGATGACCATGTCTGCTTCCGGCTTATCAAAGCTGCGCACGAG GTACTTGTTTCATCTATGATGACCATGTCTGCTTCCGGCTTATCAAAGCTGCGCACGAG *****	1080 1026
Clone-sequence SIP-428	GCAGGCGCTGCGACTGCAATTGTAAATATTGGGGTGACACGAGCTGACGATCTGTACCT GCAGGCGCTGCGACTGCAATTGTAAATATTGGGGTGACACGAGCTGACGATCTGTACCT *****	1140 1086
Clone-sequence SIP-428	TTGAAAATTAATGCTCGAGTTGGAGAGATACTCCAAGATTGCTTAATGTTGGATCCTTG TTGAAAATTAATGCTCGAGTTGGAGAGATACTCCAAGATTGCTTAATGTTGGATCCTTG *****	1200 1146
Clone-sequence SIP-428	AGTATCCCTGCTCTCTAGACTAGTAAGGGCGAATTCGCGGCCGCTAAATCATCGCCNT AGTATCCCTGCTCTCTAG----- *****	1258 1164

Figure 54: Sequence alignment of pGEMT-SIP-428-OE and SIP-428 cDNA. Sequence alignment revealed DNA sequence were identical as indicated by a star sign below the nucleotide sequence.

Cloning of SIP-428-OE into pER8 Plasmid

Sequence verified entry plasmid (pGEMT-SIP-428-OE), and the destination plasmid (pER8) were digested using AvrII and SpeI restriction enzymes. Digested products were gel purified (Figure 55). The digested fragments of SIP-428-OE (overnight digestion) was ligated with digested pER8 plasmid using T4 DNA ligase enzyme. The ligated mixture was incubated overnight at RT and transformed into chemically competent Top 10 *E. coli* by the heat shock method. Transformed cells were selected on LB agar plates with 100 µg/ml of spectinomycin. Positive clones were screened by colony PCR using DK 677 forward and DK 502 reverse primers (Figure 56). Results showed the successful cloning of SIP-428-OE fragment into the pER8 destination plasmid.

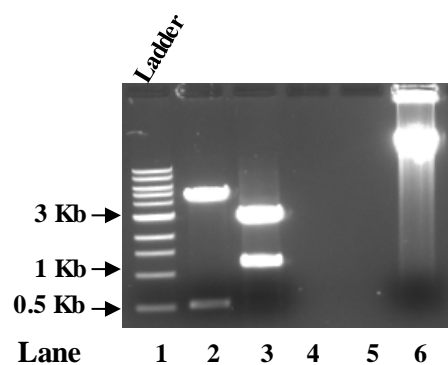


Figure 55: Restriction digestion of entry plasmid DNA and destination vector (pER8). 1.0% agarose gel electrophoresis shows digested fragment for overexpression at the expected size (lane# 3 and 6). Lane# 1; 1kb ladder, lane2# pGEMT (AvrII and SpeI digestion for 3 hrs at RT), lane# 3; pGEMT-428-OE (AvrII and SpeI digestion for overnight at RT) and lane# 6; pER8 (AvrII and SpeI digestion).

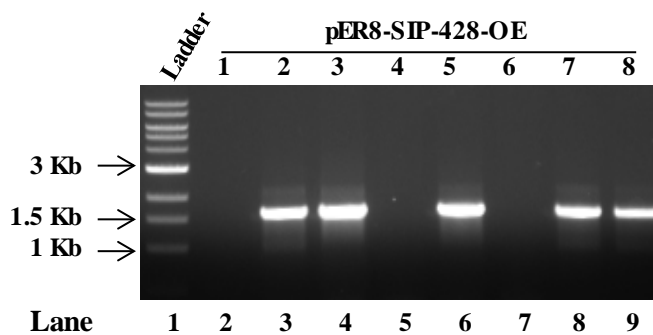


Figure 56: Colony PCR detection of pER8-SIP-428-OE. PCR amplified products of SIP-428-OE fragment in the pER8 plasmid (lane#3, 4, 6, 8 and 9) were visualized on 1.0% agarose gel containing EtBr stain.

Verification of Destination Plasmid (pER8-SIP-428-OE)

Plasmid DNA from the positive clone was isolated (Figure 57) and sequenced. Analysis showed that the nucleotide sequence of SIP-428-OE was in the right frame with pER8 plasmid as shown in Figure 58. The verified pER8- SIP-428-OE plasmid was transformed into competent *Agrobacterium* by the heat shock method and selected in LB agar plates with 100 µg/ml spectinomycin.

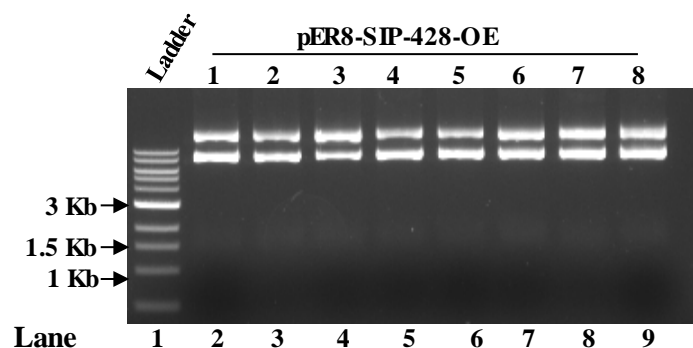


Figure 57: Isolation of plasmid DNA (pER8-SIP-428-OE) from *E. coli*. Plasmid DNA from positive destination clones containing the pER8-428-OE (lane# 2-9) was extracted and visualized on 1.0% agarose gel with EtBr stain.

5'GCAAGACCCTTCCTCTATATAAGGAAGTTCATTTCAATTTGGAGAGGACACGCTGAAGCTAGTCGACT
 CTAGCCTCGAGGCGCGCCGGGCCAGGCCTACGCGTTTAATTATTCAAAGCTATGGAGCAAAGCTCA
 TTTCTGAAGAGGACTTGAATGAAATGGAGCAAAGCTCATTCTGAAGAGGACTTGAATGAAATGGA
 GCAAAGCTCATTCTGAAGAGGACTTGAATGAAATGGAGCAAAGCTCATTCTGAAGAGGACTTGA
 ATGAAATGGAGAGCTTGGGGGACCTCACCATGGAGCAAAGCTCATTCTGAAGAGGACTTGAATTCG
 GTACCCCGGGTTCGAAATCGATGGATCCTACGTAGCCTAGGATATGTCCTCTTCGACTTTGTTC
 GAACCCTCAATTTCTGGCTTAAAGAATAAAAGAGATTTGCTGGGCTTAGATTTGGCAGCTAATCATTG
 AATATCCCAATGAGGAAATGGTTTAGTGGAGTAAAAAGTTTCATTCCCTTTGAGGGATATGTAAAGTT
 TGTGCAAACAACAGCAAGAATAACATTTCCAAAGATCTCATCAGATTGTAAAGATAATCCCCTTCGA
 ATTTTTTGTGATCACAAGGTTTCTTATTTCGGATCCCCCTAGCATGAAAGATGTGGACAGTTTGT
 ATGAATTCCTTTGATAGGAGTACCAAGCTTGTGTATTGACGGGAGCTGGCATGAGCACAGAGAGTGG
 ATTCCGGATTACAGGAGCCCAATGGAGCATATAGTACTGGTTTCAAACCAATTACCCATCAGGAGTT
 TCTCCGATCAAGCAAGGCTCGAAGGCGTTATTGGACACGGAGTTATGCTGGCTGGAGACGTTTCACTG
 CAGCTCAACCTAGTACAGGTACATATAGCTCTATCATCTCTTGGAGAAAGCAGGCCATATAAGTTTTATGA
 TTACACAGAATGTGGACAGGCTGCATCATCGGGCTGGCAGCAATCCACTTGAATTGCATGGGACCGTC
 TACATTGTTGCCTGTACAAATTGTGGTTTTACTCTACCTCGAGAAGTGTTCAGATCAAGTGAAGGCT
 CAAAATCCTAAGTGGGCAGCAGCTATCGAAAGTTTGGATTATGACAGCCGATCAGACGAGAGCTTTGG
 TATGAAGCAAAGGCTGATGGGGATATTGAGATCGATGAGAAATCTGGGAGGAGGATTTCTACATTC
 CTGATTGTGAGAGGTGCCAAGGAGTTCTCAAACCTGACGTTGTCTTCTTTGGGGATAATGTCCCTAAAG
 CTAGAGCTGATGTTGCCATGGAAGCTGCAAAGGGATGTGATGCCTTCCTTGTACTTGGTTTCATCTATGA
 TGACCATGTCTGCTTTCGGCTTATCAAAGCTGCGCACGAGGCAGGCGCTGCGACTGCAATTGTAAAT
 ATTGGGGTGACACGAGCTGACGATCTTGTACCTTTGAAAATTAATGCTCGAGTTGGAGAGATACTTCC
 AAGATTGCTTAATGTTGGATCCTTGAGTATCCCTGCTCTCTAGACTAGT3'

Figure 58: In frame cloning of SIP-428-OE in the pER8 plasmid. The start and stop codon denoted by red with an underline, while AvrII and SpeI restriction enzyme highlighted in bold red with a yellow background. Multiple Myc tag highlighted in green background.

Transient Expression of SIP-428 (pER8-SIP-428-OE) in *Nicotiana benthamiana*

Transient expression in *Nicotiana benthamiana* was performed to verify whether pER8-SIP-428-OE plasmid could express SIP-428 protein when induced with 50 μ M β -estradiol. Western blot analysis of SIP-428 transiently expressed in *Nicotiana benthamiana* confirmed successful expression of the SIP-428 protein (Figure 59).

The HcPro inhibits the endogenous gene-silencing mechanism of the plant that suppresses the expression of the exogenous protein (SIP-428 in this case) (Anandalakshmi *et al.* 1998; Kasschau and Carrington 1998). Therefore the HcPro was co-expressed along with pER8-SIP-428-OE for the transient expression of SIP-428 (Figure 59).

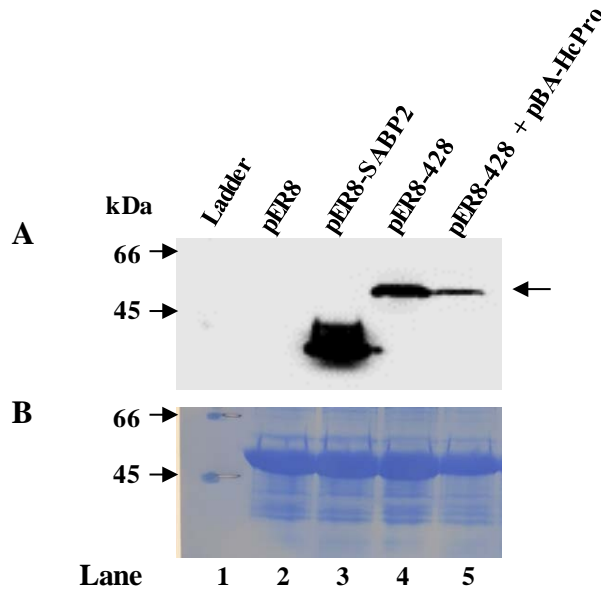


Figure 59: Transient expression of SIP-428 in *Nicotiana benthamiana*. Panel A, western blot using anti-myc tag antibody. Panel B, coomassie stained blot shows the loading control. The pER8 used as negative control (lane# 2), and pER8-SABP2 as a positive control (lane# 3). Lane# 4 and 5 shows the expression of SIP-428 in the absence and presence of pBA-HcPro respectively.

Generation of Stable SIP-428 Overexpressing Transgenic Lines

After verification of SIP-428 overexpressing construct, generation of stable SIP-428 overexpressing transgenic plants was done by the leaf disk method. Successfully transformed plants (T1 generation) overexpressing SIP-428 were selected in half MS media containing hygromycin. Leaf disk samples from each transgenic line were collected and induced with 50 μ M β -estradiol to express SIP-428. Western blot using an anti-myc tag antibody was used to screen the T1 generation of SIP-428 overexpressing lines (Figure 60). Positive lines were transferred to soil for generating seeds (lane 2 and 4). When a sample from line 13 (lane# 4) (Figure 60) was processed for a second western blot, it showed a single band that verified the SIP-428 overexpressing lines. T2 generations of SIP-428 overexpressing lines were used for further experiments.

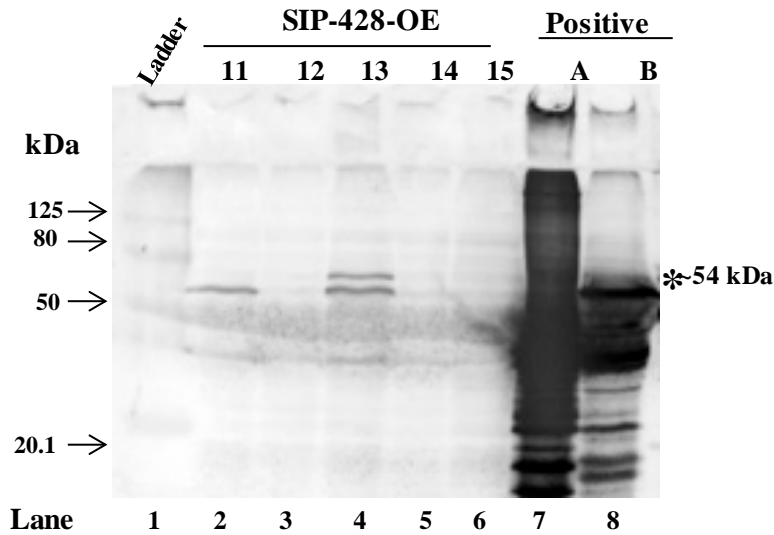


Figure 60: Western blot screening of T1 generation of SIP-428 overexpressing lines. Two positive lines (lane# 2 and 4) detected with the anti myc tag antibody. Sample A and B were used as positive controls (lane# 7 and 8).

Generation of T2 Generation of Stable SIP-428 Overexpressing Lines

Seeds from a positive T1 generation (Figure 60) were sown in the soil. Seeds from the single parental line of T1 generation of SIP-428 overexpressing line (pER8-428) was used to generate T2 generation lines for further experiments. Seedlings of individual plants were transferred to 4'x4' flat racks and grown until the 4-5 leaf stage was reached (up to 2-3 weeks). Two leaf disk (cork borer# 6) from the young healthy T2 generation of SIP-428 overexpressing lines were collected and induced with 50 μ M β -estradiol. Expression of SIP-428 was detected by western blot using anti-myc tag antibody (Figure 61). Positive lines of the T2 generation were used for the further experiment (lane# 5 and 7).

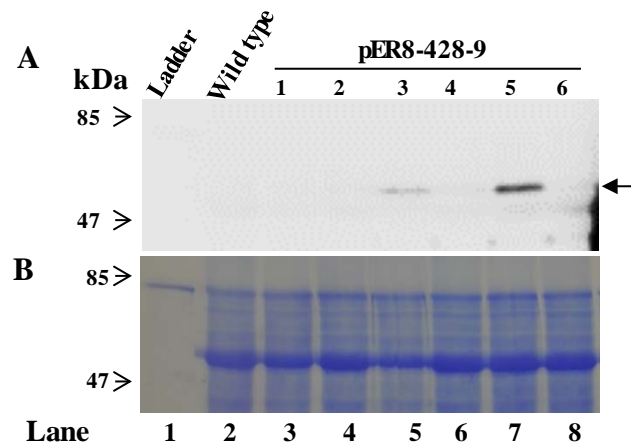


Figure 61: Western blot screening of T2 generation of SIP-428 overexpressing lines. Panel A, western blot with an anti-myc tag antibody. Panel B, the coomassie stained blot for protein loading control. Wild-type (lane# 2) was used as negative control to screen SIP-428 overexpression lines (lane# 3-8).

SIP-428 Overexpressing Lines and Biotic Stress

Overexpression of SIP-428 Compromised Basal Resistance

Role of SIP-428 in basal resistance was investigated by a bacterial growth assay. *Pseudomonas syringae* pv *tabaci* (*Pst*) is virulent tobacco pathogen. Results of this experiment showed that SIP-428 overexpressing plants allowed a significantly higher *Pst* growth (CFU/ml) as compared to wild-type control at three days post-infection (3 DPI). At 3 DPI wild-type (XNN) allowed growth of *Pst* to 5.2×10^8 CFU/ml while SIP-428 overexpressing lines allowed growth of *Pst* to 2.7×10^9 CFU/ml (Table 17 and 18 and Figure 62 and 63). Results showed SIP-428 overexpressing lines were significantly compromised to pathogen infections as compared to wild-type controls ($P < 0.05$). These results indicated SIP-428 negatively regulates basal resistance of plants.

Table 17: The bacterial growth of *Pseudomonas syringae* pv *tabaci* (CFU/ml) on three days post-infection (3DPI) of wild-type and SIP-428 overexpressing lines.

	Wild-type	SIP-428 overexpressing
Average	491666666	2331250000
STD	200346921	486135912

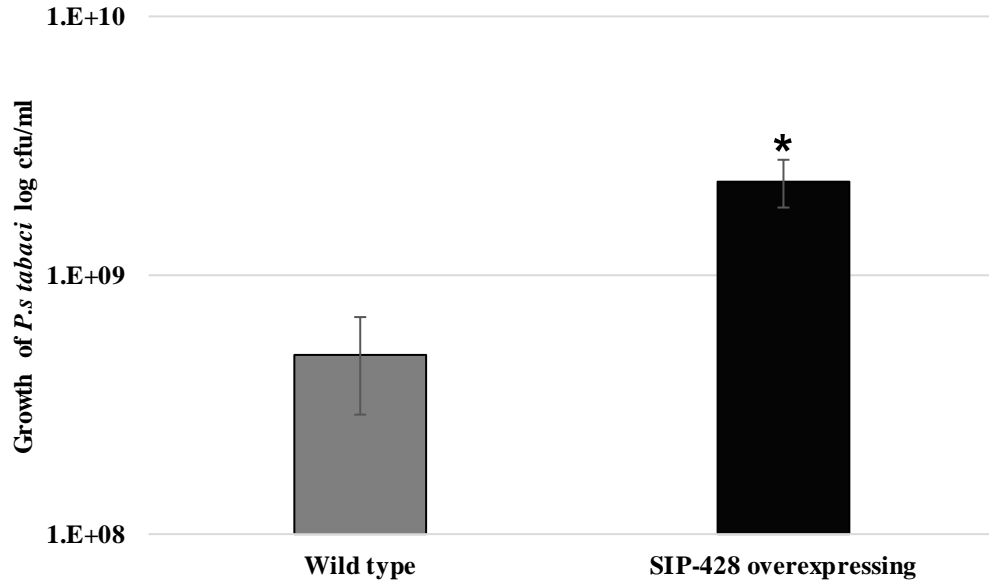


Figure 62: Bacterial growth assay of SIP-428 overexpressing lines and wild-type. Bar diagram shows the average of CFUs (*Pst*) in SIP-428 overexpressing lines (black) and the wild-type (gray) with standard deviation at 3DPI (P < 0.05).

Table 18: The bacterial growth of *Pseudomonas syringae* pv *tabaci* (CFU/ml) on three days post-infection (3DPI) of wild-type and SIP-428 overexpressing lines.

	Wild-type	SIP-428 overexpressing
Average	410000000	2100000000
Standard deviation	89442719	845576726

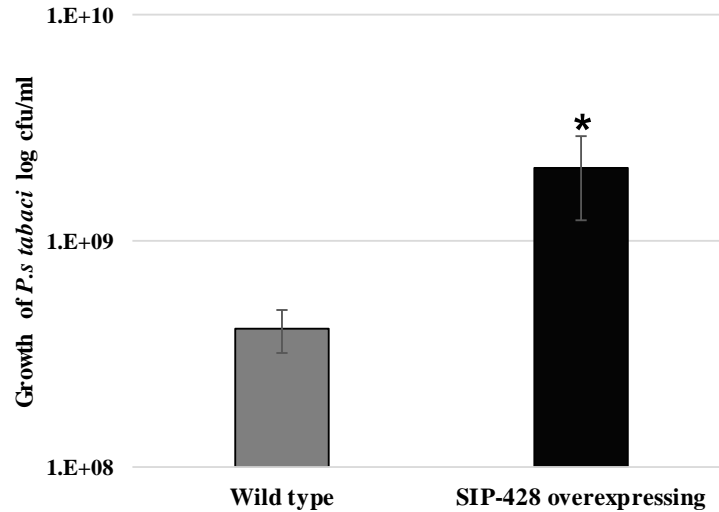


Figure 63: Bacterial growth assay of SIP-428 overexpressing lines and wild-type. Figures show CFU of *Pst* in SIP-428 overexpressing lines and the wild-type at 3DPI (t-test, $P < 0.05$).

Overexpression of SIP-428 Compromised SAR

The role of SIP-428 in SAR was investigated by infecting SIP-428 overexpressing lines and wild-type plants with Tobacco mosaic virus (TMV). T2 generations of SIP-428 overexpressing lines were used after screening (Figure 64: line 2,6 and 7). Induction of SAR resulted in a decreased size of TMV necrotic lesions in response to secondary infection. High concentration of TMV was used for primary infection, and tenfold diluted TMV was used for secondary infection. Results showed that wild-type plant TMV necrotic lesion was 2.17 ± 0.12 mm while the SAR induced wild-type plants showed TMV necrotic lesion of 1.42 ± 0.07 mm (Figure 65). This significant decrease in TMV necrotic lesion indicated the induction of SAR upon primary infection ($P < 0.05$).

Similarly, SIP-428 overexpressing lines showed TMV necrotic lesion of 2.95 ± 0.17 mm that was significantly higher than wild-type control (Figure 65). Higher concentration of primary

infection was done to induce robust SAR response in short span of time, but still, SIP-428 overexpressing lines showed TMV necrotic lesion of 2.9 ± 0.11 mm post-secondary infection indicating no induction of SAR in SIP-428 overexpressing lines even after primary infection (Figure 65). Results showed SIP-428 overexpressing lines were defective in SAR response compared to wild-type control (Figure 65 and 66).

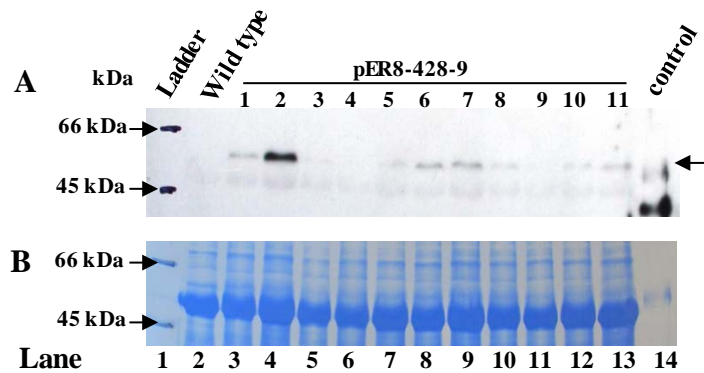
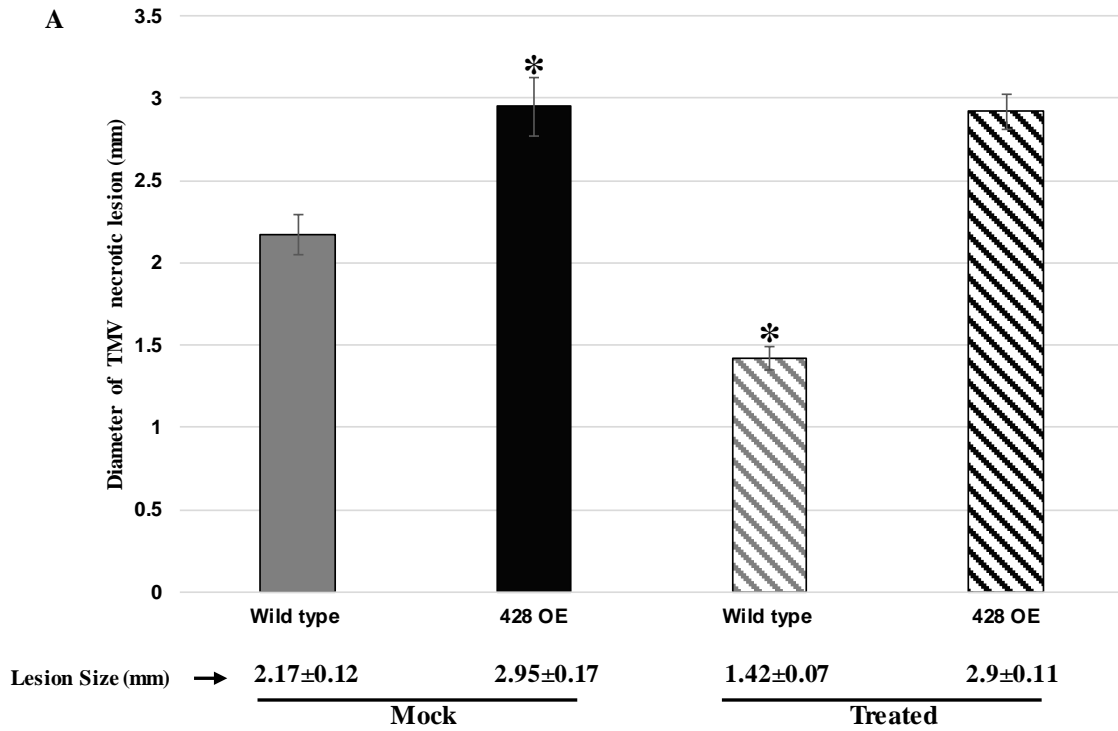


Figure 64: Western blot screening of T2 generation of SIP-428 overexpressing lines. Panel A, western blot analysis using an anti-myc tag antibody. Panel B, the coomassie stained blot for protein loading control. Wild-type (lane# 2) as a negative control and positive control (lane# 14) was used to screen SIP-428 overexpression lines (lane# 3-13).



B

	Lesion Size (mm)	
	Mock	Treated
Wild type	2.17±0.12	1.42±0.07
428 OE	2.95±0.17	2.9±0.11

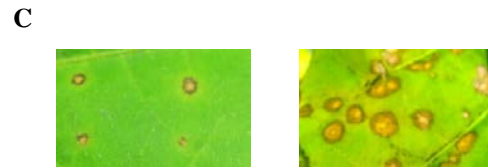
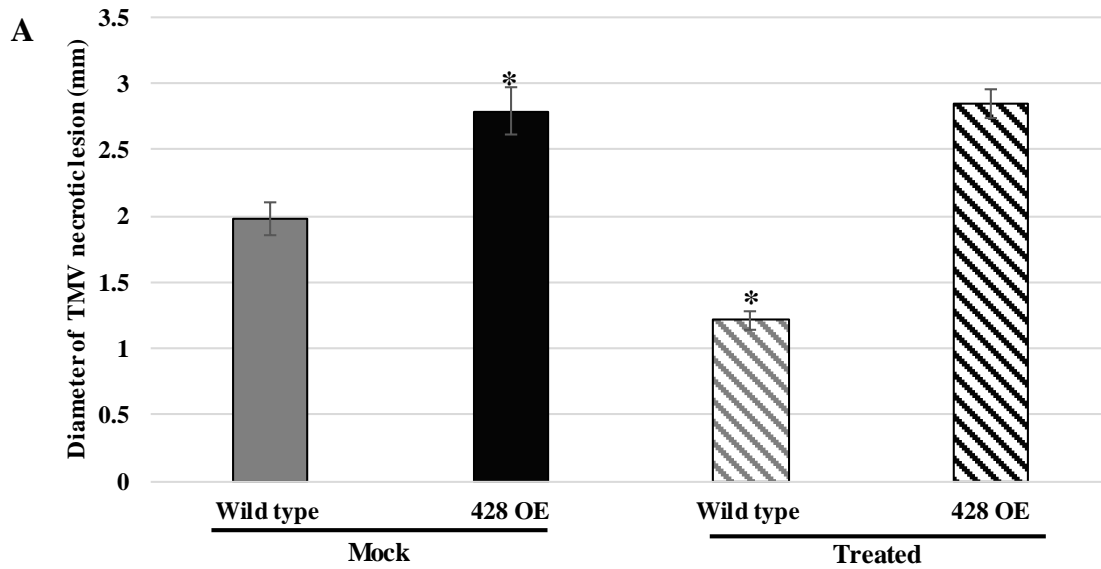


Figure 65: Systemic acquired resistance in SIP-428 overexpressing (428-OE) lines. The bar diagram representing the average diameter of TMV lesion size with error bar in wild-type, and SIP-428 overexpressing(428 OE) plants before and after primary infection (A). The measurement of average lesion (B). The visual difference observed between wild-type and SIP-428 overexpressing lines post-secondary infection (C) ($P < 0.05$).



B

Lesion Size (mm)

	Mock	Treated
Wild type	1.978±0.12	1.216±0.07
428 OE	2.789±0.17	2.845±0.11

Figure 66: Systemic acquired resistance in SIP-428 overexpressing (428-OE) lines. Panel A, the bar diagram representing the average diameter of TMV lesion size in wild-type, and SIP-428 overexpressing plants before and after primary infection. Panel B, the measurement of average TMV necrotic lesion sizes (t-test, $p < 0.05$).

Subcellular Localization of SIP-428

To understand the possible subcellular localization pattern of SIP-428, *in silico* analysis was done to determine the possible presence of a signal peptide and localization pattern of SIP-428 as shown in Table 19.

Table 19: *In silico* analysis of SIP-428 signal peptide. Various bioinformatics online tools were used to predict the signal peptide as shown below.

Prediction Tool	Chloroplast	Mitochondria	Nucleus	cytoplasm	
Localizer				Most Likely	
TargetP1.1		Mitochondria		Cytoplasm	
MultiLoc	Chloroplast	Mitochondria		Cytoplasm	
Protein Prowler		Mitochondria			
BaCeILo			Nucleus		
ChloroP1.1					None

To test the *in silico* analysis of SIP-428 signal peptide pSITE-2CA expression system was generated to express SIP-428 protein along with GFP tag localized in the N-terminus. The pDONR221 and pSITE-2CA plasmids were used as entry and destination plasmids respectively. SIP-428 was cloned into the pDONR221 plasmid, subcloned into pSITE-2CA plasmid, and transformed into competent *Agrobacterium*. Transient expression of SIP-428 in *Nicotiana benthamiana* was also done to find the possible localization pattern of SIP-428. PR1 protein expression was also detected to confirm whether the immune system of *Nicotiana benthamiana* got activated in response to transient expression of SIP-428.

PCR Amplification of SIP-428

To generate pSITE-2CA-SIP-428 construct, a Gateway cloning system was used with pDONR221 and pSITE-2CA plasmids as entry and destination plasmids respectively. Full-length SIP-428 was amplified from a verified template plasmid (TOPO-SIP-428-1) with primers flanked with attB1 and attB2 sites (DK 662 and attb2-428). Two microliters of amplified PCR product was run into the gel to verify PCR amplification of full-length SIP-428 (Figure 67).

After verification 48 μ l of PCR product was run on 1.0% agarose gel. PCR product was gel extracted, purified, and quantified. The purified SIP-428 fragment was run in 1.0% agarose gel to check the quality of the gel extracted SIP-428 fragment (Figure 68). Results showed the presence of two bands (Figure 68), so PCR product was again column purified, quantified and used for further experiments.

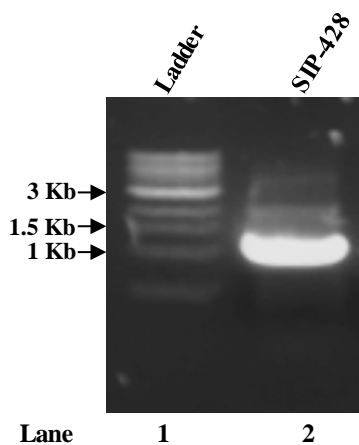


Figure 67: PCR amplification of SIP-428. Full-length SIP-428 was amplified (lane# 2) and visualized on 1.0% agarose gel with EtBr.

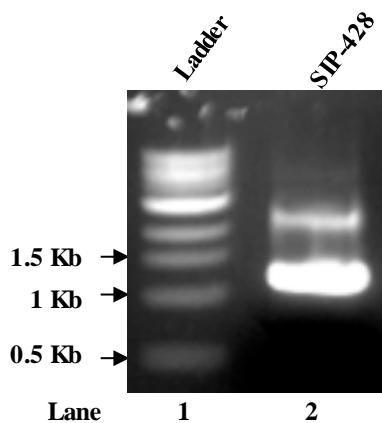


Figure 68: Gel extraction of the SIP-428 fragment. The figure shows the PCR product of SIP-428 (lane# 2) that was gel extracted, purified, and visualized on 1.0% agarose gel with EtBr.

Cloning of SIP-428 into Entry Plasmid (pDONR221) by BP Reaction

The gel purified SIP-428 fragment was cloned into entry plasmid (pDONR221) by BP reaction. The reaction was stopped with 1 μ l of proteinase K, and 2 μ l of BP reaction mixture was transformed into chemically competent Top 10 *E. coli* cells by the heat shock method. Transformed cells were selected on LB agar plates containing 100 μ g/ml kanamycin. Colony PCR of transformed cells were done (M13 forward primer and DK 504 reverse primer) to screen positive cells (Figure 69)

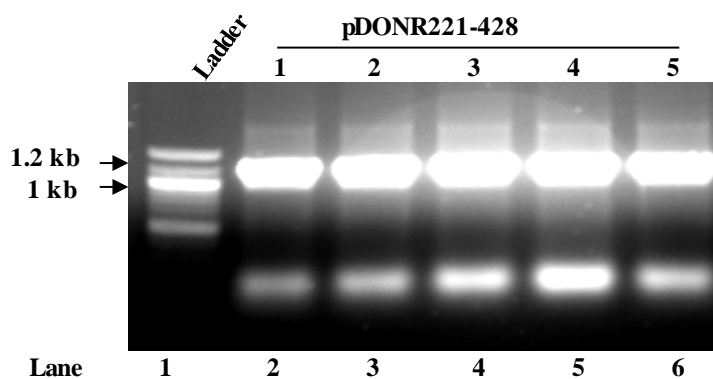


Figure 69: Colony PCR of entry plasmid (pDONR221-428). The colony PCR of transformed cells (lane#2-6) were visualized using 1.0% agarose gel with EtBr.

Plasmid DNA (pDONR221-428) from positive entry clones was isolated and purified (Figure 70). DNA sequence of entry plasmid was aligned with SIP-428 cDNA sequence (Appendix C; A-2). Sequence verified entry plasmid was used for LR cloning reaction.

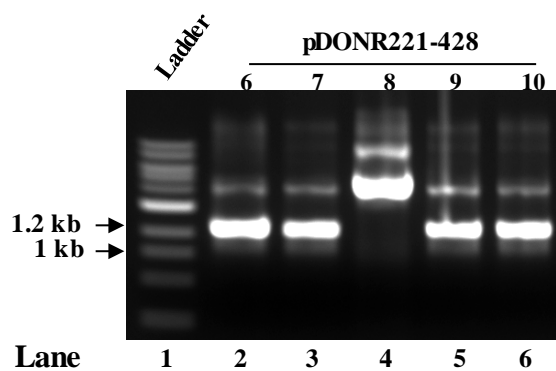


Figure 70: Isolation of entry plasmid (pDONR221-428). The plasmid extracted from positive transformed clones and visualized on 1.0% agarose gel with EtBr (lane# 2-6).

Cloning of SIP-428 into Destination Plasmid (pSITE-2CA) by LR reaction

The SIP-428 fragment from entry plasmid (pDONR221-428) was cloned into destination plasmid (pSITE-2CA) by the LR reaction. After incubation, the LR reaction was stopped by adding 1 μ l of proteinase K and 2 μ l of LR reaction mixture was transformed into chemically competent Top10 *E. coli* cells. The transformed bacterial cells were selected on LB agar plate with 100 μ g/ml of spectinomycin. Colony PCR of transformed cells were performed using vector specific forward (DK 677) and gene-specific reverse (DK 502) primers to screen positive cells (Figure 71).

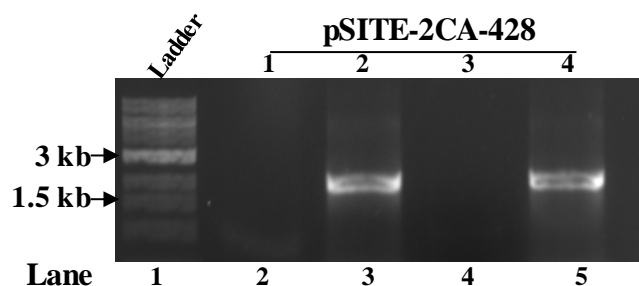


Figure 71: Colony PCR of destination plasmid (pSITE-2CA-428). Colony PCR showed the presence of SIP-428 in pSITE-2CA plasmid (lane# 3 and 5). 1.0% agarose gel with EtBr was used to visualize the PCR product.

Plasmid DNA from positive destination cells was extracted and purified. Quality of isolated destination plasmid (pSITE-2CA-428) was checked by agarose gel electrophoresis (Figure 72). One microgram of destination plasmid DNA was transformed into chemically competent *Agrobacterium*. Transformed *Agrobacterium* was screened by colony PCR using DK 677 forward and DK 502 reverse primer (Figure 73).

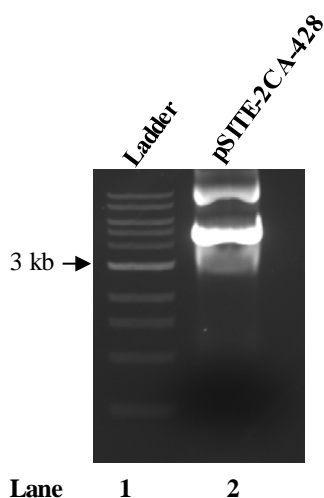


Figure 72: Isolation of destination plasmid (pSITE-2CA-428) from *E. coli*. The extracted plasmid was run and visualized on 1.0% agarose gel with EtBr (lane# 2).

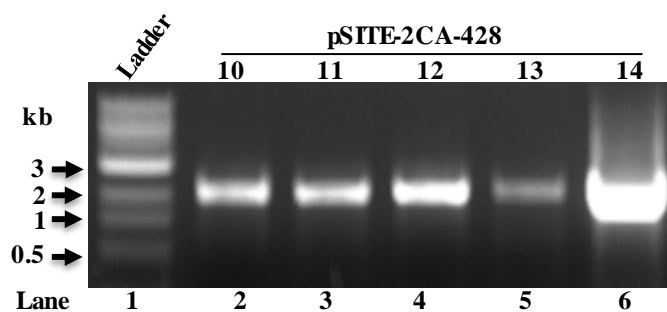


Figure 73: Colony PCR screening of transformed *Agrobacterium* with pSITE-2CA-428. The presence of pSITE-2CA-428 in transformed *Agrobacterium* (lane# 2-6) was visualized using 1.0% agarose gel.

Transient Expression of SIP-428

SIP-428 was transiently expressed in *Nicotiana benthamiana*. Time course samples were collected to determine the expression of SIP-428. Two sets of experiments were carried out simultaneously; one with pSITE-2CA-428 alone, and the next one with HcPro in combination with pSITE-2CA-428. Leaf disk samples were collected and processed using 1X SDS. SDS PAGE and western blot using anti-GFP tag antibody were done to find time point where SIP-428 expressed with maximum intensity (Figure 74). Results showed 24 hrs post infection, expression of SIP-428 was high for both combinations (with and without HcPro). Based on these results 24 hrs post infection samples were used for further experiments.

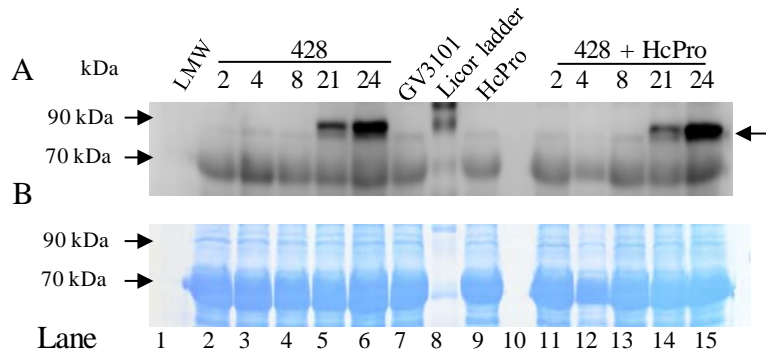


Figure 74: Time course expression of the SIP-428 protein. Panel A, western blot analysis with an anti-GFP antibody. Panel B, coomassie blue stain of the PVDF membrane. Lane# 1; low molecular weight (LMW), lanes# 2-6; 2, 4, 8, 21 and 24 hrs sample post infiltration with pSITE-2CA-428 alone respectively, lane# 7; Agrobacterium infiltrated sample (GV3101), lane# 8; liquor ladder, lane# 9; pBA-HcPro infiltrated sample, lane# 10; blank, lanes# 11-15; 2, 4, 8, 21 and 24 hrs sample post infiltration with mixture of pSITE-2CA-428 and pBA-HcPro (1:1).

To determine whether transient expression of SIP-428 induces the immune system of *Nicotiana benthamiana*, PR1 protein expression was detected from time course samples by western blot using the anti PR1 antibody. Results showed Agrobacterium (GV3101) itself induced the expression of PR1 in the absence of SIP-428 (Figure 75).

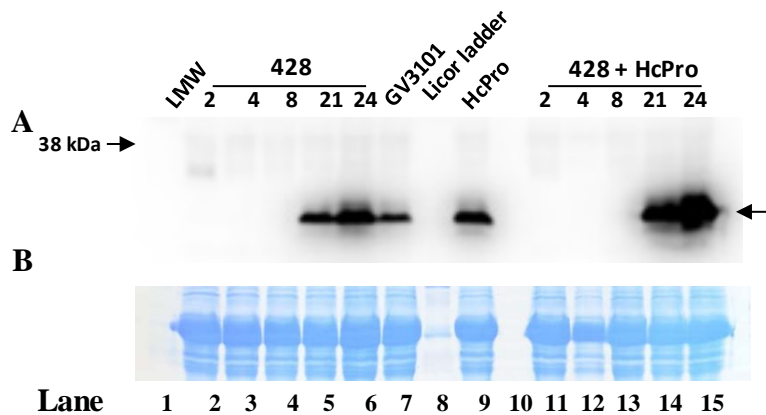


Figure 75: Time course expression of PR1. Panel A, western blot analysis with an anti-PR1 antibody. Panel B, coomassie blue stain of the PVDF membrane. Lane# 1; low molecular weight (LMW), lanes# 2-6; 2, 4, 8, 21 and 24 hrs sample post infiltration with pSITE-2CA-428 alone respectively, lane# 7; Agrobacterium infiltrated sample (GV3101), lane# 8; liquor ladder, lane# 9; pBA-HcPro infiltrated sample, lane# 10; blank, lanes# 11-15; 2, 4, 8, 21 and 24 hrs sample post infiltration with mixture of pSITE-2CA-428 and pBA-HcPro (1:1).

Confocal Microscopy of SIP-428 Expression

Transformed Agrobacterium was used for transient expression of SIP-428 in *Nicotiana benthamiana*. Transformed Agrobacterium expresses SIP-428 protein along with N-terminal GFP tag that can be detected by confocal microscopy. Two sets of experiments were carried out simultaneously; one with pSITE-2CA-428 alone, and the next one with HcPro in combination with pSITE-2CA-428. Leaf disk samples were collected 24 hr post-infection and visualized under a confocal microscope. The red channel was used to detect the auto-fluorescence components of the cells (chloroplasts). The epidermal cell of the plant leaf tissue contains vacuole which occupies a large volume of the plant cell (Chakrabarty *et al.* 2007; Speth *et al.* 2009). Most of the cellular content concentrated between cell wall and vacuoles. The merged figure indicates the possible location of SIP-428 in a plant cell. The signal of SIP-428 in the

absence of pBA-HcPro construct was weak (Figure 76) although SIP-428 appeared to localize around the periphery of the cells.

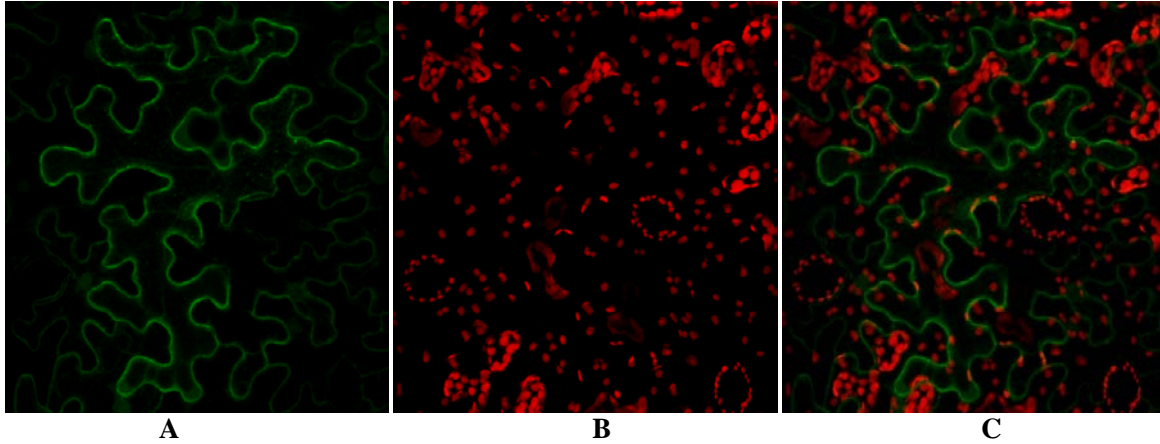


Figure 76: Confocal microscopy of SIP-428 expression. Panel A shows green expression of GFP detected by the microscope. Panel B shows auto-fluorescence component detected in a plant cell. Panel C shows the merged figure of A and B.

Transformed clone (pSITE-2CA-428), when expressed with the HcPro construct, showed higher and persistent signal at 24 hrs post infiltration (Figure 77). The leaf disk sample was visualized under the confocal microscope as described earlier. The GFP signal was persistent and detected towards the edge of the cell that could be from mitochondria, tonoplast, plasma membrane, cytoplasm, cytoskeleton, and peroxisome. Results showed that SIP-428 did not localize to nucleus or chloroplast.

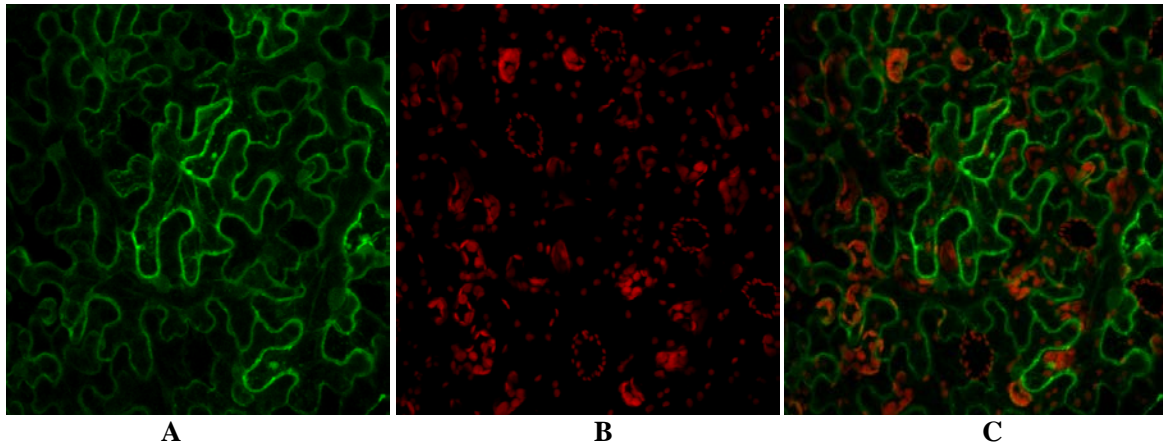


Figure 77: Confocal microscopy of SIP-428 expression in the presence of pBA-HcPro. Panel A shows green expression of GFP detected by the microscope. Panel B shows auto-fluorescence component detected in a plant cell. Panel C shows merged figure of A and B.

Subcellular Fractionation of SIP-428

The localization of SIP-428 was detected by subcellular fractionation of SIP-428 proteins expressed in *Nicotiana benthamiana*. Differential centrifugation followed by sucrose gradient separation techniques were used (Singer 1972; Ueoka-Nakanishi *et al.* 2000). Different cellular components were separated and processed for western blot using anti-GFP antibody. Confocal microscopy helped to narrow down the possible localization of SIP-428 in mitochondria or plasma membrane or cytosolic component. Subcellular fractionation followed by western blot showed that SIP-428 localized in mitochondria (Figure 78). Multiple experiments yielded a similar pattern of SIP-428 localization. Subcellular fractionation of SIP-428 protein with N-terminal myc tag (pER8-SIP-428) was also done to verify independently whether GFP tag determined the localization pattern of SIP-428. Western blot analysis using an anti-myc tag antibody showed the localization of SIP-428 in mitochondria (Figure 79). Taken together these results showed that SIP-428 localized in mitochondria (Figure 78 and 79).

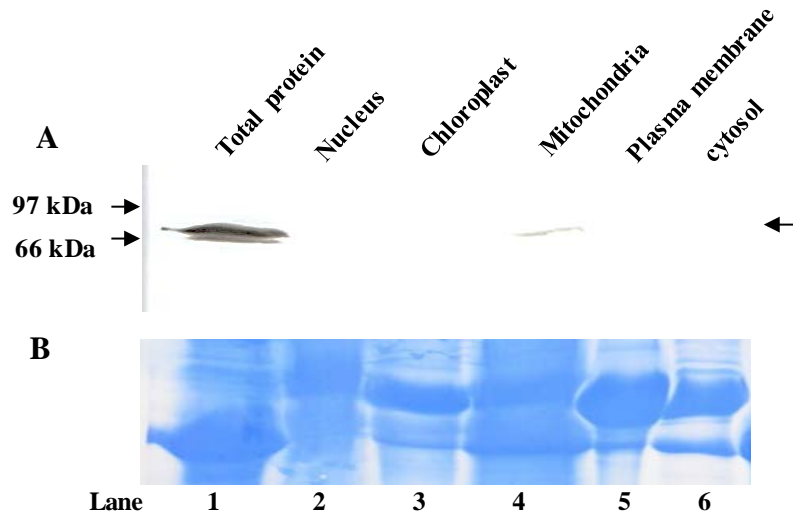


Figure 78: Western blot analysis of subcellular fractions. Panel A, western blot analysis using anti-GFP antibody. Panel B, coomassie blue stain of the membrane, which serves as a loading control. Lane# 1; total protein and lanes# 2-6; nucleus, chloroplast, mitochondria, plasma membrane, and cytosol fractions respectively. Arrow indicates the detection of SIP-428 expression.

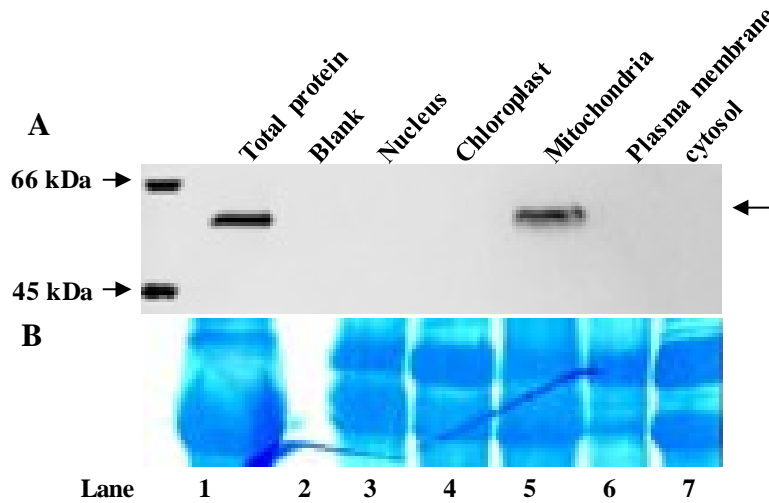


Figure 79: Western blot analysis of subcellular fractions. Panel A, western blot analysis using anti-c-myc antibody. Panel B, coomassie blue stain of the membrane, which serves as a loading control. Lane# 1; total protein and lanes# 2-7; blank, nucleus, chloroplast, mitochondria, plasma membrane, and cytosol fractions respectively. Arrow indicates the detection of SIP-428 expression.

CHAPTER 4

DISCUSSION

Salicylic acid (SA), a plant hormone, plays an important role in the activation of both local and systemic acquired resistance (SAR) (Chen *et al.* 1995; Wobbe and Klessig 1996). SA-binding protein 2 (SABP2) is an important component of the SA signaling pathway. It catalyzes the conversion of MeSA into SA by its methylsterase activity. This likely results in an increase in the cytosolic concentration of SA that in turn activates the SA responsive genes (PR1, 2 and 5) through NPR1. SABP2 is essential for both basal resistance and SAR in plants (Kumar and Klessig 2003; Forouhar *et al.* 2005). In order to know more about SABP2, a yeast two-hybrid (Y2H) screening was performed using SABP2 as bait and tobacco leaf proteins as prey. Several interacting proteins were identified, including SIP-428 (Kumar *et al.*, 2018 unpublished).

This study is aimed to determine the possible role of SIP-428 in plant physiology. Our approach included biochemical characterization of the SIP-428. *In silico* analysis predicted SIP-428 to be a putative SIR2 deacetylase enzyme. The amino acid sequence of SIP-428 has a SIR2-like conserved catalytic domain with 72% identity with *Arabidopsis thaliana* sirtuin (AtSRT2) and 45% identity with human sirtuin-4, respectively (Figure 7).

The SIP-428 cDNA without signal predicted signal peptide (SIP-428-72) was expressed in *E. coli* and used to determine its enzymatic activity (Figure 13). Deacetylase activity of SIP-428-72 was only detected with the acetylated p53 substrate (Figure 18 and 19). NAD-dependent deacetylation of acetylated proteins is essential for gene silencing, aging, DNA damage repair, glucose homeostasis, fatty acid oxidation, fine-tuning of energy metabolism, cell cycle

regulation, and lifespan extension (Jackson and Denu 2002; Argmann and Auwerx 2006; Hirschey *et al.* 2009; Zhong and Kowluru 2010; König *et al.* 2014). SIR2 deacetylase enzymes serve as the sensor of free NAD⁺ maintaining the cellular energy status (Imai *et al.* 2000).

SIP-428 Negatively Regulates Plant Immune System

Since SIP-428 is a SABP2-interacting protein, it is likely involved in the plant immune signaling. AtSRT2, an Arabidopsis homolog of SIP-428, acts as a negative regulator of basal resistance by suppressing the SA biosynthesis via PAD4, EDS5, and SID2 (Wang *et al.* 2010). AtSRT2 expression was downregulated in an SA independent manner when exposed to *Pseudomonas syringae* pv. *tomato* DC3000 (*Pst* DC3000) (Wang *et al.* 2010). NPR1 is an essential component of the SA mediated plant immune system, which leads to the induction of PR1 (Zhou *et al.* 2000). Enhanced expression of NPR1 was observed in *atsrt2* mutant when treated with the *Pst*DC3000. Increased expression of PR1 in *atsrt2* mutant indicated that AtSRT2 negatively regulates PR1 expression (Wang *et al.* 2010). The PR1 is an antimicrobial protein that binds and sequesters sterol (required by pathogens for their growth) causing the inhibitory effect on the pathogen growth (Gamir *et al.* 2017). Arabidopsis mutant *atsrt2* showed higher resistance to the pathogen infection compared to wild-type control (Figure 23 and 24). These results were in line with the previous finding that demonstrated AtSRT2 negatively regulates the plant immune system (Wang *et al.* 2010).

The transgenic SIP-428 silenced tobacco lines were more resistant to pathogen infection as SIP-428 silenced lines allowed a significantly decreased bacterial growth (*Pst*) compared to wild-type controls (Figure 46 and 47). The SIP-428 overexpressing transgenic tobacco lines showed compromised basal resistance as more *Pst* growth was detected in these plants compared

to the wild type control at 3 DPI (Figure 62 and 63). Like transgenic Arabidopsis plants where AtSRT2 was overexpressed, it most likely due to reduced expression of PR1 compared to the wild-type control (Wang *et al.* 2010). Reduced expression of PR1 in AtSRT2 overexpressing Arabidopsis also indicated the low level of SA induction after *Psm* infection. Taken together the results from *atsrt2* mutant plants, SIP-428 silenced and overexpressed lines we demonstrated that SIP-428 negatively regulates the basal resistance of tobacco plants.

Systemic acquired resistance (SAR) is broad range long-lasting immunity of plants, and SA is important for the induction of SAR (Gaffney *et al.* 1993). MeSA is a mobile SAR signal molecule that is transported to the systemic tissue from the site of infection to make systemic tissue prime for subsequent infections (Park *et al.* 2007). SAR response was detected in the *atsrt2* mutant (Figure 25 and 26) while transgenic SIP-428 silenced tobacco lines showed enhanced SAR response as TMV induced necrotic lesions were significantly reduced in SIP-428 silenced plants compared to the wild-type controls (Figure 48 and 49). The difference in the SAR response of SIP-428 and its homolog in Arabidopsis (AtSRT2) could be, due to the difference in experimental design. Both plants (Arabidopsis and tobacco) were exposed to long day environment (16 hrs of light and 8 hrs of dark) for basal resistance and SAR. The *atsrt2* mutant plants are exhibiting SAR response similar to the wild-type control (Figure 25 and 26). When Arabidopsis plants infected with *Ps tomato* DC3000 AvrRPT2 were exposed for 3.5 hrs or more of light, plants develop SAR in the absence of MeSA (Liu *et al.* 2011). For our experimental design, we infiltrated the plants before noon and exposed to the lights for more than 8 hrs. The *atsrt2* mutant plants exhibited SAR in the absence of MeSA while SIP-428 silenced plants showed enhanced SAR compared to wild-type plants. SIP-428 overexpressing lines were compromised in SAR (Figure 65 and 66). As in the case of basal resistance exhibited by SIP-428

overexpression lines (Figure 62 and 63), it most likely due to the inhibition of SA biosynthesis when SIP-428 is overexpressed. The inhibition of SA biosynthesis in SIP-428 overexpression lines most likely inhibited the generation of MeSA, a SAR mobile signal (Park *et al.* 2007). Together, these data suggested that SIP-428 negatively regulated SAR in tobacco plants.

SIP-428 in SABP2 Signaling Pathway

SIP-428 was identified based on its physical interaction with SABP2 in a yeast two-hybrid screen. GST pull-down assay using GST fused SABP2 and 6x Histidine fused to SIP-428 confirmed the interaction between SABP2 and SIP-428.

Tetra FA (2,2,2,2'-tetra-fluoroacetophenone) is a synthetic SA analog that inhibits methylesterase activity of SABP2 (Park *et al.* 2009). Tetra FA treatment of SIP-428 silenced lines did not show any effect while wild-type control plants showed enhanced susceptibility in bacterial growth assay (Figure 50). This result indicated the methylesterase activity of SABP2 did not affect the SIP-428 response to pathogen infection. The expression of SABP2 in SIP-428 silenced lines were not changed (Figure 45) which showed that SIP-428 did not regulate the SABP2 expression. SABP2 is an essential component of the SA signaling pathway as it converts MeSA to SA by activating plant immune response (Kumar and Klessig 2003). It is likely that SIP-428 regulates the SA biosynthesis as was shown in case of its *Arabidopsis* homolog, AtSRT2 (Wang *et al.* 2010). As tetra FA treatment did not affect the resistance exhibited by SIP-428 silenced lines it could be concluded that SIP-428 most likely act upstream of SABP2 in the SA signaling pathway.

Subcellular Localization of SIP-428

Various localization patterns have been detected in the human homologs of SIP-428 (North and Verdin 2004; Herskovits and Guarente 2013). Localization of AtSRT2 was shown to be both nuclear and mitochondrial (Wang *et al.* 2010; König *et al.* 2014). *In silico* analysis of SIP-428 predicted a different localization pattern (Table 19). Confocal microscopy and subcellular fractionation demonstrated that SIP-428 is localized in the mitochondria.

The acetylation level of many mitochondrial proteins (cytochrome c, α subunit of ATP synthase complex, ATP/ADP carrier (AAC1 to AAC3), a putative carboxylate transporter, the mitochondrial metabolite carrier protein BOU, and the di- and tricarboxylate transporter) in *atsrt2* mutant shown to be increased (König *et al.* 2014).

Future Directions

Transgenic tobacco lines (SIP-428 silenced and SIP-428 overexpression) could be used to identify the in-planta substrate for the SIP-428. The finding of the possible substrate could help to understand the signaling pathway of SIP-428. SIP-428 silenced line, and wild-type control treated with tetra FA showed that SIP-428 likely acts upstream of SABP2 in the SA signaling pathway. It would be interesting to study the effect of SIP-428 on the methyltransferase activity of SABP2 in pathogen infected plants.

Analysis of the *atsrt2* mutant plants it was shown that AtSRT2 negatively regulated the SA biosynthesis (Wang *et al.* 2010). Treatment of SIP-428 overexpressing plants with MeSA would be one approach that would help to verify further whether or not SIP-428 negatively

regulate SA biosynthesis. Inhibition of SA synthesis caused a decreased level of MeSA, mobile SAR signal molecules. Treatment of SIP-428 overexpressing plants with MeSA expected to behave like a wild-type control as it helps to rescue the deficiency of MeSA.

REFERENCES

- Abramovitch RB, Kim YJ, Chen S, Dickman MB, Martin GB. 2003. Pseudomonas type iii effector avrptob induces plant disease susceptibility by inhibition of host programmed cell death. *The EMBO journal*. 22(1):60-69.
- AbuQamar S, Moustafa K, Tran LS. 2017. Mechanisms and strategies of plant defense against botrytis cinerea. *Crit Rev Biotechnol*. 37(2):262-274.
- Alvarez-Venegas R, Abdallat AA, Guo M, Alfano JR, Avramova Z. 2007. Epigenetic control of a transcription factor at the cross section of two antagonistic pathways. *Epigenetics*. 2(2):106-113.
- Anandalakshmi R, Pruss GJ, Ge X, Marathe R, Mallory AC, Smith TH, Vance VB. 1998. A viral suppressor of gene silencing in plants. *Proceedings of the National Academy of Sciences of the United States of America*. 95(22):13079-13084.
- Anderson RM, Bitterman KJ, Wood JG, Medvedik O, Sinclair DA. 2003a. Nicotinamide and pnc1 govern lifespan extension by calorie restriction in *saccharomyces cerevisiae*. *Nature*. 423(6936):181-185.
- Anderson RM, Latorre-Esteves M, Neves AR, Lavu S, Medvedik O, Taylor C, Howitz KT, Santos H, Sinclair DA. 2003b. Yeast life-span extension by calorie restriction is independent of nad fluctuation. *Science (New York, NY)*. 302(5653):2124-2126.
- Antoniw JF, Dunkley AM, White RF, Wood J. 1980. Soluble leaf proteins of virus-infected tobacco (*nicotiana tabacum*) cultivars [proceedings]. *Biochem Soc Trans*. 8(1):70-71.
- Aquea F, Timmermann T, Arce-Johnson P. 2010. Analysis of histone acetyltransferase and deacetylase families of *vitis vinifera*. *Plant Physiol Biochem*. 48(2-3):194-199.
- Argmann C, Auwerx J. 2006. Insulin secretion: Sirt4 gets in on the act. *Cell*. 126(5):837-839.

- Axtell MJ. 2013. Classification and comparison of small rnas from plants. *Annu Rev Plant Biol.* 64:137-159.
- Balan V, Miller GS, Kaplun L, Balan K, Chong ZZ, Li F, Kaplun A, VanBerkum MF, Arking R, Freeman DC *et al.* 2008. Life span extension and neuronal cell protection by drosophila nicotinamidase. *J Biol Chem.* 283(41):27810-27819.
- Banday ZZ, Nandi AK. 2015. Interconnection between flowering time control and activation of systemic acquired resistance. *Front Plant Sci.* 6:174.
- Bertil D. 2006. Advanced information: Rna interference. *The Nobel Prize in Physiology or Medicine.*
- Bitterman KJ, Anderson RM, Cohen HY, Latorre-Esteves M, Sinclair DA. 2002. Inhibition of silencing and accelerated aging by nicotinamide, a putative negative regulator of yeast sir2 and human sirt1. *The Journal of biological chemistry.* 277(47):45099-45107.
- Blander G, Guarente L. 2004. The sir2 family of protein deacetylases. *Annual review of biochemistry.* 73:417-435.
- Boller T, Felix G. 2009. A renaissance of elicitors: Perception of microbe-associated molecular patterns and danger signals by pattern-recognition receptors. *Annual review of plant biology.* 60:379-406.
- Bonnemain J-L, Chollet J-F, Rocher F. 2013. Transport of salicylic acid and related compounds. *Salicylic acid.* Springer. p. 43-59.
- Borges F, Martienssen RA. 2015. The expanding world of small rnas in plants. *Nat Rev Mol Cell Biol.* 16(12):727-741.
- Bowles DJ. 1990. Defense-related proteins in higher plants. *Annual review of biochemistry.* 59:873-907.

- Brachmann CB, Sherman JM, Devine SE, Cameron EE, Pillus L, Boeke JD. 1995. The sir2 gene family, conserved from bacteria to humans, functions in silencing, cell cycle progression, and chromosome stability. *Genes Dev.* 9(23):2888-2902.
- Brown I, Trethowan J, Kerry M, Mansfield J, Bolwell GP. 1998. Localization of components of the oxidative cross-linking of glycoproteins and of callose synthesis in papillae formed during the interaction between non-pathogenic strains of *Xanthomonas campestris* and french bean mesophyll cells. *The Plant Journal.* 15(3):333-343.
- Buck SW, Sandmeier JJ, Smith JS. 2002. Rna polymerase i propagates unidirectional spreading of rDNA silent chromatin. *Cell.* 111(7):1003-1014.
- Burow MD, Chlan CA, Sen P, Lisca A, Murai N. 1990. High-frequency generation of transgenic tobacco plants after modified leaf disk cocultivation with *Agrobacterium tumefaciens*. *Plant Molecular Biology Reporter.* 8(2):124-139.
- Busconi M, Reggi S, Fogher C, Bavaresco L. 2009. Evidence of a sirtuin gene family in grapevine (*Vitis vinifera* L.). *Plant Physiol Biochem.* 47(7):650-652.
- Butterbrodt T, Thurow C, Gatz C. 2006. Chromatin immunoprecipitation analysis of the tobacco *pr-1a*- and the truncated *camv 35s* promoter reveals differences in salicylic acid-dependent TGA factor binding and histone acetylation. *Plant Mol Biol.* 61(4-5):665-674.
- Chadha KC, Brown SA. 1974. Biosynthesis of phenolic acids in tomato plants infected with *Agrobacterium tumefaciens*. *Canadian Journal of Botany.* 52(9):2041-2047.
- Chai J, Liu J, Zhou J, Xing D. 2014. Mitogen-activated protein kinase 6 regulates *npr1* gene expression and activation during leaf senescence induced by salicylic acid. *J Exp Bot.* 65(22):6513-6528.

- Chakrabarty R, Banerjee R, Chung SM, Farman M, Citovsky V, Hogenhout SA, Tzfira T, Goodin M. 2007. Psite vectors for stable integration or transient expression of autofluorescent protein fusions in plants: Probing nicotiana benthamiana-virus interactions. *Mol Plant Microbe Interact.* 20(7):740-750.
- Chan HM, La Thangue NB. 2001. P300/cbp proteins: Hats for transcriptional bridges and scaffolds. *J Cell Sci.* 114(Pt 13):2363-2373.
- Chang JH, Kim HC, Hwang KY, Lee JW, Jackson SP, Bell SD, Cho Y. 2002. Structural basis for the nad-dependent deacetylase mechanism of sir2. *J Biol Chem.* 277(37):34489-34498.
- Chapagai DP. 2014. Biochemical characterization of sbip-470 and its role in sa-mediated signaling in plants. East Tennessee State University.
- Chaumont F, Bernier B, Buxant R, Williams ME, Levings CS, Boutry M. 1995. Targeting the maize t-urf13 product into tobacco mitochondria confers methomyl sensitivity to mitochondrial respiration. *Proc Natl Acad Sci U S A.* 92(4):1167-1171.
- Chen Z, Malamy J, Henning J, Conrath U, Sanchez-Casas P, Silva H, Ricigliano J, Klessig DK. 1995. Induction, modification, and transduction of the salicylic acid signal in plant defense responses. *Proceedings of the National Academy of Sciences of the United States of America.* 92(10):4134-4137.
- Chen Z, Zheng Z, Huang J, Lai Z, Fan B. 2009. Biosynthesis of salicylic acid in plants. *Plant Signal Behav.* 4(6):493-496.
- Cheng HL, Mostoslavsky R, Saito S, Manis JP, Gu Y, Patel P, Bronson R, Appella E, Alt FW, Chua KF. 2003. Developmental defects and p53 hyperacetylation in sir2 homolog (sirt1)-deficient mice. *Proc Natl Acad Sci U S A.* 100(19):10794-10799.

- Chigurupati P, Haq I, Kumar D. 2016. Tobacco methyl salicylate esterase mediates nonhost resistance. *Current Plant Biology*. 6:48-55.
- Chinchilla D, Boller T, Robatzek S. 2007. Flagellin signalling in plant immunity. *Adv Exp Med Biol*. 598:358-371.
- Choi HW, Klessig DF. 2016. Damps, mamps, and namps in plant innate immunity. *BMC Plant Biol*. 16(1):232.
- Choi SM, Song HR, Han SK, Han M, Kim CY, Park J, Lee YH, Jeon JS, Noh YS, Noh B. 2012. Hda19 is required for the repression of salicylic acid biosynthesis and salicylic acid-mediated defense responses in arabidopsis. *Plant J*. 71(1):135-146.
- Choudhary C, Kumar C, Gnad F, Nielsen ML, Rehman M, Walther TC, Olsen JV, Mann M. 2009. Lysine acetylation targets protein complexes and co-regulates major cellular functions. *Science (New York, NY)*. 325(5942):834-840.
- Curto M, Camafeita E, Lopez JA, Maldonado AM, Rubiales D, Jorrín JV. 2006. A proteomic approach to study pea (*pisum sativum*) responses to powdery mildew (*erysiphe pisi*). *Proteomics*. 6 Suppl 1:S163-174.
- Dean JV, Mills JD. 2004. Uptake of salicylic acid 2-o-beta-d-glucose into soybean tonoplast vesicles by an atp-binding cassette transporter-type mechanism. *Physiologia plantarum*. 120(4):603-612.
- Dean JV, Mohammed LA, Fitzpatrick T. 2005. The formation, vacuolar localization, and tonoplast transport of salicylic acid glucose conjugates in tobacco cell suspension cultures. *Planta*. 221(2):287-296.
- Defossez PA, Lin SJ, McNabb DS. 2001. Sound silencing: The sir2 protein and cellular senescence. *Bioessays*. 23(4):327-332.

- Despres C, DeLong C, Glaze S, Liu E, Fobert PR. 2000. The arabidopsis npr1/nim1 protein enhances the dna binding activity of a subgroup of the tga family of bzip transcription factors. *The Plant cell*. 12(2):279-290.
- Devoto A, Nieto-Rostro M, Xie D, Ellis C, Harmston R, Patrick E, Davis J, Sherratt L, Coleman M, Turner JG. 2002. Coi1 links jasmonate signalling and fertility to the scf ubiquitin-ligase complex in arabidopsis. *Plant J*. 32(4):457-466.
- Ding B, Bellizzi MeR, Ning Y, Meyers BC, Wang GL. 2012. Hdt701, a histone h4 deacetylase, negatively regulates plant innate immunity by modulating histone h4 acetylation of defense-related genes in rice. *Plant Cell*. 24(9):3783-3794.
- Ding B, Wang GL. 2015. Chromatin versus pathogens: The function of epigenetics in plant immunity. *Front Plant Sci*. 6:675.
- Ding Y, Dommel M, Mou Z. 2016. Abscisic acid promotes proteasome-mediated degradation of the transcription coactivator npr1 in arabidopsis thaliana. *The Plant Journal*. 86(1):20-34.
- Dong X. 2001. Genetic dissection of systemic acquired resistance. *Current opinion in plant biology*. 4(4):309-314.
- Duan Y, Jiang Y, Ye S, Karim A, Ling Z, He Y, Yang S, Luo K. 2015. Ptrwrky73, a salicylic acid-inducible poplar wrky transcription factor, is involved in disease resistance in arabidopsis thaliana. *Plant Cell Rep*. 34(5):831-841.
- Dudareva N, Raguso RA, Wang J, Ross JR, Pichersky E. 1998. Floral scent production in clarkia breweri: Iii. Enzymatic synthesis and emission of benzenoid esters. *Plant Physiology*. 116(2):599-604.
- Dutta TK, Banakar P, Rao U. 2015. The status of rnai-based transgenic research in plant nematology. *Frontiers in microbiology*. 5:760.

- Fan W, Dong X. 2002. In vivo interaction between npr1 and transcription factor tga2 leads to salicylic acid-mediated gene activation in arabidopsis. *The Plant cell*. 14(6):1377-1389.
- Fink Jr R. 1993. *Pseudomonas aeruginosa the opportunist: Pathogenesis and disease*. Boca Raton, FL: CRC.1-5.
- Finkemeier I, Laxa M, Miguet L, Howden AJ, Sweetlove LJ. 2011. Proteins of diverse function and subcellular location are lysine acetylated in arabidopsis. *Plant physiology*. 155(4):1779-1790.
- Fire A, Xu S, Montgomery MK, Kostas SA, Driver SE, Mello CC. 1998. Potent and specific genetic interference by double-stranded rna in caenorhabditis elegans. *Nature*. 391(6669):806-811.
- Fischle W, Kiermer V, Dequiedt F, Verdin E. 2001. The emerging role of class ii histone deacetylases. *Biochem Cell Biol*. 79(3):337-348.
- Fong PM, Tian L, Chen ZJ. 2006. Arabidopsis thaliana histone deacetylase 1 (athd1) is localized in euchromatic regions and demonstrates histone deacetylase activity in vitro. *Cell research*. 16(5):479-488.
- Forouhar F, Yang Y, Kumar D, Chen Y, Fridman E, Park SW, Chiang Y, Acton TB, Montelione GT, Pichersky E. 2005. Structural and biochemical studies identify tobacco sabp2 as a methyl salicylate esterase and implicate it in plant innate immunity. *Proceedings of the National Academy of Sciences of the United States of America*. 102(5):1773-1778.
- Frye RA. 2000. Phylogenetic classification of prokaryotic and eukaryotic sir2-like proteins. *Biochemical and biophysical research communications*. 273(2):793-798.

- Fu ZQ, Yan S, Saleh A, Wang W, Ruble J, Oka N, Mohan R, Spoel SH, Tada Y, Zheng N *et al.* 2012. Npr3 and npr4 are receptors for the immune signal salicylic acid in plants. *Nature*. 486(7402):228-232.
- Fulco M, Schiltz RL, Iezzi S, King MT, Zhao P, Kashiwaya Y, Hoffman E, Veech RL, Sartorelli V. 2003. Sir2 regulates skeletal muscle differentiation as a potential sensor of the redox state. *Mol Cell*. 12(1):51-62.
- Gaffney T, Friedrich L, Vernooij B, Negrotto D, Nye G, Uknes S, Ward E, Kessmann H, Ryals J. 1993. Requirement of salicylic acid for the induction of systemic acquired resistance. *Science*. 261(5122):754-756.
- Gamir J, Darwiche R, Van't Hof P, Choudhary V, Stumpe M, Schneiter R, Mauch F. 2017. The sterol-binding activity of pathogenesis-related protein 1 reveals the mode of action of an antimicrobial protein. *Plant J*. 89(3):502-509.
- Gao QM, Zhu S, Kachroo P, Kachroo A. 2015. Signal regulators of systemic acquired resistance. *Front Plant Sci*. 6:228.
- Garner CM, Kim SH, Spears BJ, Gassmann W. 2016. Express yourself: Transcriptional regulation of plant innate immunity. *Semin Cell Dev Biol*. 56:150-162.
- Glozak MA, Sengupta N, Zhang X, Seto E. 2005. Acetylation and deacetylation of non-histone proteins. *Gene*. 363:15-23.
- Greiss S, Gartner A. 2009. Sirtuin/sir2 phylogeny, evolutionary considerations and structural conservation. *Mol Cells*. 28(5):407-415.
- Grozinger CM, Chao ED, Blackwell HE, Moazed D, Schreiber SL. 2001. Identification of a class of small molecule inhibitors of the sirtuin family of nad-dependent deacetylases by phenotypic screening. *The Journal of biological chemistry*. 276(42):38837-38843.

- Gu W, Roeder RG. 1997. Activation of p53 sequence-specific dna binding by acetylation of the p53 c-terminal domain. *Cell*. 90(4):595-606.
- Guo HS, Fei JF, Xie Q, Chua NH. 2003. A chemical-regulated inducible rna system in plants. *The Plant Journal*. 34(3):383-392.
- Gururani MA, Venkatesh J, Upadhyaya CP, Nookaraju A, Pandey SK, Park SW. 2012. Plant disease resistance genes: Current status and future directions. *Physiological and molecular plant pathology*. 78:51-65.
- Haq MI. 2014. Characterization of a putative sir2 like deacetylase and its role in sabp2 dependent salicylic acid mediated pathways in plant.
- Heil M, Land WG. 2014. Danger signals - damaged-self recognition across the tree of life. *Front Plant Sci*. 5:578.
- Hein I, Gilroy EM, Armstrong MR, Birch PR. 2009. The zig-zag-zig in oomycete-plant interactions. *Mol Plant Pathol*. 10(4):547-562.
- Hekimi S, Guarente L. 2003. Genetics and the specificity of the aging process. *Science*. 299(5611):1351-1354.
- Henderson IR, Zhang X, Lu C, Johnson L, Meyers BC, Green PJ, Jacobsen SE. 2006. Dissecting arabidopsis thaliana dicer function in small rna processing, gene silencing and dna methylation patterning. *Nat Genet*. 38(6):721-725.
- Herskovits AZ, Guarente L. 2013. Sirtuin deacetylases in neurodegenerative diseases of aging. *Cell Res*. 23(6):746-758.
- Hirao M, Posakony J, Nelson M, Hraby H, Jung M, Simon JA, Bedalov A. 2003. Identification of selective inhibitors of nad⁺-dependent deacetylases using phenotypic screens in yeast. *J Biol Chem*. 278(52):52773-52782.

- Hirschey MD, Shimazu T, Huang JY, Verdin E. 2009. Acetylation of mitochondrial proteins. *Methods Enzymol.* 457:137-147.
- Hollender C, Liu Z. 2008. Histone deacetylase genes in arabidopsis development. *J Integr Plant Biol.* 50(7):875-885.
- Howitz KT, Bitterman KJ, Cohen HY, Lamming DW, Lavu S, Wood JG, Zipkin RE, Chung P, Kisielewski A, Zhang LL *et al.* 2003. Small molecule activators of sirtuins extend *saccharomyces cerevisiae* lifespan. *Nature.* 425(6954):191-196.
- Huang J, Gu M, Lai Z, Fan B, Shi K, Zhou YH, Yu JQ, Chen Z. 2010. Functional analysis of the arabidopsis pal gene family in plant growth, development, and response to environmental stress. *Plant Physiol.* 153(4):1526-1538.
- Huang L, Sun Q, Qin F, Li C, Zhao Y, Zhou DX. 2007. Down-regulation of a silent information regulator2-related histone deacetylase gene, *ossrt1*, induces dna fragmentation and cell death in rice. *Plant physiology.* 144(3):1508-1519.
- Imai S, Johnson FB, Marciniak RA, McVey M, Park PU, Guarente L. 2000. Sir2: An nad-dependent histone deacetylase that connects chromatin silencing, metabolism, and aging. *Cold Spring Harb Symp Quant Biol.* 65:297-302.
- Jackson MD, Denu JM. 2002. Structural identification of 2'- and 3'-o-acetyl-adp-ribose as novel metabolites derived from the sir2 family of beta -nad+-dependent histone/protein deacetylases. *J Biol Chem.* 277(21):18535-18544.
- Jakoby M, Weisshaar B, Dröge-Laser W, Vicente-Carbajosa J, Tiedemann J, Kroj T, Parcy F, Group bR. 2002. Bzip transcription factors in arabidopsis. *Trends Plant Sci.* 7(3):106-111.

- Jeandet P, Douillet-Breuil AC, Bessis R, Debord S, Sbaghi M, Adrian M. 2002. Phytoalexins from the vitaceae: Biosynthesis, phytoalexin gene expression in transgenic plants, antifungal activity, and metabolism. *Journal of agricultural and food chemistry*. 50(10):2731-2741.
- Johnson ES, Kornbluth S. 2012. Life, death, and the metabolically controlled protein acetylome. *Curr Opin Cell Biol*. 24(6):876-880.
- Jones AM, Grossmann G, Danielson J, Sosso D, Chen LQ, Ho CH, Frommer WB. 2013. In vivo biochemistry: Applications for small molecule biosensors in plant biology. *Curr Opin Plant Biol*. 16(3):389-395.
- Jones JD, Dangl JL. 2006. The plant immune system. *Nature*. 444(7117):323-329.
- Kaeberlein M, McVey M, Guarente L. 1999. The sir2/3/4 complex and sir2 alone promote longevity in *saccharomyces cerevisiae* by two different mechanisms. *Genes Dev*. 13(19):2570-2580.
- Kasschau KD, Carrington JC. 1998. A counterdefensive strategy of plant viruses: Suppression of posttranscriptional gene silencing. *Cell*. 95(4):461-470.
- Kasuga T, Bui MQ. 2011. Evaluation of automated cell disruptor methods for oomycetous and ascomycetous model organisms. *Fungal Genetics Reports*. 58(1):4-13.
- Kesarwani M, Yoo J, Dong X. 2007. Genetic interactions of tga transcription factors in the regulation of pathogenesis-related genes and disease resistance in *arabidopsis*. *Plant Physiol*. 144(1):336-346.
- Kiefer IW, Slusarenko AJ. 2003. The pattern of systemic acquired resistance induction within the *arabidopsis* rosette in relation to the pattern of translocation. *Plant physiology*. 132(2):840-847.

- Kim E, Bisson WH, Löhr CV, Williams DE, Ho E, Dashwood RH, Rajendran P. 2016. Histone and non-histone targets of dietary deacetylase inhibitors. *Curr Top Med Chem.* 16(7):714-731.
- Klessig DF, Malamy J, Hennig J, Sanchez-Casas P, Indulski J, Grynkiewicz G, Chen Z. 1994. Induction, modification, and perception of the salicylic acid signal in plant defence. *Biochem Soc Symp.* 60:219-229.
- Kumar D. 2014. Salicylic acid signaling in disease resistance. *Plant Sci.* 228:127-134.
- Kumar D, Klessig DF. 2003. High-affinity salicylic acid-binding protein 2 is required for plant innate immunity and has salicylic acid-stimulated lipase activity. *Proceedings of the National Academy of Sciences of the United States of America.* 100(26):16101-16106.
- König AC, Hartl M, Pham PA, Laxa M, Boersema PJ, Orwat A, Kalitventseva I, Plöschinger M, Braun HP, Leister D *et al.* 2014. The arabidopsis class ii sirtuin is a lysine deacetylase and interacts with mitochondrial energy metabolism. *Plant Physiol.* 164(3):1401-1414.
- Landry J, Sutton A, Tafrov ST, Heller RC, Stebbins J, Pillus L, Sternglanz R. 2000. The silencing protein sir2 and its homologs are nad-dependent protein deacetylases. *Proc Natl Acad Sci U S A.* 97(11):5807-5811.
- Latrasse D, Jégu T, Li H, de Zelicourt A, Raynaud C, Legras S, Gust A, Samajova O, Veluchamy A, Rayapuram N *et al.* 2017. Mapk-triggered chromatin reprogramming by histone deacetylase in plant innate immunity. *Genome Biol.* 18(1):131.
- Legrand M, Kauffmann S, Geoffroy P, Fritig B. 1987. Biological function of pathogenesis-related proteins: Four tobacco pathogenesis-related proteins are chitinases. *Proc Natl Acad Sci U S A.* 84(19):6750-6754.

- Leon J, Shulaev V, Yalpani N, Lawton MA, Raskin I. 1995. Benzoic acid 2-hydroxylase, a soluble oxygenase from tobacco, catalyzes salicylic acid biosynthesis. *Proceedings of the National Academy of Sciences of the United States of America*. 92(22):10413-10417.
- Li J, Brader G, Palva ET. 2004. The wrky70 transcription factor: A node of convergence for jasmonate-mediated and salicylate-mediated signals in plant defense. *The Plant cell*. 16(2):319-331.
- Li R, Weldegergis BT, Li J, Jung C, Qu J, Sun Y, Qian H, Tee C, van Loon JJ, Dicke M. 2014. Virulence factors of geminivirus interact with myc2 to subvert plant resistance and promote vector performance. *The Plant Cell*. 26(12):4991-5008.
- Li X, Ye J, Ma H, Lu P. 2018. Proteomic analysis of lysine acetylation provides strong evidence for involvement of acetylated proteins in plant meiosis and tapetum function. *Plant J*. 93(1):142-154.
- Lin J, Mazarei M, Zhao N, Hatcher CN, Wuddineh WA, Rudis M, Tschaplinski TJ, Pantalone VR, Arelli PR, Hewezi T *et al*. 2016. Transgenic soybean overexpressing gmsamt1 exhibits resistance to multiple-hg types of soybean cyst nematode heterodera glycines. *Plant Biotechnol J*. 14(11):2100-2109.
- Lin SJ, Defossez PA, Guarente L. 2000. Requirement of nad and sir2 for life-span extension by calorie restriction in *saccharomyces cerevisiae*. *Science*. 289(5487):2126-2128.
- Liu J, Elmore JM, Coaker G. 2009. Investigating the functions of the rin4 protein complex during plant innate immune responses. *Plant Signal Behav*. 4(12):1107-1110.
- Liu L, Sonbol FM, Huot B, Gu Y, Withers J, Mwimba M, Yao J, He SY, Dong X. 2016a. Salicylic acid receptors activate jasmonic acid signalling through a non-canonical pathway to promote effector-triggered immunity. *Nat Commun*. 7:13099.

- Liu L, Wang G, Song L, Lv B, Liang W. 2016b. Acetylome analysis reveals the involvement of lysine acetylation in biosynthesis of antibiotics in *Bacillus amyloliquefaciens*. *Sci Rep.* 6:20108.
- Liu PP, von Dahl CC, Klessig DF. 2011. The extent to which methyl salicylate is required for signaling systemic acquired resistance is dependent on exposure to light after infection. *Plant physiology.* 157(4):2216-2226.
- Losson H, Schneckeburger M, Dicato M, Diederich M. 2016. Natural compound histone deacetylase inhibitors (hdaci): Synergy with inflammatory signaling pathway modulators and clinical applications in cancer. *Molecules.* 21(11):1608.
- Luna E, Pastor V, Robert J, Flors V, Mauch-Mani B, Ton J. 2011. Callose deposition: A multifaceted plant defense response. *Mol Plant Microbe Interact.* 24(2):183-193.
- Luo J, Li M, Tang Y, Laszkowska M, Roeder RG, Gu W. 2004. Acetylation of p53 augments its site-specific dna binding both in vitro and in vivo. *Proceedings of the National Academy of Sciences of the United States of America.* 101(8):2259-2264.
- Malinovsky FG, Fangel JU, Willats WG. 2014. The role of the cell wall in plant immunity. *Front Plant Sci.* 5:178.
- McBurney MW, Yang X, Jardine K, Hixon M, Boekelheide K, Webb JR, Lansdorp PM, Lemieux M. 2003. The mammalian sir2alpha protein has a role in embryogenesis and gametogenesis. *Molecular and cellular biology.* 23(1):38-54.
- Melotto M, Underwood W, He SY. 2008. Role of stomata in plant innate immunity and foliar bacterial diseases. *Annu Rev Phytopathol.* 46:101-122.
- Min J, Landry J, Sternglanz R, Xu RM. 2001. Crystal structure of a sir2 homolog-nad complex. *Cell.* 105(2):269-279.

- Monaghan J, Zipfel C. 2012. Plant pattern recognition receptor complexes at the plasma membrane. *Curr Opin Plant Biol.* 15(4):349-357.
- Montgomery MK, Xu S, Fire A. 1998. Rna as a target of double-stranded rna-mediated genetic interference in *caenorhabditis elegans*. *Proceedings of the National Academy of Sciences.* 95(26):15502-15507.
- Moreau M, Tian M, Klessig DF. 2012. Salicylic acid binds npr3 and npr4 to regulate npr1-dependent defense responses. *Cell research.* 22(12):1631-1633.
- Mou Z, Fan W, Dong X. 2003. Inducers of plant systemic acquired resistance regulate npr1 function through redox changes. *Cell.* 113(7):935-944.
- Niderman T, Genetet I, Bruyère T, Gees R, Stintzi A, Legrand M, Fritig B, Mössinger E. 1995. Pathogenesis-related pr-1 proteins are antifungal. Isolation and characterization of three 14-kilodalton proteins of tomato and of a basic pr-1 of tobacco with inhibitory activity against *phytophthora infestans*. *Plant Physiol.* 108(1):17-27.
- Nimchuk Z, Eulgem T, Holt BF, Dangl JL. 2003. Recognition and response in the plant immune system. *Annu Rev Genet.* 37:579-609.
- North BJ, Marshall BL, Borra MT, Denu JM, Verdin E. 2003. The human sir2 ortholog, sirt2, is an nad⁺-dependent tubulin deacetylase. *Molecular cell.* 11(2):437-444.
- North BJ, Verdin E. 2004. Sirtuins: Sir2-related nad-dependent protein deacetylases. *Genome Biol.* 5(5):224.
- Pajerowska-Mukhtar KM, Emerine DK, Mukhtar MS. 2013. Tell me more: Roles of nprs in plant immunity. *Trends Plant Sci.* 18(7):402-411.
- Pandey R, Muller A, Napoli CA, Selinger DA, Pikaard CS, Richards EJ, Bender J, Mount DW, Jorgensen RA. 2002. Analysis of histone acetyltransferase and histone deacetylase

- families of arabidopsis thaliana suggests functional diversification of chromatin modification among multicellular eukaryotes. *Nucleic acids research*. 30(23):5036-5055.
- Park S-W, Kaimoyo E, Kumar D, Mosher S, Klessig DF. 2007. Methyl salicylate is a critical mobile signal for plant systemic acquired resistance. *Science*. 318(5847):113-116.
- Park SW, Liu PP, Forouhar F, Vlot AC, Tong L, Tietjen K, Klessig DF. 2009. Use of a synthetic salicylic acid analog to investigate the roles of methyl salicylate and its esterases in plant disease resistance. *The Journal of biological chemistry*. 284(11):7307-7317.
- Patel JH, Du Y, Ard PG, Phillips C, Carella B, Chen C-J, Rakowski C, Chatterjee C, Lieberman PM, Lane WS. 2004. The c-myc oncoprotein is a substrate of the acetyltransferases hgc5/pcaf and tip60. *Molecular and cellular biology*. 24(24):10826-10834.
- Pieterse CM, Van der Does D, Zamioudis C, Leon-Reyes A, Van Wees SC. 2012. Hormonal modulation of plant immunity. *Annual review of cell and developmental biology*. 28:489-521.
- Pontier D, Privat I, Trifa Y, Zhou JM, Klessig DF, Lam E. 2002. Differential regulation of tga transcription factors by post-transcriptional control. *Plant J*. 32(5):641-653.
- Porra R, Thompson W, Kriedemann P. 1989. Determination of accurate extinction coefficients and simultaneous equations for assaying chlorophylls a and b extracted with four different solvents: Verification of the concentration of chlorophyll standards by atomic absorption spectroscopy. *Biochimica et Biophysica Acta (BBA)-Bioenergetics*. 975(3):384-394.
- Poulose N, Raju R. 2015. Sirtuin regulation in aging and injury. *Biochim Biophys Acta*. 1852(11):2442-2455.

- Qiao Y, Liu L, Xiong Q, Flores C, Wong J, Shi J, Wang X, Liu X, Xiang Q, Jiang S *et al.* 2013. Oomycete pathogens encode rna silencing suppressors. *Nat Genet.* 45(3):330-333.
- Rafty LA, Schmidt MT, Perraud AL, Scharenberg AM, Denu JM. 2002. Analysis of o-acetyl-adp-ribose as a target for nudix adp-ribose hydrolases. *J Biol Chem.* 277(49):47114-47122.
- Raguso RA, Light DM, Pickersky E. 1996. Electroantennogram responses of *hyalophora lineata* (sphingidae: Lepidoptera) to volatile compounds from *clarkia breweri* (onagraceae) and other moth-pollinated flowers. *Journal of Chemical Ecology.* 22(10):1735-1766.
- Raguso RA, Pichersky E. 1995. Floral volatiles from *clarkia breweri* and *Concinna* (onagraceae): Recent evolution of floral scent and moth pollination. *Plant Systematics and Evolution.* 194(1-2):55-67.
- Rairdan GJ, Delaney TP. 2002. Role of salicylic acid and *nim1/npr1* in race-specific resistance in *arabidopsis*. *Genetics.* 161(2):803-811.
- Ribnicky DM, Shulaev V, Raskin I. 1998. Intermediates of salicylic acid biosynthesis in tobacco. *Plant Physiol.* 118(2):565-572.
- Rivas-San Vicente M, Plasencia J. 2011. Salicylic acid beyond defence: Its role in plant growth and development. *Journal of experimental botany.* 62(10):3321-3338.
- Robyr D, Suka Y, Xenarios I, Kurdistani SK, Wang A, Suka N, Grunstein M. 2002. Microarray deacetylation maps determine genome-wide functions for yeast histone deacetylases. *Cell.* 109(4):437-446.
- Ross JR, Nam KH, D'Auria JC, Pichersky E. 1999. S-adenosyl-l-methionine:Salicylic acid carboxyl methyltransferase, an enzyme involved in floral scent production and plant

- defense, represents a new class of plant methyltransferases. *Archives of biochemistry and biophysics*. 367(1):9-16.
- Saleh A, Withers J, Mohan R, Marqués J, Gu Y, Yan S, Zavaliev R, Nomoto M, Tada Y, Dong X. 2015. Posttranslational modifications of the master transcriptional regulator npr1 enable dynamic but tight control of plant immune responses. *Cell Host Microbe*. 18(2):169-182.
- Sambrook J, Russell DW. 2006. The hanahan method for preparation and transformation of competent e. Coli: High-efficiency transformation. *CSH Protoc*. 2006(1).
- Sanders BD, Jackson B, Marmorstein R. 2010. Structural basis for sirtuin function: What we know and what we don't. *Biochimica et Biophysica Acta (BBA)-Proteins and Proteomics*. 1804(8):1604-1616.
- Schmid J, Amrhein N. 1995. Molecular organization of the shikimate pathway in higher plants. *Phytochemistry*. 39(4):737-749.
- Schmid M, Davison TS, Henz SR, Pape UJ, Demar M, Vingron M, Schölkopf B, Weigel D, Lohmann JU. 2005. A gene expression map of arabidopsis thaliana development. *Nat Genet*. 37(5):501-506.
- Schwessinger B, Zipfel C. 2008. News from the frontline: Recent insights into pamp-triggered immunity in plants. *Curr Opin Plant Biol*. 11(4):389-395.
- Sels J, Mathys J, De Coninck BM, Cammue BP, De Bolle MF. 2008. Plant pathogenesis-related (pr) proteins: A focus on pr peptides. *Plant Physiol Biochem*. 46(11):941-950.
- Serino L, Reimmann C, Baur H, Beyeler M, Visca P, Haas D. 1995. Structural genes for salicylate biosynthesis from chorismate in pseudomonas aeruginosa. *Mol Gen Genet*. 249(2):217-228.

- Shah J. 2003. The salicylic acid loop in plant defense. *Current opinion in plant biology*. 6(4):365-371.
- Sheen J, Hwang S, Niwa Y, Kobayashi H, Galbraith DW. 1995. Green-fluorescent protein as a new vital marker in plant cells. *Plant J*. 8(5):777-784.
- Shine MB, Yang JW, El-Habbak M, Nagyabhyru P, Fu DQ, Navarre D, Ghabrial S, Kachroo P, Kachroo A. 2016. Cooperative functioning between phenylalanine ammonia lyase and isochorismate synthase activities contributes to salicylic acid biosynthesis in soybean. *New Phytol*. 212(3):627-636.
- Silverman P, Seskar M, Kanter D, Schweizer P, Metraux JP, Raskin I. 1995. Salicylic acid in rice (biosynthesis, conjugation, and possible role). *Plant physiology*. 108(2):633-639.
- Singer B. 1972. Protein synthesis in virus-infected plants. Ii. The synthesis and accumulation of tmv and tmv coat protein in subcellular fractions of tmv-infected tobacco. *Virology*. 47(2):397-404.
- Singh S, Singh A, Yadav S, Gautam V, Sarkar AK. 2017. Sirtinol, a sir2 protein inhibitor, affects stem cell maintenance and root development in arabis thaliana by modulating auxin-cytokinin signaling components. *Sci Rep*. 7:42450.
- Speth EB, Imboden L, Hauck P, He SY. 2009. Subcellular localization and functional analysis of the arabidopsis gtpase rabe. *Plant Physiol*. 149(4):1824-1837.
- Spoel S, Mou Z, Zhang X, Pieterse C, Dong X. 2006. Regulatory roles of npr1 in plant defense: Regulation and function.
- Spoel SH, Mou Z, Tada Y, Spivey NW, Genschik P, Dong X. 2009. Proteasome-mediated turnover of the transcription coactivator npr1 plays dual roles in regulating plant immunity. *Cell*. 137(5):860-872.

- Tada Y, Spoel SH, Pajerowska-Mukhtar K, Mou Z, Song J, Wang C, Zuo J, Dong X. 2008. Plant immunity requires conformational changes of npr1 via s-nitrosylation and thioredoxins. *Science*. 321(5891):952-956.
- Tai TH, Dahlbeck D, Clark ET, Gajiwala P, Pasion R, Whalen MC, Stall RE, Staskawicz BJ. 1999. Expression of the bs2 pepper gene confers resistance to bacterial spot disease in tomato. *Proceedings of the National Academy of Sciences of the United States of America*. 96(24):14153-14158.
- Tang G, Reinhart BJ, Bartel DP, Zamore PD. 2003. A biochemical framework for rna silencing in plants. *Genes Dev*. 17(1):49-63.
- Tanner KG, Landry J, Sternglanz R, Denu JM. 2000. Silent information regulator 2 family of nad- dependent histone/protein deacetylases generates a unique product, 1-o-acetyl-adp-ribose. *Proceedings of the National Academy of Sciences of the United States of America*. 97(26):14178-14182.
- Ueoka-Nakanishi H, Tsuchiya T, Sasaki M, Nakanishi Y, Cunningham KW, Maeshima M. 2000. Functional expression of mung bean ca^{2+}/h^{+} antiporter in yeast and its intracellular localization in the hypocotyl and tobacco cells. *Eur J Biochem*. 267(10):3090-3098.
- van Lohuizen M. 1999. The trithorax-group and polycomb-group chromatin modifiers: Implications for disease. *Curr Opin Genet Dev*. 9(3):355-361.
- van Loon LC, Rep M, Pieterse CM. 2006. Significance of inducible defense-related proteins in infected plants. *Annu Rev Phytopathol*. 44:135-162.
- Wanderley-Nogueira AC, Belarmino LC, Soares-Cavalcanti NaM, Bezerra-Neto JP, Kido EA, Pandolfi V, Abdelnoor RV, Binneck E, Carazzole MF, Benko-Iseppon AM. 2012. An overall evaluation of the resistance (r) and pathogenesis-related (pr) superfamilies in

- soybean, as compared with medicago and arabidopsis. *Genet Mol Biol.* 35(1 (suppl)):260-271.
- Wang C, Gao F, Wu J, Dai J, Wei C, Li Y. 2010. Arabidopsis putative deacetylase *atsrt2* regulates basal defense by suppressing *pad4*, *eds5* and *sid2* expression. *Plant & cell physiology.* 51(8):1291-1299.
- Wang Y, Hu Q, Wu Z, Wang H, Han S, Jin Y, Zhou J, Zhang Z, Jiang J, Shen Y *et al.* 2017. Histone deacetylase 6 represses pathogen defence responses in *arabidopsis thaliana*. *Plant Cell Environ.* 40(12):2972-2986.
- Weissmann G. 1991. Aspirin. *Scientific American.* 264(1):84-91.
- Wendehenne D, Gao QM, Kachroo A, Kachroo P. 2014. Free radical-mediated systemic immunity in plants. *Curr Opin Plant Biol.* 20:127-134.
- White RF. 1979. Acetylsalicylic acid (aspirin) induces resistance to tobacco mosaic virus in tobacco. *Virology.* 99(2):410-412.
- Wielopolska A, Townley H, Moore I, Waterhouse P, Helliwell C. 2005. A high-throughput inducible *rnai* vector for plants. *Plant Biotechnol J.* 3(6):583-590.
- Wildermuth MC, Dewdney J, Wu G, Ausubel FM. 2001. Isochorismate synthase is required to synthesize salicylic acid for plant defence. *Nature.* 414(6863):562-565.
- Wobbe KK, Klessig DF. 1996. Salicylic acid—an important signal in plants. *Signal transduction in plant growth and development.* Springer. p. 167-196.
- Wu T, Pi EX, Tsai SN, Lam HM, Sun SM, Kwan YW, Ngai SM. 2011. *Gm*phd5 acts as an important regulator for crosstalk between histone h3k4 di-methylation and h3k14 acetylation in response to salinity stress in soybean. *BMC Plant Biol.* 11:178.

- Xing S, Poirier Y. 2012. The protein acetylome and the regulation of metabolism. *Trends in plant science*. 17(7):423-430.
- Yan S, Dong X. 2014. Perception of the plant immune signal salicylic acid. *Current opinion in plant biology*. 20C:64-68.
- Yang H, Murphy A. 2013. Membrane preparation, sucrose density gradients and two-phase separation fractionation from five-day-old arabidopsis seedlings. *The Plant Journal*.
- Yang XJ, Seto E. 2007. Hats and hdacs: From structure, function and regulation to novel strategies for therapy and prevention. *Oncogene*. 26(37):5310-5318.
- Yuan Z-l, Guan Y-j, Chatterjee D, Chin YE. 2005. Stat3 dimerization regulated by reversible acetylation of a single lysine residue. *Science*. 307(5707):269-273.
- Zhang Y, Fan W, Kinkema M, Li X, Dong X. 1999. Interaction of npr1 with basic leucine zipper protein transcription factors that bind sequences required for salicylic acid induction of the pr-1 gene. *Proc Natl Acad Sci U S A*. 96(11):6523-6528.
- Zhang Y, Li N, Caron C, Matthias G, Hess D, Khochbin S, Matthias P. 2003. Hdac-6 interacts with and deacetylates tubulin and microtubules in vivo. *The EMBO journal*. 22(5):1168-1179.
- Zhao B, Lin X, Poland J, Trick H, Leach J, Hulbert S. 2005. A maize resistance gene functions against bacterial streak disease in rice. *Proc Natl Acad Sci U S A*. 102(43):15383-15388.
- Zheng Z, Qamar SA, Chen Z, Mengiste T. 2006. Arabidopsis wrky33 transcription factor is required for resistance to necrotrophic fungal pathogens. *Plant J*. 48(4):592-605.
- Zhong Q, Kowluru RA. 2010. Role of histone acetylation in the development of diabetic retinopathy and the metabolic memory phenomenon. *J Cell Biochem*. 110(6):1306-1313.

- Zhou C, Zhang L, Duan J, Miki B, Wu K. 2005. Histone deacetylase19 is involved in jasmonic acid and ethylene signaling of pathogen response in arabidopsis. *The Plant cell*. 17(4):1196-1204.
- Zhou JM, Trifa Y, Silva H, Pontier D, Lam E, Shah J, Klessig DF. 2000. Npr1 differentially interacts with members of the tga/obf family of transcription factors that bind an element of the pr-1 gene required for induction by salicylic acid. *Mol Plant Microbe Interact*. 13(2):191-202.
- Zuo J, Niu QW, Chua NH. 2000. Technical advance: An estrogen receptor-based transactivator xve mediates highly inducible gene expression in transgenic plants. *Plant J*. 24(2):265-273.

APPENDICES

APPENDIX A – Abbreviations

SABP2 - Salicylic acid binding protein 2

SIP-428 – SABP2 Interacting Protein-428

PRRs - Pattern recognition receptors

PAMPs - Pathogen-associated molecular patterns

R protein - Resistance protein

Avr - Avirulence

ICS 1 - Isochorismate synthase 1

PCD - Program cell death

SA - Salicylic acid

JA - Jasmonic acid

ET - Ethylene

SAR - Systemic acquired resistance

SAMT - Salicylic acid methyltransferase

MeSA - Methyl salicylate

SDS PAGE - Sodium dodecyl sulphate-polyacrylamide gel electrophoresis

TMV - Tobacco mosaic virus

PR - Pathogenesis-related

ROS - Reactive oxygen species

NPR1 - Non-expresser of pathogenesis-related protein 1

CFU - colony forming units

β ME - β mercaptoethanol

Ps - *Pseudomonas syringae*

E α 1 - *Elongation Factor alpha 1*

PAD4 - *Phytoalexin Deficient*

R-genes - *Resistance genes*

TAE - Tris-Acetate EDTA

KBM - King's B Medium

KDa - Kilo Dalton

OD - Optical Density

UV - Ultraviolet

μ g - microgram

μ l - microliter

ml - milliliter

mM - milli Molar

APPENDIX B – Buffers and Reagents

Ammonium Persulfate (20% in 1ml)

Dissolve Ammonium persulfate (200mg) in 1ml of water

Ampicillin (100mg/ml)

Ampicillin: 1gm

Add to 10 ml of milli-Q water

Filter sterilized and stored at -20°C

Bicine buffer (buffer B) (1L)

Bicine (1.63g), M.W. = 163.2g/mol, final concentration = 10Mm

Adjust pH to 8.5 with 1 N NaOH

1ml of β -ME (14.4mM final concentration), 1ml of PMSF (100mM) (0.1mM final concentration),

0.15g of benzamidine HCl (156.61g/mol, final concentration 1mM).

Edward's solution

200 mM Tris-HCl, pH 7.5,

250 mM NaCl,

25 mM EDTA,

0.5% SDS

Gentamycin (30 mg/ml)

Gentamycin (powder) = 0.3 gm

Add to 10 ml of milli-Q water

Filter sterilized and stored at -20°C.

Grinding Buffer (1L)

Mannitol (60.12g), M.W. = 182.17g/mol, final concentration = 0.33M

Glycine (0.75g), M.W. = 75.07g/mol, final concentration = 10mM

MOPS (4.19g), M.W. = 209.26g/mol, final concentration = 20mM

EDTA (0.42g), M.W. = 416.20g/mol, final concentration = 1mM

Adjust pH to 7.2

Then autoclave at 121°C and 15 psi atmospheric pressure for 20 minutes

Stored at 4°C

Infiltration buffer

10mM of MES (pH 5.5)

10mM MgCl₂

Kanamycin (50 or 100 mg/ml)

Kanamycin= 0.5 or 1gm

Add to 10 ml of milli-Q water

Filter sterilized and stored at -20°C.

KING'S B Medium

Protease peptone # 3 = 20 g

Potassium phosphate dibasic = 1.50 g

Magnesium sulfate = 1.50 g

Glycerol = 10 ml

Adjust the volume to 1 liter with distilled water

Adjust the pH to 7.0

Agar = 17.50 g (for solid medium)

Then autoclave at 121°C and 15 psi atmospheric pressure for 20 minutes

LB Medium (1 L)

LB Broth = 25 g

Makeup to 1000 ml with distilled water

Then autoclave at 121°C and 15 psi atmospheric pressure for 20 minutes

Store at room temperature

MES (2-(*N*-morpholino) ethanesulfonic acid) Buffer (0.55M)

MES powder = 9.762 gm

Dissolved in 60 ml of milli-Q water

Adjusted to pH 5.5 with 1M NaOH

Adjust the volume to 100 ml with milli-Q water

Then filter sterilized and stored in -20°C

MS media with Gamborg's Vitamins

MS media (4.4g/L)

Myo-Inositol (100mg/L)

Nicotinic Acid (1mg/L)

Pytodoxine. HCl (1mg/ml)

Thiamine. HCl (10mg/ml)

Ponceau S Stain (100ml)

Ponceau S (0.1g), final concentration = 0.1%

Acetic acid (5ml), final concentration = 5%

Rifampicin (20 mg/ml)

Rifampicin= 0.2 g

Add to 10 ml of Methanol

Stored at 4°C covered with aluminum foil

RIM (Root Inducing Media)

MS salt medium + 1% sucrose + Agar

+Vitamin

+Carbenicillin and Kanamycin into a RIM

SDS Gel Loading Buffer (2 X):

50mM Tris-HCl (pH 6.8)

100mM DTT

2% (wt/vol) SDS

0.1% (wt/vol) bromophenol blue

10% (vol/vol) glycerol

Shoot Inducing Media (SIM)

4.31g of MS salts (1 liter)

3% Sucrose

Adjust pH to 5.9 with 1M KOH

Add 0.9% Agar

Add Vitamins

+0.1mg/litre alpha NAA

+1mg/liter BAP

+1ml 1000X vitamin solution

SIM with antibiotics

Carbenicillin 250mg/litre

Kanamycin 300mg/litre

Cefatoxim 100mg/ml

Spectinomycin (100 mg/ml)

Spectinomycin (powder) = 1gm

Add to 10 ml of milli-Q water

Filter sterilized and stored at -20⁰C.

STE buffer

100mM NaCl

10mM Tris-HCl, pH 8

1mM EDTA

STET buffer

10mM Tris-HCl

1mM EDTA

100mM NaCl

5% Triton X-100

Sucrose gradient in Grinding Buffer (50 ml)

Dissolved 18, 25, 35, 40 and 50% sucrose in 50 ml of grinding buffer respectively.

Filter sterilized

Stored at 4⁰C

TE buffer

10 mM Tris-HCl, pH 8.0

1 mM EDTA, pH 8.0

Wash solution

20% (v/v) commercial bleach

0.1% Tween-20

Western Blotting Blocking Buffer (100ml)

1x PBS buffer, 100ml

Dry Milk (1g), final concentration = 1%

BSA (3g), final concentration = 3%

10x Phosphate Buffer Saline (10x PBS)

Sodium Chloride (76g), M.W. = 58.44g/mol, final concentration = 1.3M

Sodium Phosphate dibasic (10g), M.W. = 141.96g/mol, final concentration = 70mM

Sodium Phosphate monobasic (4.1g), M.W. = 119.96g/mol, final concentration = 30mM

For 1x PBS (1 L), dilute 100ml of 10x PBS in 900ml of water. 88

For 1x PBS (1 L) with 0.03% Tween 20, dilute 100ml of 10x PBS in 899.7ml of water,
then add 300 μ L of tween 20.

4x SDS-PAGE Stacking gel Buffer (500ml)

Tris base (30.28), M.W. = 121.1g/mol, final concentration = 0.5M

Adjust pH to 6.8

Add SDS (0.2g), final concentration = 0.04%

10x SDS-PAGE Running Buffer (1 L)

Tris base (30g), M.W. = 121.1g/mol

Glycine (144g), M.W. 75.07g/mol

SDS (10g) 89

10x Western Blotting Transfer Buffer (1L)

Tris base (30.3g), M.W. = 121.1g/mol, final concentration = 125mM

Glycine (72.06g), M.W. = 75.07g/mol, final concentration 960mM

For western, 1x transfer buffer is prepared by mixing 100ml of 10x transfer buffer, 100ml of 100% methanol, and 800ml of cold water.

2x SDS-PAGE Loading Dye (100ml)

1M Tris-Cl, pH 6.8 (10ml), final concentration = 100mM

SDS (0.4g), final concentration = 0.4%

Glycerol (20ml), final concentration, 20%

Bromophenol blue (0.2g), final concentration = 0.2%

Add 5ml of ME before use.

1X Ni-NTA lysis buffer

50 mM sodium phosphate monobasic

300 mM sodium chloride

10 mM imidazole, (pH 8.0)

1mM PMSF (had to be added fresh)

1X Ni-NTA wash buffer

50 mM sodium phosphate monobasic

300 mM sodium chloride

20 mM imidazole, (pH 8.0)

1mM PMSF (had to be added fresh)

1X Ni-NTA elution buffer

50 mM sodium phosphate monobasic

300 mM sodium chloride

250 mM imidazole, (pH 8.0)

1mM PMSF (had to be added fresh)

10 mM Magnesium Chloride

$\text{MgCl}_2 = 0.952 \text{ g}$

Adjust the volume to 1 liter with distilled water 88

Then autoclave at 121°C and 15 psi atmospheric pressure for 20 minutes

1M Magnesium Sulfate

$\text{MgSO}_4 = 246.48 \text{ g}$

Adjust the volume to 1 liter with distilled water

Then autoclave at 121°C and 15 psi atmospheric pressure for 20 minutes

0.1M Sucrose Solution

Sucrose = 34.2 g

Adjust the volume to 1 liter with distilled water.

Filter sterilize the solution and store at -20°C

0.1% Diethyl Pyrocarbonate Treated Water (DEPC)

Diethyl pyrocarbonate = 0.1 ml

Add to 100 ml of distilled water

Incubate for overnight at 37°C

Then autoclave at 121°C and 15 psi atmospheric pressure for 20 minutes

APPENDIX C – Figures and Tables

TGAGACTTTTCAACAAAGGATAATTTTCGGGAAACCTCCTCGGATTCCATTGCCAGCTATCTGTCACTT
 CATCGAAAGGACAGTAGAAAAGGAAGGTGGCTCCTACAAATGCCATCATTGCGATAAAGGAAAGGCT
 ATCATTCAAGATCTCTCTGCCGACAGTGGTCCCAAAGATGGACCCCCACCCACGAGGAGCATCGTGG
 AAAAGAAGACGTTCCAACCACGTCTTCAAAGCAAGTGGATTGATGTGACATCTCCACTGACGTAAGGG
 ATGACGCACAATCCCACTATCCTTCGCAAGACCTTCCTCTATATAAGGAAGTTCATTTCAATTTGGAGA
 GGACA

Figure 80 (A-1): 35S CaMV promoter sequence of pHELLSGATE8 vector.

pDR221-428-predicted	TGCTTTTTTATAATGCCAACTTTGTACAAAAAGCAGGCTATATGTCCATGTCCTTCGA
pDR221-428-colony-8	TGCTTTTTTATAATGCCAACTTTGTACAAAAAGCAGGCTATATGTCCATGTCCTTCGA
pDR221-428-colony-9	TGCTTTTTTATAATGCCAACTTTGTACAAAAAGCAGGCTATATGTCCATGTCCTTCGA
pDR221-428-colony-10	TGCTTTTTTATAATGCCAACTTTGTACAAAAAGCAGGCTATATGTCCATGTCCTTCGA
pDR221-428-colony-6	TGCTTTTTTATAATGCCAACTTTGTACAAAAAGCAGGCTATATGTCCATGTCCTTCGA
pDR221-428-colony-7	TGCTTTTTTATAATGCCAACTTTGTACAAAAAGCAGGCTATATGTCCATGTCCTTCGA

pDR221-428-predicted	CTTTGTTCGGAACCTCAATTTCTGGCTTAAAGAATAAAAGAGATTTGCTGGGCTTAGAT
pDR221-428-colony-8	CTTTGTTCGGAACCTCAATTTCTGGCTTAAAGAATAAAAGAGATTTGCTGGGCTTAGAT
pDR221-428-colony-9	CTTTGTTCGGAACCTCAATTTCTGGCTTAAAGAATAAAAGAGATTTGCTGGGCTTAGAT
pDR221-428-colony-10	CTTTGTTCGGAACCTCAATTTCTGGCTTAAAGAATAAAAGAGATTTGCTGGGCTTAGAT
pDR221-428-colony-6	CTTTGTTCGGAACCTCAATTTCTGGCTTAAAGAATAAAAGAGATTTGCTGGGCTTAGAT
pDR221-428-colony-7	CTTTGTTCGGAACCTCAATTTCTGGCTTAAAGAATAAAAGAGATTTGCTGGGCTTAGAT

pDR221-428-predicted	TTGGCAGCTAATCATTGAAATATCCCAATGAGGAAATGGTTTGTAGTGGAGTAAAAAGTTC
pDR221-428-colony-8	TTGGCAGCTAATCATTGAAATATCCCAATGAGGAAATGGTTTGTAGTGGAGTAAAAAGTTC
pDR221-428-colony-9	TTGGCAGCTAATCATTGAAATATCCCAATGAGGAAATGGTTTGTAGTGGAGTAAAAAGTTC
pDR221-428-colony-10	TTGGCAGCTAATCATTGAAATATCCCAATGAGGAAATGGTTTGTAGTGGAGTAAAAAGTTC
pDR221-428-colony-6	TTGGCAGCTAATCATTGAAATATCCCAATGAGGAAATGGTTTGTAGTGGAGTAAAAAGTTC
pDR221-428-colony-7	TTGGCAGCTAATCATTGAAATATCCCAATGAGGAAATGGTTTGTAGTGGAGTAAAAAGTTC

pDR221-428-predicted	ATTCCCTTTGAGGGATATGTTAAGTTTGTGCAAAACACAGCAAGAATAACATTTCCAAG
pDR221-428-colony-8	ATTCCCTTTGAGGGATATGTTAAGTTTGTGCAAAACACAGCAAGAATAACATTTCCAAG
pDR221-428-colony-9	ATTCCCTTTGAGGGATATGTTAAGTTTGTGCAAAACACAGCAAGAATAACATTTCCAAG
pDR221-428-colony-10	ATTCCCTTTGAGGGATATGTTAAGTTTGTGCAAAACACAGCAAGAATAACATTTCCAAG
pDR221-428-colony-6	ATTCCCTTTGAGGGATATGTTAAGTTTGTGCAAAACACAGCAAGAATAACATTTCCAAG
pDR221-428-colony-7	ATTCCCTTTGAGGGATATGTTAAGTTTGTGCAAAACACAGCAAGAATAACATTTCCAAG

pDR221-428-predicted	ATCTCATCAGATTGTAAGATAATTCCTTCGAATTTTTTGAGTCACAAAAAGAAGGTT
pDR221-428-colony-8	ATCTCATCAGATTGTAAGATAATTCCTTCGAATTTTTTGAGTCACAAAAAGAAGGTT
pDR221-428-colony-9	ATCTCATCAGATTGTAAGATAATTCCTTCGAATTTTTTGAGTCACAAAAAGAAGGTT
pDR221-428-colony-10	ATCTCATCAGATTGTAAGATAATTCCTTCGAATTTTTTGAGTCACAAAAAGAAGGTT
pDR221-428-colony-6	ATCTCATCAGATTGTAAGATAATTCCTTCGAATTTTTTGAGTCACAAAAAGAAGGTT
pDR221-428-colony-7	ATCTCATCAGATTGTAAGATAATTCCTTCGAATTTTTTGAGTCACAAAAAGAAGGTT

pDR221-428-predicted	CCTTATTCGGATCCCCCTAGCATGAAAGATGTGGACAGTTGTATGAATTCCTTGATAGG
pDR221-428-colony-8	CCTTATTCGGATCCCCCTAGCATGAAAGATGTGGACAGTTGTATGAATTCCTTGATAGG
pDR221-428-colony-9	CCTTATTCGGATCCCCCTAGCATGAAAGATGTGGACAGTTGTATGAATTCCTTGATAGG
pDR221-428-colony-10	CCTTATTCGGATCCCCCTAGCATGAAAGATGTGGACAGTTGTATGAATTCCTTGATAGG
pDR221-428-colony-6	CCTTATTCGGATCCCCCTAGCATGAAAGATGTGGACAGTTGTATGAATTCCTTGATAGG
pDR221-428-colony-7	CCTTATTCGGATCCCCCTAGCATGAAAGATGTGGACAGTTGTATGAATTCCTTGATAGG

pDR221-428-predicted	AGTACCAAGCTTGTGTATTGACGGGAGCTGGCATGAGCACAGAGAGTGAATTCGGAT
pDR221-428-colony-8	AGTACCAAGCTTGTGTATTGACGGGAGCTGGCATGAGCACAGAGAGTGAATTCGGAT
pDR221-428-colony-9	AGTACCAAGCTTGTGTATTGACGGGAGCTGGCATGAGCACAGAGAGTGAATTCGGAT

pDR221-428-colony-10 AGTACCAAGCTTGTGTATTGACGGGAGCTGGCATGAGCACAGAGAGTGAATTCGGAT
pDR221-428-colony-6 AGTACCAAGCTTGTGTATTGACGGGAGCTGGCATGAGCACAGAGAGTGAATTCGGAT
pDR221-428-colony-7 AGTACCAAGCTTGTGTATTGACGGGAGCTGGCATGAGCACAGAGAGTGAATTCGGAT

pDR221-428-predicted TACAGGAGCCCAAATGGAGCATATAGTACTGGTTTCAAACCAATTACCCATCAGGAGTTT
pDR221-428-colony-8 TACAGGAGCCCAAATGGAGCATATAGTACTGGTTTCAAACCAATTACCCATCAGGAGTTT
pDR221-428-colony-9 TACAGGAGCCCAAATGGAGCATATAGTACTGGTTTCAAACCAATTACCCATCAGGAGTTT
pDR221-428-colony-10 TACAGGAGCCCAAATGGAGCATATAGTACTGGTTTCAAACCAATTACCCATCAGGAGTTT
pDR221-428-colony-6 TACAGGAGCCCAAATGGAGCATATAGTACTGGTTTCAAACCAATTACCCATCAGGAGTTT
pDR221-428-colony-7 TACAGGAGCCCAAATGGAGCATATAGTACTGGTTTCAAACCAATTACCCATCAGGAGTTT

pDR221-428-predicted CTCCGATCAAGCAAGGCTCGAAGGCGTTATTGGACACGGAGTTATGCTGGCTGGAGACGT
pDR221-428-colony-8 CTCCGATCAAGCAAGGCTCGAAGGCGTTATTGGACACGGAGTTATGCTGGCTGGAGACGT
pDR221-428-colony-9 CTCCGATCAAGCAAGGCTCGAAGGCGTTATTGGACACGGAGTTATGCTGGCTGGAGACGT
pDR221-428-colony-10 CTCCGATCAAGCAAGGCTCGAAGGCGTTATTGGACACGGAGTTATGCTGGCTGGAGACGT
pDR221-428-colony-6 CTCCGATCAAGCAAGGCTCGAAGGCGTTATTGGACACGGAGTTATGCTGGCTGGAGACGT
pDR221-428-colony-7 CTCCGATCAAGCAAGGCTCGAAGGCGTTATTGGACACGGAGTTATGCTGGCTGGAGACGT

pDR221-428-predicted TTCCTGCAGCTCAACCTAGTACAGGTCATATAGCTCTATCATCTCTTGAGAAAGCAGGC
pDR221-428-colony-8 TTCCTGCAGCTCAACCTAGTACAGGTCATATAGCTCTATCATCTCTTGAGAAAGCAGGC
pDR221-428-colony-9 TTCCTGCAGCTCAACCTAGTACAGGTCATATAGCTCTATCATCTCTTGAGAAAGCAGGC
pDR221-428-colony-10 TTCCTGCAGCTCAACCTAGTACAGGTCATATAGCTCTATCATCTCTTGAGAAAGCAGGC
pDR221-428-colony-6 TTCCTGCAGCTCAACCTAGTACAGGTCATATAGCTCTATCATCTCTTGAGAAAGCAGGC
pDR221-428-colony-7 TTCCTGCAGCTCAACCTAGTACAGGTCATATAGCTCTATCATCTCTTGAGAAAGCAGGC

pDR221-428-predicted CATATAAGTTTTATGATTACACAGAATGTGGACAGGCTGCATCATCGGGCTGGCAGCAAT
pDR221-428-colony-8 CATATAAGTTTTATGATTACACAGAATGTGGACAGGCTGCATCATCGGGCTGGCAGCAAT
pDR221-428-colony-9 CATATAAGTTTTATGATTACACAGAATGTGGACAGGCTGCATCATCGGGCTGGCAGCAAT
pDR221-428-colony-10 CATATAAGTTTTATGATTACACAGAATGTGGACAGGCTGCATCATCGGGCTGGCAGCAAT
pDR221-428-colony-6 CATATAAGTTTTATGATTACACAGAATGTGGACAGGCTGCATCATCGGGCTGGCAGCAAT
pDR221-428-colony-7 CATATAAGTTTTATGATTACACAGAATGTGGACAGGCTGCATCATCGGGCTGGCAGCAAT

pDR221-428-predicted CCCTTGAATTGCATGGGACCGTCTACATTGTTGCCTGTACAATTTGGTTTTACTCTA
pDR221-428-colony-8 CCCTTGAATTGCATGGGACCGTCTACATTGTTGCCTGTACAATTTGGTTTTACTCTA
pDR221-428-colony-9 CCCTTGAATTGCATGGGACCGTCTACATTGTTGCCTGTACAATTTGGTTTTACTCTA
pDR221-428-colony-10 CCCTTGAATTGCATGGGACCGTCTACATTGTTGCCTGTACAATTTGGTTTTACTCTA
pDR221-428-colony-6 CCCTTGAATTGCATGGGACCGTCTACATTGTTGCCTGTACAATTTGGTTTTACTCTA
pDR221-428-colony-7 CCCTTGAATTGCATGGGACCGTCTACATTGTTGCCTGTACAATTTGGTTTTACTCTA

pDR221-428-predicted CCTCGAGAAGTGTTC AAGATCAAGTGAAGGCTCAAAATCCTAAGTGGGCAGCAGCTATC
pDR221-428-colony-8 CCTCGAGAAGTGTTC AAGATCAAGTGAAGGCTCAAAATCCTAAGTGGGCAGCAGCTATC
pDR221-428-colony-9 CCTCGAGAAGTGTTC AAGATCAAGTGAAGGCTCAAAATCCTAAGTGGGCAGCAGCTATC
pDR221-428-colony-10 CCTCGAGAAGTGTTC AAGATCAAGTGAAGGCTCAAAATCCTAAGTGGGCAGCAGCTATC
pDR221-428-colony-6 CCTCGAGAAGTGTTC AAGATCAAGTGAAGGCTCAAAATCCTAAGTGGGCAGCAGCTATC
pDR221-428-colony-7 CCTCGAGAAGTGTTC AAGATCAAGTGAAGGCTCAAAATCCTAAGTGGGCAGCAGCTATC

pDR221-428-predicted GAAAGTTTGGATTATGACAGCCGATCAGACGAGAGCTTTGGTATGAAGCAAAGGCCTGAT
pDR221-428-colony-8 GAAAGTTTGGATTATGACAGCCGATCAGACGAGAGCTTTGGTATGAAGCAAAGGCCTGAT
pDR221-428-colony-9 GAAAGTTTGGATTATGACAGCCGATCAGACGAGAGCTTTGGTATGAAGCAAAGGCCTGAT
pDR221-428-colony-10 GAAAGTTTGGATTATGACAGCCGATCAGACGAGAGCTTTGGTATGAAGCAAAGGCCTGAT
pDR221-428-colony-6 GAAAGTTTGGATTATGACAGCCGATCAGACGAGAGCTTTGGTATGAAGCAAAGGCCTGAT
pDR221-428-colony-7 GAAAGTTTGGATTATGACAGCCGATCAGACGAGAGCTTTGGTATGAAGCAAAGGCCTGAT

pDR221-428-predicted GGGGATATTGAGATCGATGAGAAATTC TGGGAGGAGGATTTCTACATTCTGATTGTGAG
pDR221-428-colony-8 GGGGATATTGAGATCGATGAGAAATTC TGGGAGGAGGATTTCTACATTCTGATTGTGAG
pDR221-428-colony-9 GGGGATATTGAGATCGATGAGAAATTC TGGGAGGAGGATTTCTACATTCTGATTGTGAG
pDR221-428-colony-10 GGGGATATTGAGATCGATGAGAAATTC TGGGAGGAGGATTTCTACATTCTGATTGTGAG
pDR221-428-colony-6 GGGGATATTGAGATCGATGAGAAATTC TGGGAGGAGGATTTCTACATTCTGATTGTGAG
pDR221-428-colony-7 GGGGATATTGAGATCGATGAGAAATTC TGGGAGGAGGATTTCTACATTCTGATTGTGAG

```

pDR221-428-predicted      AGGTGCCAAGGAGTTCTCAAACCTGACGTTGTCTTCTTTGGGGATAATGTCCTTAAAGCT
pDR221-428-colony-8      AGGTGCCAAGGAGTTCTCAAACCTGACGTTGTCTTCTTTGGGGATAATGTCCTTAAAGCT
pDR221-428-colony-9      AGGTGCCAAGGAGTTCTCAAACCTGACGTTGTCTTCTTTGGGGATAATGTCCTTAAAGCT
pDR221-428-colony-10     AGGTGCCAAGGAGTTCTCAAACCTGACGTTGTCTTCTTTGGGGATAATGTCCTTAAAGCT
pDR221-428-colony-6      AGGTGCCAAGGAGTTCTCAAACCTGACGTTGTCTTCTTTGGGGATAATGTCCTTAAAGCT
pDR221-428-colony-7      AGGTGCCAAGGAGTTCTCAAACCTGACGTTGTCTTCTTTGGGGATAATGTCCTTAAAGCT
*****

pDR221-428-predicted      AGAGCTGATGTTGCCATGGAAGCTGCAAAGGGATGTGATGCCTTCCTTGTACTTGGTTCA
pDR221-428-colony-8      AGAGCTGATGTTGCCATGGAAGCTGCAAAGGGATGTGATGCCTTCCTTGTACTTGGTTCA
pDR221-428-colony-9      AGAGCTGATGTTGCCATGGAAGCTGCAAAGGGATGTGATGCCTTCCTTGTACTTGGTTCA
pDR221-428-colony-10     AGAGCTGATGTTGCCATGGAAGCTGCAAAGGGATGTGATGCCTTCCTTGTACTTGGTTCA
pDR221-428-colony-6      AGAGCTGATGTTGCCATGGAAGCTGCAAAGGGATGTGATGCCTTCCTTGTACTTGGTTCA
pDR221-428-colony-7      AGAGCTGATGTTGCCATGGAAGCTGCAAAGGGATGTGATGCCTTCCTTGTACTTGGTTCA
*****

pDR221-428-predicted      TCTATGATGACCATGTCTGCTTTCGGCTTATCAAAGCTGCGCAGGAGGCAGGCGCTGCG
pDR221-428-colony-8      TCTATGATGACCATGTCTGCTTTCGGCTTATCAAAGCTGCGCAGGAGGCAGGCGCTGCG
pDR221-428-colony-9      TCTATGATGACCATGTCTGCTTTCGGCTTATCAAAGCTGCGCAGGAGGCAGGCGCTGCG
pDR221-428-colony-10     TCTATGATGACCATGTCTGCTTTCGGCTTATCAAAGCTGCGCAGGAGGCAGGCGCTGCG
pDR221-428-colony-6      TCTATGATGACCATGTCTGCTTTCGGCTTATCAAAGCTGCGCAGGAGGCAGGCGCTGCG
pDR221-428-colony-7      TCTATGATGACCATGTCTGCTTTCGGCTTATCAAAGCTGCGCAGGAGGCAGGCGCTGCG
*****

pDR221-428-predicted      ACTGCAATTGTAATATTGGGGTGACACGAGCTGACGATCTTGTACCTTTGAAAATTAAT
pDR221-428-colony-8      ACTGCAATTGTAATATTGGGGTGACACGAGCTGACGATCTTGTACCTTTGAAAATTAAT
pDR221-428-colony-9      ACTGCAATTGTAATATTGGGGTGACACGAGCTGACGATCTTGTACCTTTGAAAATTAAT
pDR221-428-colony-10     ACTGCAATTGTAATATTGGGGTGACACGAGCTGACGATCTTGTACCTTTGAAAATTAAT
pDR221-428-colony-6      ACTGCAATTGTAATATTGGGGTGACACGAGCTGACGATCTTGTACCTTTGAAAATTAAT
pDR221-428-colony-7      ACTGCAATTGTAATATTGGGGTGACACGAGCTGACGATCTTGTACCTTTGAAAATTAAT
*****

pDR221-428-predicted      GCTCGAGTTGGAGAGATACTTCCAAGATTGCTTAATGTTGGATCCTTGAGTATCCCTGCT
pDR221-428-colony-8      GCTCGAGTTGGAGAGATACTTCCAAGATTGCTTAATGTTGGATCCTTGAGTATCCCTGCT
pDR221-428-colony-9      GCTCGAGTTGGAGAGATACTTCCAAGATTGCTTAATGTTGGATCCTTGAGTATCCCTGCT
pDR221-428-colony-10     GCTCGAGTTGGAGAGATACTTCCAAGATTGCTTAATGTTGGATCCTTGAGTATCCCTGCT
pDR221-428-colony-6      GCTCGAGTTGGAGAGATACTTCCAAGATTGCTTAATGTTGGATCCTTGAGTATCCCTGCT
pDR221-428-colony-7      GCTCGAGTTGGAGAGATACTTCCAAGATTGCTTAATGTTGGATCCTTGAGTATCCCTGCT
*****

pDR221-428-predicted      CTCTAGTACCCAGCTTCTTGTACAAAGTTGGCATTATAAGAAAGCATTGCTTATCAATT
pDR221-428-colony-8      CTCTAGTACCCAGCTTCTTGTACAAAGTTGGCATTATAAGAAAGCATTGCTTATCAATT
pDR221-428-colony-9      CTCTAGTACCCAGCTTCTTGTACAAAGTTGGCATTATAAGAAAGCATTGCTTATCAATT
pDR221-428-colony-10     CTCTAGTACCCAGCTTCTTGTACAAAGTTGGCATTATAAGAAAGCATTGCTTATCAATT
pDR221-428-colony-6      CTCTAGTACCCAGCTTCTTGTACAAAGTTGGCATTATAAGAAAGCATTGCTTATCAATT
pDR221-428-colony-7      CTCTAGTACCCAGCTTCTTGTACAAAGTTGGCATTATAAGAAAGCATTGCTTATCAATT
*****

```

Figure 81 (A-2): Sequence alignment of SIP-428 with attb sites and pDONR221-SIP-428 entry clone. Sanger sequencing method was used for DNA sequencing the pDONR221-SIP-428 entry clone using M13 forward and reverse primers. Blue highlights sequence represent the start and stop codon. Clone 6, 8, and 10 showed SIP-428 in the proper reading frame.

VITA

BAL KRISHNA CHAND THAKURI

Education:

East Tennessee State University, Johnson City, TN, USA,
Biomedical Science, Ph.D., 2018

Tribhuvan University, Kathmandu, Nepal
MS., Biotechnology, 2012

Tribhuvan University, Kathmandu, Nepal
B.S., Microbiology, 2008

Professional Experience:

Graduate Assistant, East Tennessee State University, Department
of Biological Science, Johnson City, TN, USA, 2013-2018.

Presentations:

Bal Krishna Chand Thakuri, and Kumar D. (2018). “*SIR2 Like Deacetylase Enzyme and Its Possible Role in SABP2 Signaling Pathway*”, 2018 Annual meeting of Southern Section of American Society of Plant Biologist (SS-ASPB), March 24-26, 2018, New Orleans, LA. (Seminar)

Bal Krishna Chand Thakuri, and Kumar D. (2018). “*Sir2 Deacetylase Enzyme and Its Possible Role in Pathogen Infection*”, Appalachian Student Research Forum. Johnson City, TN. April 4 - 5, 2018 (Seminar)

Bal Krishna Chand Thakuri, and Kumar D. (2017). “*Role of SIR2 like Deacetylase Enzyme in plant stress signaling mechanism*”. 56th Annual Meeting of the Phytochemical Society of North America. August 5-9, 2017, University of Missouri, Bond Life Sciences Center, 1201 Rollins, Columbia, MO, IL. (Poster)

Bal Krishna Chand Thakuri, and Kumar D. (2017). “*Characterization of SIR2 like Deacetylase for its Role in Plant Stress Signaling Mechanism*”, Appalachian Student Research Forum. April 11 - 12, 2017, Johnson City, TN. (Poster)

Bal Krishna Chand Thakuri, and Kumar D. (2016). “*Characterization of SIR2 like Deacetylase for Its Role in Stress*”, Appalachian Student Research Forum. April 6 - 7, 2016, Johnson City, TN. (Poster)

Bal Krishna Chand Thakuri, and Kumar D. (2015). “*Characterization of a Tobacco SIR2 like Enzyme for its Role in Plant Stress Signaling*”. 53rd Annual Meeting of the Phytochemical Society of North America. August 8–12, 2015, Urbana-Champagne, IL, USA. (Poster)

Bal Krishna Chand Thakuri, and Kumar D. (2015). “*Putative SIR2 like Enzyme and Its Role in Plant Stress Signaling*”, Appalachian Student Research Forum. April 8 - 9, 2015, Johnson City, TN. (Poster)

Honors and Awards:

Frank and Mary Loews Travel Award by the *Phytochemical Society of North America* (2015)

Frank and Mary Loews Travel Award by the *Phytochemical Society of North America* (2017)

Publications:

Tripathi D, Thakuri BC and Kumar D (2017). Role of Multiple Phytohormones in Regulating Stress Responses in Plants. A Functional Genomic Frontier, Chapter: Mechanism of Plant Hormone Signaling under Stress: A Functional Genomic Frontier, Publisher: John Wiley & Sons, Inc. (Book Chapter)

Thakuri BC, Haq I and Kumar D. SIP-428, an SIR2 deacetylase enzyme and its role in plant immune system. (Manuscript in progress)

Mathema VB, Koh YS, Thakuri BC and Sillanpää M (2012). Parthenolide, a sesquiterpene lactone, expresses multiple anti-cancer and anti-inflammatory activities. *Inflammation* 2012 Apr; 35(2):560-565

Thakuri BC, Mathema VB, Maharjan J, Basnet B and Malla R (2012). Microbial Polyhydroxyalkanoates (PHAs) as a Source of Biodegradable Plastics. *Environment and Biotechnology, Biotechnological Approaches for Environmental Science*. Lambert Academic Publishing (Book Chapter).

Mathema VB, Thakuri BC and Sillanpää M (2011). Bacterial mer operon-mediated detoxification of mercurial compounds: a short review. *Arch Microbiol* (2011) 193:837–844.

Mathema VB, Thakuri BC, Sillanpää M and Shrestha RA (2011). Study of mercury (II) chloride tolerant bacterial isolates from Baghmata River with estimation of plasmid size and growth variation for the high mercury(II) resistant *Enterobacter* spp. *Journal of Biotech Research* [ISSN: 1944-3285]